The mechanism of glucose-induced RCAN1 expression in β-cells

Rakhvinder Kaur Kashmir Singh
(BSc, Hons)

A thesis submitted in partial fulfilment of the requirements for the award of the degree of Masters of Biotechnology (Research)

March 28, 2012

Supervisor: Dr. Damien Keating

Centre for Neuroscience,

Department of Human Physiology,

Flinders University

School of Medicine,

Adelaide, South Australia.

Dedication

This thesis is dedicated to my mother

Harcharan Kaur Dhillon

(1937-2011)

This work contains no material which has been accepted for the award of any other degree or diploma in any university of other tertiary institution and, to the best of my knowledge and belief, the thesis contains no material previously published or written by another person, except where due reference has been made in the text.

I give consent to this copy of my thesis, when deposited in the University Library, being available for loan and photocopying.

Rakhvinder Kaur Kashmir Singh

March 2012

Acknowledgements

I would like to express my gratitude by thanking the following people who have supported and helped me throughout the year.

First and foremost, my utmost gratitude to my supervisor Dr.Damien Keating, whose encouragement, guidance and support from the initial to the final level I will never forget. Dr. Keating has helped me see this project through as I hurdle all the obstacles in the completion of this research work.

Dr. Mary-Louise Rogers, my co-supervisor who always had kind concern and consideration regarding my research work. Her unselfish, unfailing support and friendship meant a lot to me.

The members of the Molecular and Cellular Neuorscience Laboratory; Dr. Ravinarayan Raghupathi for his advice, time, experience and friendship during this journey, Dr. Heshan Pieris for his patience and time in sharing his knowledge of RT-PCR, Dr. Claire Jessup for her cheerful nature which always made everything seem easy; my fellow lab mates; Petra Unteweger and Leah Zelkas; for their friendship, the stimulating "discussions", and for all the fun we have had in the last year.

Dr. Michael Duffield for his patience, motivation, enthusiasm, immense knowledge and best of all his friendship and coffee/lunch chats; the best friend anyone could ever ask for. Most of all for reading the many drafts of this thesis patiently. I also thank Pam Simpson and Robyn Flook for all the kind words and pick-me-up hugs throughout the year.

My greatest appreciation goes to my husband, Vishnu Prathap Nair who has been my pillar of strength throughout this period, and my daughters Myrna and Nithaa Nair. You have each allowed me to be a student more than I was a wife or a mother. My time is all yours now.

Within the Department of Human Physiology I would like to acknowledge Dr. Nick Spencer, Dr. Rainer Haberberger, Dr. William Blessing, and members of their respective laboratories for their continued support and friendship. I would also like to thank Dr. Jonathan Gleandle Dr. Tim Chataway, Dr. Hakan Muyderman, Dr. Neil Sims and the members of their respective laboratories for their support. My sincere appreciation to Dr. Michael Jackson for his kind generosity in donating the MIN6 cells.

My final appreciation goes to the one above all of us, the omnipresent God, for answering my prayers for giving me the strength to plod on despite my constitution wanting to give up and throw in the towel, thank you so much Dear Lord.

Table of Contents

Table of Figures

ABSTRACT

Regulator of calcineurin 1 (RCAN1) is a gene located on chromosome 21 that is highly expressed in the brain, heart, and also in numerous endocrine cells. RCAN1 is an endogenous inhibitor of the protein phosphatase calcineurin which is essential for β cell function and circulatory insulin levels. Changes in RCAN1 expression regulate exocytosis, mitochondrial function, apoptosis, proliferation and susceptibility to oxidative stress. Previous work with RCAN1 in β cells, showed that elevated expression of RCAN1 has a profound effect on β cell function resulting in altered gene expression, elevated ROS accumulation, reduced insulin secretion, hypoinsulinemia and fasting hyperglycemia. Furthermore, an increase in RCAN1 expression is also seen in chronic hyperglycemia in pancreatic islets. However, the mechanisms underlying this in β cells are unknown. As RCAN1 expression is induced by oxidative stress in neuronal cultures and oxidative stress can occur in β cells during periods of cell stress such as hypoxia, there could potentially be a role of RCAN1 in hypoxia. Hence, the aims of this study were firstly to investigate potential mechanisms underlying the glucose-induced expression of RCAN1 followed by the effects of hypoxia on the expression of RCAN1 in MIN6 β cells.

Glucose induction of both the RCAN1 isoforms, RCAN1-1 and RCAN1-4, was dependent on the production of ROS and Ca^{2+} entry in the MIN6 β cells at the gene and protein level. This is because reversal of the glucose-induction of these RCAN1 isoforms was seen in the presence of antioxidants and Ca^{2+} channel blockers. However, the inhibition of calcineurin via the usage of FK506 and Cyclosporine A was seen to effect the expression of RCAN1-4 significantly at

the gene and protein level but not that of RCAN1-1. These results suggest a common ROS and Ca^{2+}-associated pathway for the control of both RCAN1 isoforms but a calcineurin-associated pathway regulating RCAN1-4 expression but not RCAN1-1. Hypoxia at various levels and durations had no effect on the expression of either of the RCAN1 isoforms. This study provides new insights into the mechanisms by which glucose induces the expression of RCAN1. Given that increased RCAN1 has negative effects on β cell function and induces diabetes, the findings further our understanding of the mechanisms linking chronic high glucose and β cell dysfunction.

Commonly Used Abbreviations

µM	Micromole
ADP	Adenosine diphosphate
ANT	Adenine nucleotide translocator
AP-1	Activator protein-1
Arx	Aristaless related homeobox
ATP	Adenosine triphosphate
Bcl-2	B-cell lymphoma-2
bp	Base pairs
Cabin1	Calcineurin binding protein 1
CDK4	Cyclin-dependent kinase 4
CoQ	Coenzyme Q
CPT-1	Carnitine-palmitoyl transferanse-1
CsA	Cyclosporine A
DAPI	4’,6-diamino-2-phenylindole,dihydrochloride
DNA	Deoxyribose nucleic acid
DMEM	Dulbecco’s Minimal Essential Medium
DMSO	Dimethyl sulphoxide

ELISA	Enzyme-linked immunosorbent assay
FAD	Flavin adenine dinucleotide
FFA’s	Free fatty acids
FKBP	FK-binding proteins
FLIP	FLICE inhibitory protein
GAD	Glutamic acid carboxylase
GLUT1	Glucose transporter 1
GLUT2	Glucose transporter 2
GLUT4	Glucose transporter type 4
GSK-3β	Glycogen synthase kinase 3β
GTP	Guanosine triphosphate
Hes-1	*Hairy and Enhancer* of split homologue-1
HLA	Human leucocyte antigen
HNF	Hepatocyte nuclear factor
IA-2	Islet specific antigen-2
IL	Interleukin
Insm1	Insulinoma-associated 1
IRS	Insulin receptor substrate
K_{ATP}	ATP sensitive potassium channels

K_m	Michaelis constant
kDa	Kilo Dalton
LC-CoA	Long-chain acyl-CoA esters
MaFA	Musculoaponeurotic fibrosarcoma oncogene homolog A
MIN6	Mouse Insulinoma
mg	Milligram
ml	Millilitre
mM	Millimolar
MODY	Maturity-onset diabetes of the young
mRNA	Messenger ribonucleic acid
NAD	Nicotinamide adenine dinucleotide
NEFA	Non-esterified fatty acids
Neurod-1	Neurogenic differentiation-1
NFAT	Nuclear factor of activated T-cells
Ng3	Neurogenin 3
NHR	NFAT homology region
NLS	Nuclear localisation sequence
nm	Nanometre
PAX4	Paired box gene 4

PBS	Phosphate buffered saline
PCR	Polymerase chain reaction
Pdx-1	Pancreatic and duodenum homeobox 1
PKC	Protein-kinase C
PP1	Protein phosphtase-1
PP2	Protein phosphtase-2
PPARγ	Peroxisome proliferator-activated receptor gamma
PPI	Peptidyl-propyl cis-trans isomerase
Ptf1a	Pancreas transcription factor 1 alpha
RCAN1	Regulator of calcineurin 1
RCANs	Regulators of calcineurin
ROS	Reactive oxygen species
RRP	Readily releasable pool
RT-PCR	Reverse transcription polymerase chain reaction
SIRT1	sirtuin – (silent-mating type information regulation 2- homolog)-1)
SNAP-25	Synaptosomal-associated protein 25
SNARE	Soluble NSF attachment protein receptor
TBE	Tris boric acid EDTA buffer
TBS	Tris buffered saline

TCA	Tricarboxylic acid
VDCC	Voltage dependent Calcium channels

1 INTRODUCTION

1.1 The Pancreas and β cells

Pancreas is an elongated organ situated close to the first part of the intestine. An adult mammalian pancreas is composed of two main parts; the exocrine and the endocrine component. The exocrine part is a lobulated, branched acinar gland involved in the secretion of pancreatic juices containing digestive enzymes whereas the endocrine pancreas is embedded in the acinar gland. The latter refers to those cells within the pancreas that synthesize and secrete hormones responsible in maintaining appropriate level of glucose in the blood through two of its main hormones insulin and glucagon (Mishra et al., 2011). These cells which are responsible in hormone secretion are made up of many small clusters of cells called **islets of Langerhans** or, more simply, islets.

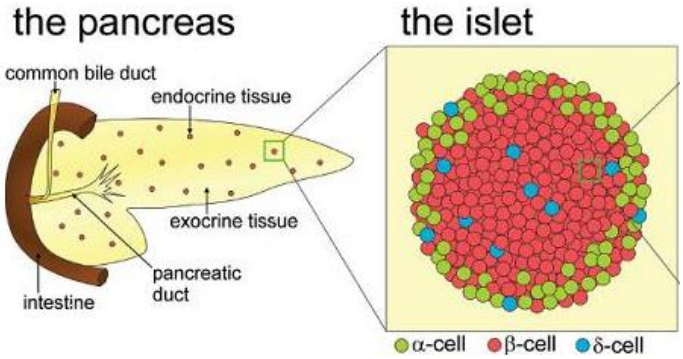

Figure 1-1: Cellular composition of an islet of Langerhans
Cellular composition of an islet of Langerhans and the β-cell signalling pathway. Glucose enters the β-cell via the Glut-2 transporter. Glucose metabolism within the mitochondria increases the ATP:ADP ratio which closes ATP sensitive K^+ channels (K_{ATP}). This depolarises the β-cell, opens voltage-dependent Ca^{2+} channels (VDCC) which triggers insulin release (MacDonald and Rorsman, 2006).

The Islets of Langerhans constitutes approximately 1-2 % of the total pancreatic mass (Kobayashi et al., 2004). The ~1 million Islet of Langerhans

making up a normal pancreas (Marchetti et al., 2006) comprises of ~3000-5000 endocrine cells forming an islet aggregate with a diameter of 100-200 µm (Rorsman et al., 2011, Kitsou-Mylona et al., 2008)

Four main types of endocrine cells make up the islets

a) Insulin producing β cells (65 – 90%)
b) Glucagon producing α cells (15 – 20%)
c) Somatostatin producing δ cells (3 – 10%) and
d) ghrelin and pancreatic polypeptide producing PP cells which are usually located on the surface (1%)

The distribution of these cells in the islets is species-dependent. For example, in rodents and rabbit a core of β cells is surrounded by a ring of α cell, whereas the islets of primates and humans have all the four endocrine cell types intermingled with each other (Kim et al., 2009). However, irrespective of species, mature pancreatic islets are highly vascularised to ensure an efficient secretion of islet hormones into the blood stream. These hormones are responsible in ensuring effective glucose homeostasis and the islet cells work together to maintain glucose homeostasis. However, of the four islet cell types, β cells, representing the majority of islet endocrine cells, are the most important. β cells play the most important role in glucose homeostasis amongst all islet cells by coupling nutrient uptake and metabolism to culminate in electrical activity which regulates the release of β cell insulin.

1.1.1 Glucose uptake and metabolism by β-cells

In healthy β cells, the internalisation of glucose occurs via facilitative transport through the membrane-associated β cell glucose transporter, GLUT-2. This

protein transports glucose into the cell where glucose is rapidly metabolized to pyruvate, following an initial phosphorylation step by glucokinase to glucose-6-phosphate. The phosphorylation of glucose by glucokinase, which has a high K_m for glucose, determines the rate of glucose metabolism by the β cell (Newsholme et al., 2010). Glucose ensures a functional β cell mass by stimulating protein synthesis with a preferential effect on proinsulin and other granule proteins, and stimulation of the transcription of genes important for β cell function such as GLUT2 and glycolytic enzymes including glucokinase. (Jonas et al., 2009).

At the end of glycolysis, each molecule of glucose produces two molecules each of ATP and pyruvate. The latter is then transferred to the mitochondria where it is a substrate for both pyruvate dehydrogenase and pyruvate carboxylase (Figure 1-2). These enzymes cause the formation of acetyl CoA or oxaloacetate from pyruvate respectively, resulting in enhanced mitochondrial tricarboxylic acid (TCA) cycle activity (Maechler, 2002). In the mitochondria, oxidation of pyruvate via the tricarboxylic acid (TCA) or Krebs cycle produces metabolic coupling factors such as ATP, NADPH, glutamate, long chain acyl-CoA and diacylglycerol ((Newsholme et al., 2010).

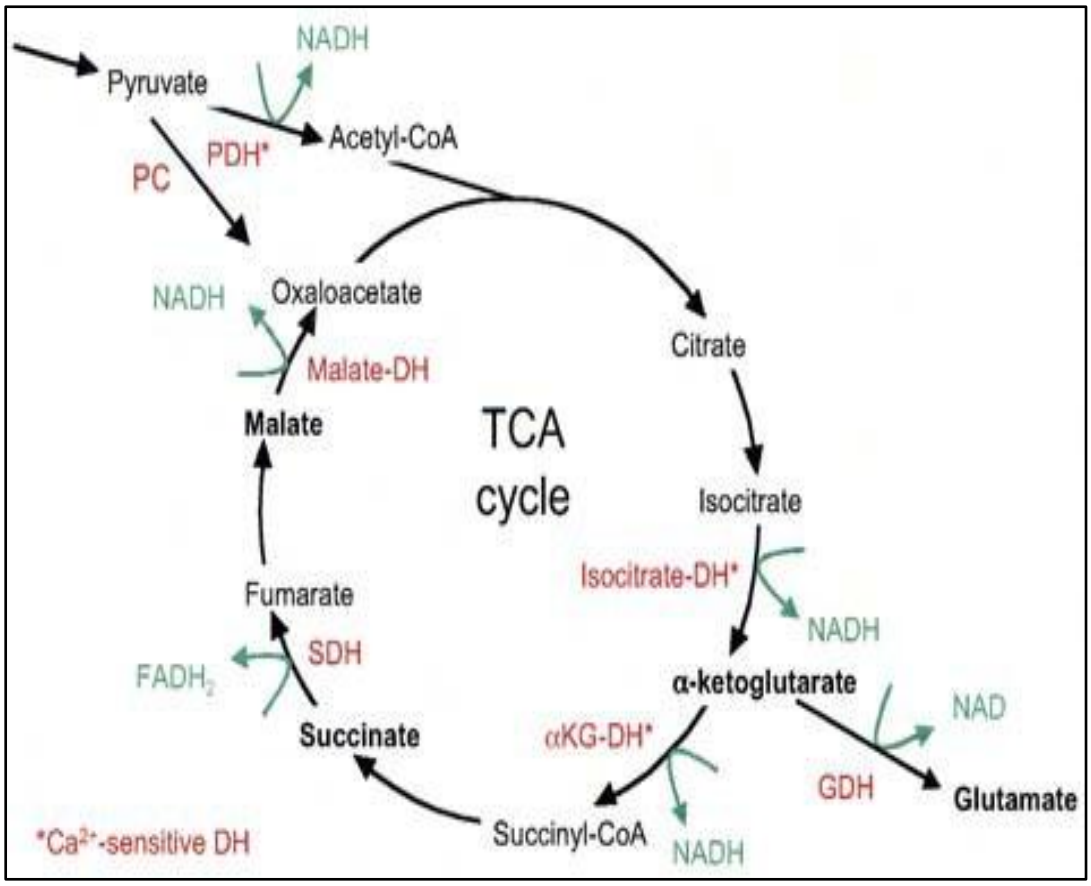

Figure 1-2: The tricarboxylic acid (TCA) cycle with Ca2+-sensitive dehydrogenase.
In the mitochondria, pyruvate is a substrate for both pyruvate dehydrogenase (PDH) and pyruvate carboxylase (PC). Glutamate is produced from an intermediate in the TCA cycle, α-ketoglutarate. (Maechler, 2002)

Transfer of electrons from the TCA cycle to the mitochondrial electron transport chain is mediated by formation of the pyridine nucleotide NADH and the flavin nucleotide $FADH_2$ (Maechler, 2002). Electrons enter the respiratory chain at complexes I and II; and this flow of electron drives protons out of the mitochondrial matrix resulting in hyperpolarisation of the mitochondrial membrane. The mitochondrial membrane potential generated therefore is negative inside the mitochondria and is created by complexes I, III and IV. Complex V catalyses the condensation of ADP with inorganic phosphate to yield ATP and the formation of a high-energy bond powered by the diffusion of protons back into the mitochondrial matrix. The ATP produced is then transferred to the cytoplasm by the adenine

nucleotide translocator (ANT) in exchange for ADP and results in an increase of ATP in the cytoplasm (Maechler, 2002). This leads to an increase in the intracellular ATP to ADP ratio which is essential in the secretion of insulin. This forms the backbone of a series of events which triggers the release of insulin from β cells via a well characterised pathway known as Glucose Stimulated Insulin Secretion (GSIS).

1.1.2 Glucose Stimulated Insulin Secretion (GSIS) in β-cells

β-cells are electrically excitable. By generating changes in β cell membrane potential to depolarised potentials to trigger the entry of Ca^{2+}, fluctuations in blood glucose concentration result in changes in the secretion of insulin. The control of insulin secretion is dependent on the metabolism of glucose. At substimulatory glucose concentrations, K^+ channels are open allowing for the efflux of K^+ from the cell which maintains the resting membrane potential of β cells at a hyperpolarized level around -70mV (Tarasov et al., 2004).

An increase in blood glucose concentration results in an increased uptake and metabolism of glucose in β cells leading to an increase in the intracellular ATP/ADP ratio (Figure 1-3). This results in closure of the ATP-sensitive K^+ (K_{ATP}) channels, a decrease in the efflux of K^+ resulting in the inside of the cell becoming more positive and depolarization of the membrane (Tarasov et al., 2004). Once the membrane potential reaches -30 to -40mV, voltage-dependent Ca^{2+} channels (VDCCs) open leading to an influx of Ca^{2+} along its electrochemical gradient and a rapid increase in cytosolic Ca^{2+} levels. The resultant rise in intracellular Ca^{2+} triggers the exocytosis of insulin by the fusion of insulin containing large dense core vesicles with the plasma membrane (Rutter et al., 2006a).

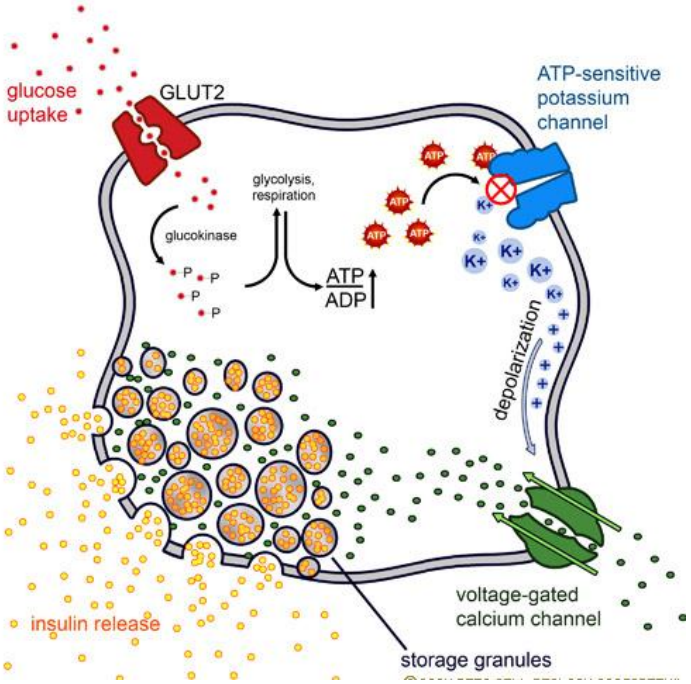

Figure 1-3: Mechanism of glucose-induced insulin secretion
The uptake of glucose into the cell followed by its metabolism results in the secretion of insulin from β-cells

VDCCs are broadly categorised into two groups; low voltage activated (LVA) and the high voltage (HVA) activated Ca^{2+} channels. From these two subtypes, electrophysiologists have further classified VDCCs into L-, P/Q, N- and R-type which belongs to the HVA Ca^{2+} channel group and T-type Ca^{2+} channels within the LVA Ca^{2+} channel group (Yang and Berggren, 2006). The expression of these channels in β cells are heterogenous; with the L-type calcium channels being the most dominant type and as being important for exocytosis of insulin-containing granules (Sher et al., 2003, Schulla et al., 2003). In addition to the exocytosis of insulin, the increase in Ca^{2+} concentration in β cells will also cause the opening of the voltage-sensitive K^+ channels, thereby restoring the resting membrane potential to -70 to -60mV leading to a decrease in cytoplasmic free calcium.

The intermittent opening of VDCCs due to the oscillating of the membrane potential is translated to oscillations in Ca^{2+} concentration and insulin release. The

increase of Ca^{2+} concentration and insulin secretion in β cells occurs rapidly in two distinct phases (Figure 1-4), with a transient first phase and a second, sustained phase (Maechler, 2002). The first phase is dependent on ATP generation, closure of K_{ATP} channels and a rise in intracellular Ca^{2+}. This occurs within 10-15 minutes of stimulation whereby the entry of Ca^{2+} via VDCCs triggers exocytosis of a small pool of pre-formed insulin granules. The second phase of insulin release sees the release of newly synthesised insulin and can lasts up to 2 hours (Henquin, 2000) and is dependent on mitochondrial metabolism with a resulting rise in intracellular Ca^{2+} (K_{ATP} independent).

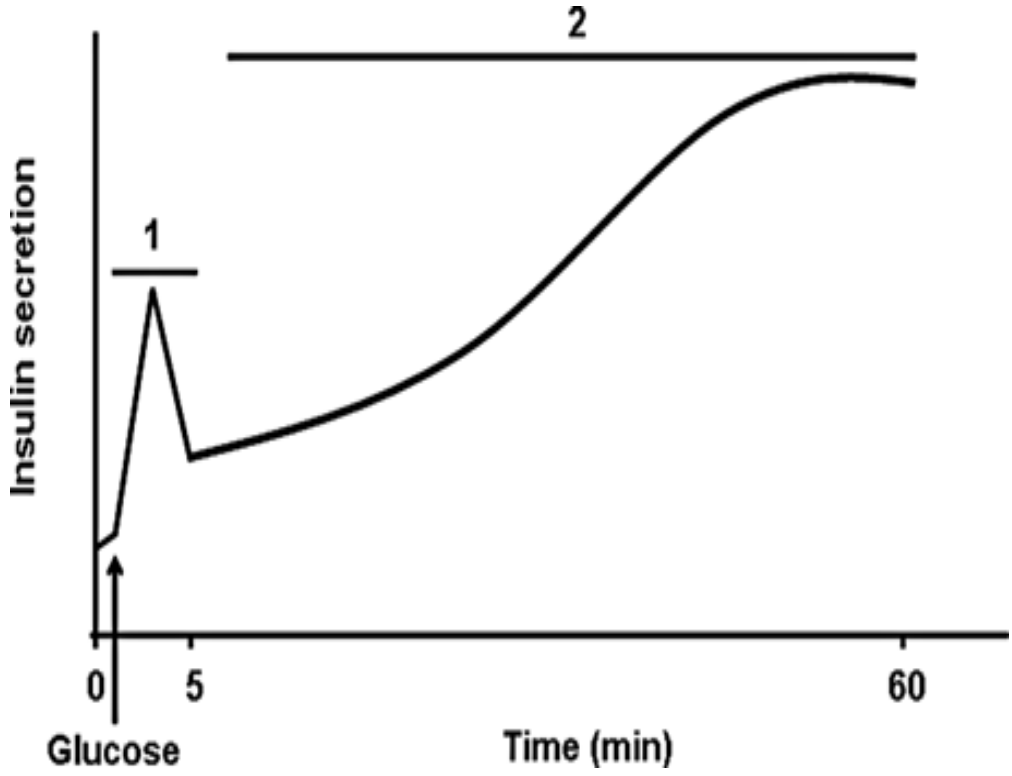

Figure 1-4: Biphasic insulin secretion
Insulin secretion from islet β-cells occurs very rapidly after glucose administration, and occurs with biphasic kinetics. (1): rapid first phase insulin secretion and (2) slower second phase insulin secretion.

The biphasic nature of insulin release is connected to the various functional insulin pool in β-cells ((Rorsman, 2005). Secretory granules vary in regard to their

release competence. These include an intracellular reserve pool (90%), a morphologically docked pool (~10%), and a readily releasable pool (RRP) that is chemically primed for release (0.3-2.2%) (Schulla et al., 2003). The size of the RRP is a major determinant of the magnitude of the initial secretory response. While in the short term, priming of granules already docked at the membrane may release sufficient levels of insulin, ultimately granules must be mobilised from the intracellular reserve pools if stimulation is maintained (Rorsman, 2005). Second phase secretion on the other hand, is dependent on vesicle mobilization towards the membrane and subsequent priming and can only be elicited by metabolizable fuel supplies (Gembal et al., 1992, Henquin, 2000). Hence, glucose-derived signals are important for amplifying and maintaining secretion by promoting the mobilization and priming of insulin granules from reserve pools.

The process of glucose metabolism and secretion of insulin from pancreatic β cells has been shown in the earlier sections to occur via a regulated pathway which is dependent on the changes of glucose concentration in the blood. This primary function of the β cell in correlating its insulin secretion to changes in blood glucose level is crucial in maintaining glucose homeostasis in the body.

1.2 Glucose Homeostasis

The body requires a continuous supply of glucose to ensure its function and survival as glucose is a major fuel supply. However, the control of glucose concentration in the blood is crucial and is dependent on the rate of glucose entering and exiting the circulation. This ensures that despite periods of feeding and fasting the concentration of glucose remains in the narrow range of 4 and 7mM in a normal individual (Saltiel and Kahn, 2001). In order to maintain plasma glucose

concentrations within a normal range, changes in dietary intake or endogenous glucose production must be precisely matched by comparable changes in tissue uptake: this forms the basis of glucose homeostasis. This tight regulation is possible due to the balance between glucose appearance and its disappearance which protects the body from hypogylcemia during periods of fasting and hyperglycemia after the ingestion of a high carbohydrate meal (Aronoff et al., 2004).

Circulating glucose in the blood is obtained via three sources a) Internal absorption of glucose after a meal; b) Glycogenolysis and c) Gluconeogenesis; whereas the removal of glucose from the blood is due to a) its uptake and utilization by peripheral organs such as the skeletal muscles and adipose tissue b) suppression of endogenous glucose production and c) paracrine effects within the pancreas which leads to the suppression of glucagon production.

Internal absorption of glucose occurs after a meal where glucose in the intestine is absorbed from the jejunum and ileum by two routes; intracellular and paracellular. The former occurs across the tight junction between enterocytes into clefts between cells whereas the latter refers to the transport via glucose transporters such as GLUTs (Zierler, 1999). The maximum blood glucose concentration is dependent on the rate at which the stomach empties its content. This is however controlled with hypoglycemia accelerating it whereas hyperglycemia does the opposite (Zierler, 1999).

After the breakdown of carbohydrates by digestive enzymes leading to an increase in blood glucose level a set of physiological responses are triggered to return the blood glucose level to the normal range. At this stage, the removal of glucose from the blood is carried out by another glucoregulatory hormone, insulin.

Insulin binds to specific insulin receptors present on various cells of the body, including muscle cells, fat and liver. Skeletal and cardiac muscles and adipose tissues are signalled to increase their uptake of glucose into these cells upon insulin binding these receptors. Glycogenesis, which is the production of glycogen from glucose, will also take place in the liver as a means to dispose of glucose from the blood. As endogenous glucose production in not necessary during and immediately after a meal, glucagon production will be supressed. This will result in the cessation of glycogenolysis and gluconeogenesis due to the inhibition of glucagon secretion by insulin (Aronoff et al., 2004). To maintain normal blood glucose levels during fasting, it is vital for endogenous glucose supply and production within the body. This task, performed by the liver, is known as hepatic glucose production and it is primarily regulated by a glucoregulatory hormone, glucagon (secreted by the α-cells in the Islet of Langerhans), which maintains the basal blood glucose concentration. A decrease in the plasma glucose concentration causes an increase in the secretion of glucagon which would result in an increase in the hepatic glucose production and hence, ensures that the plasma glucose level returns to normal.

Glucose uptake into skeletal muscle and other tissues is regulated by insulin secreted from the β-cells of the pancreas. Skeletal muscle is capable of utilizing both glucose and free fatty acids as fuel sources. Following the ingestion of a meal, insulin secretion from pancreatic β-cells reduces the rate of lipolysis while stimulating glucose uptake into skeletal muscle (Groop et al., 1989). The binding of insulin to the insulin receptor on the surface of myocytes results in the translocation of the glucose transporter type 4 (GLUT4) to the plasma membrane (Epstein et al., 1999). Glucose is transported into the myocyte via the GLUT4 transporter, and once inside the cell glucose undergoes phosphorylation by hexokinase. The

phosphorylated glucose is either converted to and stored as glycogen or enters the glycolytic pathway depending on the energy requirement of the body (Thiebaud et al., 1982).

As mentioned earlier, the insulin producing β-cells of the pancreas are important regulators of glucose homeostasis. β-cells are capable of sensing increases in blood glucose levels and respond by secreting insulin which inhibits glucose production in the liver and stimulates the uptake of glucose into skeletal muscle. Normally, β-cells are able to adapt to changes in metabolic homeostasis by increasing insulin production and secretion. A prolonged increase in insulin demand due to obesity, however, may result in β-cell increasing its mass. Four major mechanism regulates the β-cell mass; apoptosis (programmed cell death), size modification, replication and neogenesis (Marchetti et al., 2008). The normal adaptation by β-cells to changes in glucose homeostasis is by increasing its mass through an increase in replication, neogenesis and size (Marchetti et al., 2006). As obesity and insulin resistance becomes more prominent, a loss in β-cell mass will occur due to a marked increase in β-cell apoptosis which outweighs replication and neogenesis (Kahn, 2003). This results in poorly controlled glucose levels leading to the metabolic disorder known as Diabetes Mellitus.

1.3 Diabetes Mellitus

Diabetes is a metabolic disorder in which the body is deficient in producing insulin or, alternatively, when the body cannot effectively use the insulin it produces. It is potentially one of the major health problems facing Australians in the 21st century with 898,000 Australians diagnosed with diabetes (AIHW, 2011). Worldwide the number of people living with diabetes is projected to increase from

366 million in 2011 to 552 million by 2030; which equates to approximately three new cases every 10 seconds (IDF, 2011).

There are two main types of diabetes:

a) Type 1 diabetes (insulin-dependent diabetes mellitus)
b) Type 2 diabetes (non–insulin dependent diabetes)

1.3.1 Type 1 diabetes

Type 1 diabetes (or juvenile onset diabetes) is characterised by autoimmune destruction of pancreatic β cells which results in an absolute deficiency in β cell mass and insulin. In Type 1 diabetes, pancreatic islets undergo autoimmune attack and β-cells are destroyed by a combination of autoreactive T cells, islet specific autoantibodies and cytokines (Bluestone et al., 2010). Patients having this form of diabetes normalise their plasma glucose levels via an exogenous supply of insulin Although Type 1 diabetes can occur at any age, the common age of diagnosis ranges from infancy to 14 years of age (Planas et al., 2010). By this stage, however, only 10-20% of the β cells which produce insulin are functional (Knip et al., 2005)

There is a genetic predisposition to Type 1 diabetes, with over 50% of identified genetic causes due to polymorphisms in the human leucocyte antigen (HLA) class II region on chromosome 6. The appearance of diabetes-associated autoantibodies is the first sign of β-cell autoimmunity. Four disease-related autoantibodies against insulin, glutamic acid carboxylase (GAD), islet cell antigen-2 (IA-2) and islet specific glucose-6-phospahte (IGRP) together with macrophage/dendritic cells, B lymphocytes and T lymphocytes are involved in the rapid destruction of pancreatic β-cells (Yoon and Jun, 2001).

The onset of type 1 diabetes is due to the activity between macrophages, T cells, B cells and β-cell autoantibodies. β-cell autoantigens produced by the β-cell are processed by macrophages and presented to helper T cells. The macrophages then activate $CD4^+$ T cells via the secretion of IL-12. These $CD4^+$ T cells secrete a number of cytokines directed at the β-cell which also activate $CD8^+$ effector T cells. Interferon gamma released by the helper T cells cause the macrophages to become cytotoxic, resulting in the secretion of substantial amounts of β-cell toxic cytokines. These cytokines induce the expression of Fas on pancreatic β-cells resulting in Fas-mediated apoptosis of pancreatic β-cells. The rate of apoptosis varies between individuals; however, the complete destruction of insulin-producing β-cells is the end-point in type 1 diabetes.

1.3.2 Type 2 diabetes

Type 2 diabetes (T2D) which accounts for almost 90% of the cases of diabetes (Marchetti et al., 2008), is a condition of insulin resistance characterized by initial hyperinsulinaemia, followed by β-cell exhaustion, β-cell death and ultimate loss of glycaemic control. (Prentki and Nolan, 2006). Studies have shown that insulin resistance precedes the development of hyperglycemia (Kahn et al., 2006).

During the insulin resistant state, a given insulin concentration produces a lower than expected biological effect on glucose levels (Robertson and Harmon, 2006). In this state, fat, muscle and liver cells do not respond as normal to the insulin in the blood; hence reducing glucose uptake into fat and muscle tissues and the inhibition by insulin of glucose production in the liver. Insulin resistance, a common precursor to type 2 diabetes, involves a number of molecular mechanisms which can be directly linked to obesity. One of these is the increased concentrations of non-esterified fatty acids (NEFA) which inhibit insulin-stimulated glucose storage in

skeletal muscle and stimulate gluconeogenesis in the liver. Insulin resistance in skeletal muscle is closely linked to obesity via an increased accumulation of fat in myocytes (Pan et al., 1997). Insulin is an inhibitor of lipolysis and regulates the release of free fatty acids (FFAs) from adipocytes. In insulin resistant individuals the ability of insulin to inhibit lipolysis is impaired resulting in elevated FFAs levels which further affect insulin resistance (Groop et al., 1991). The excess glucose and fat in the blood can also cause additional organ and vascular damage, resulting in morbidity and mortality associated with type 2 diabetes (Deedwania and Fonseca, 2005)

There is significant evidence linking insulin resistance and hyperglycemia, to the presence of abdominal obesity Increased concentrations of non-esterified fatty acids (NEFA) and inflammatory cytokines released by expanded visceral adipose tissue adversely affect the insulin signalling cascade (Rajala and Scherer, 2003, Ravussin and Smith, 2002). Plasma levels of free fatty acids are increased due to insulin resistance in adipose tissue. This will disrupt firstly, the glucose transport system in adipocytes and secondly, the activity of muscle glycogen synthase in skeletal muscle (Camastra et al., 1999). Elevated NEFA levels inhibit the expression of insulin-responsive GLUT4 transporter; essential for glucose uptake and metabolism in skeletal muscle (Vettor et al., 2002). Hence, the increase release of cytokines due to to obesity contributes to the development of insulin resistance (Xu et al., 2003, Arya, 2006)

β-cells overcome insulin resistance by firstly increasing the secretion of insulin. The response by the pancreatic islets in increasing the secretion of insulin returns the blood glucose level to normal levels (5.5mM) under conditions of peripheral insulin resistance. The increase in insulin secretion, results in hyperinsulinaemia and is

known as β-cell compensation (Leahy, 2005). Eventually, β-cell compensation for insulin resistance is unsustainable by the islets. Hyperglycemia then sets in which leads to deterioration of β-cells. Firstly, the raised levels of lipids and reactive oxygen species which affects β-cell function, by impairing proinsulin gene transcription and increase in the degradation of proinsulin mRNA (Leibowitz et al., 2010). Hyperglycemia will also lead to alteration in the expression of apoptosis regulators by upregulating pro-apoptotic genes and down-regulating anti-apoptotic (Federici et al., 2001). These changes will increase β-cells susceptibility to apoptosis. Hence, the deterioration in β-cell function during hyperglycemia (Prentki and Nolan, 2006) will result in pancreatic β-cell damage and worsening of glucose homeostasis resulting in type 2 diabetes..

Failure of the insulin secreting β cells has been identified as the major characteristic of both Type 1 and Type 2 diabetes (Li et al, 2009). In the former, the β cells are destroyed whereas in the latter, genetic and environmental factors lead to a defect in β cells function.

1.4 β cell dysfunction in Type 2 diabetes

The imbalance between the demand on the β cell due to nutrient overload and the body's reduced insulin sensitivity, and the capacity of β cell to increase insulin secretion leads to hyperglycemia. Glucotoxicity is the first outcome of this event which leads on to the deregulation of lipid metabolism and increase in free fatty acids. This would further compound β cell dysfunction. The increase in free fatty acid concentration in the presence of glucose amplifies β cell dysfunction further and is known as glucolipotoxicity (Leibowitz et al., 2010). External factors in the form of free fatty-acids, oxidative stress and glucotoxicity have been correlated with β-cell function. Prolonged exposure to such factors leads onto uncontrolled hyperglycemia

generating cellular stress in β cells resulting in β-cell dysfunction (Prentki and Nolan, 2006). Factors which are associated with β-cell dysfunction in the presence of hyperglycemia include oxidative stress, apoptosis and altered gene expression.

1.4.1 Oxidative Stress

In a generic cell type as shown in Figure 1-5, metabolism of physiological nutrient causes an increase in the generation of reactive oxygen species (ROS) through glucose metabolism in mitochondria (by electron transport chain (ETC) activity) and in the plasma membrane (through NAPDH oxidase). However, this is usually counteracted by their quick detoxification by antioxidants present in the cell such as superoxide dismutase, catalase, glutathione peroxidase and peroxiredoxin (Li et al., 2009). For example, superoxide anions, a major contributor to other reactive species inside the mitochondrion, are enzymatically converted to hydrogen peroxide by a superoxide dismutase within mitochondria of a cell. The hydrogen peroxide produced is rapidly converted to oxygen and water by the mitochondrial enzyme glutathione peroxidase, catalase or peroxideroxin before it causes damage to the cell (Newsholme et al., 2007). As hydrogen peroxide has a long life span in the cell and is able to penetrate nuclear and plasma membrane, its quick removal from the cell by antioxidant enzymes is crucial in the survival of cells (Kaneto et al., 1999).

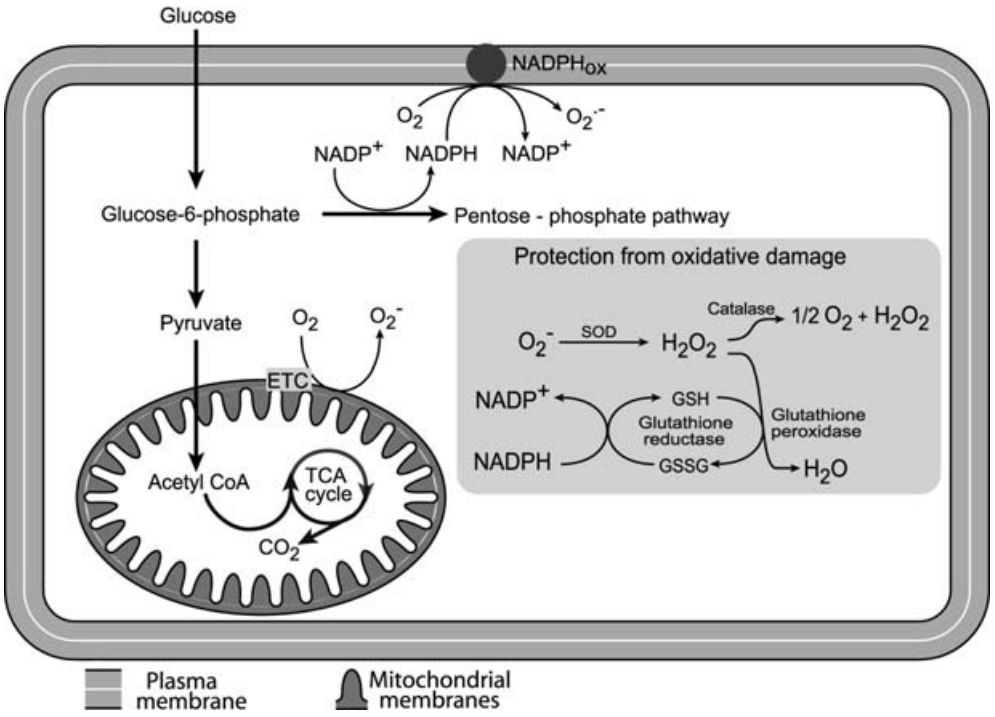

Figure 1-5: Relevant sites of production of reactive oxygen species (ROS) and antioxidant systems in a generic cell type
ROS can be generated through glucose metabolism in mitochondria by electron transport chain activity and in the plasma membrane through NADPH oxidase. The main antioxidant enzymes are superoxide dismutase (SOD), glutathione reductase, glutathione peroxidase and catalase (Newsholme et al., 2007).

Oxidative stress is a measure of free radical oxygen or reactive oxygen species in a system. The key characteristic of oxidative stress are the imbalance between the production of reactive oxygen species (ROS) and the limited antioxidant defences (Li et al., 2009). In both types of diabetes, ROS has been identified as having a role in beta cell dysfunction either as the cause for autoimmune reactions as in Type 1 Diabetes (Rabinovitch, 1998) or by causing a decrease in insulin synthesis and promoting apoptosis as in Type 2 Diabetes (Evans et al., 2002). In β cells, there are several biochemical pathways involved in the generation of ROS (Kajimoto and Kaneto, 2004) and these pathways have been identified to be activated by the overproduction of ROS by the mitochondria during hyperglycemia (Giacco and Brownlee, 2010). The major pathways identified are:

a) glucose oxidation,
b) electron transport chain in mitochondria,
c) activation of the NOX family of NAPDH oxidases,
d) nonenzymatic glycosylation reaction followed by the activation of the advanced glycation end product (AGE) receptors and
e) Hexosamine pathway.

In conditions of high glucose, the metabolic flux in mitochondria increases due to the presence of GLUT2 transporter, which is highly expressed on β cells. Hence, the uptake of glucose into β cells when exposed to high glucose concentration increases. Although during normal metabolism only 0.1% of total oxygen consumption leaks from the respiratory chain to generate ROS, in conditions of hyperglycemia there is an increase in ROS production. This is due to an increase in the electron transport donors (NADH and $FADH_2$) which results in an increase in electron flux through the mitochondrial transport chain during hyperglycemia. Partial inhibition of the electron transport chain in Complex III occurs due to the high electrochemical potential difference generated by the proton gradient. This would then lead to an accumulation of electrons to Coenzyme Q which will in turn drive the partial reduction of O_2 to generate the free radical anion superoxide (Giacco and Brownlee, 2010).

The pancreatic β cells are rendered more susceptible to ROS during oxidative stress. This is due to the relatively low expression of the antioxidant enzymes such as superoxide dismutase, catalase and glutathione peroxidase. Excessive levels of ROS damage cells directly by oxidising DNA, protein and lipids and indirectly by activating stress-sensitive intracellular signalling pathways such as JNK/SAPK and MAPK. This in turn leads to an increase in the production of gene products which

may cause cellular damage and impaired insulin secretion (Newsholme et al., 2007). Interestingly, antioxidant treatment in a diabetic obese mouse model suppressed β cell dysfunction in response to high glucose, *in vivo* (Kaneto et al., 1999). These findings suggest that oxidative stress may be an important pathway by which glucotoxicity leads to β cell dysfunction.

1.4.2 Apoptosis

Glucotoxicity results in an increased production of ROS which has a significant impact in decreasing β cell mass via the induction of apoptosis (Kaneto et al., 1999). Studies in human islets illustrate that incubation in high glucose increases the expression of pro-apoptotic genes and decreases expression of the anti-apoptotic genes (Federici et al., 2001). Furthermore, in rodent islets, higher glucose concentrations are seen to induce apoptosis (Efanova et al., 1998, Maedler et al., 2001). This could be due to the long-term increase in cytosolic Ca^{2+} which occurs due to increase nutrient signalling and may be proapoptotic and induce β cell dysfunction (Chang-Chen et al., 2008).

IL-1 has also been identified recently by numerous studies as causing β cell apoptosis during glucotoxicity (Bendtzen et al., 1986, Maedler et al., 2002b, Mandrup-Poulsen et al., 1985). IL-1 produced by β-cells during normal conditions causes an up-regulation of Fas in the presence of the caspase-8 inhibitor FLICE inhibitory protein (FLIP). This up-regulation of FAS results in β-cell proliferation. During glucotoxicity, the production of the FLIP protein is inhibited. This will then lead to a switch from proliferation to apoptosis of β-cells (Maedler et al., 2002a). The involvement of FLIP in the proliferation-apoptotic pathway is consistent with the initial increase in β-cell mass and function followed by the rapid decrease in β-cell function consistent with the later stages of type 2 diabetes.

1.4.3 Changes in gene expression

Glucotoxicity and the resulting β-cell ROS production have a detrimental effect on the transcription of numerous genes essential for β-cell function and insulin secretion (Robertson et al., 1992). Reduction in insulin is linked to irreversible decreases in the level of two transcription factors Pdx-1 and Musculoaponeurotic fibrosarcoma oncogene homolog A (MafA) (Rolo and Palmeira, 2006). The binding of Pdx-1 (Olson et al., 1993) and MafA (Poitout et al., 1996) to the insulin promoter is reduced and in some cases completely ablated in glucotoxic cell lines and rodent primary β-cells maintained in high glucose conditions (Harmon et al., 1999). Pdx-1 regulates genes involved in β cell function, energy sensing and insulin secretion whereas MafA is involved in the regulation of β cell function via the regulation of β cell genes such as insulin, GLUT-2 and glucokinase (Newsholme et al., 2007, Kulkarni et al., 2004).

β cells from hyperglycaemic animals have also been shown to have changes in the expression of genes . Genes which are normally expressed at very low levels such as the glycolytic enzymes hexokinase 1 (Hk1) and lactate dehydrogenase 1 (LdhA) and transcription factors such as c-Myc are seen to increase in hyperglycemia conditions (Ainscow et al., 2000, Kaneto et al., 2002). These genes are normally expressed in response to various types of stress in the cell, including oxidative stress and hypoxia. The overexpression of genes such as LdhA and c-Myc induce β-cell dysfunction either due to apoptosis or loss of β cell differentiation.

Studies using transgenic mouse models may identify potential genes regulating β cell function. One such gene, RCAN1 (Regulator of Calcineurin 1), has been studied recently in our laboratory. The expression of RCAN1 is upregulated during hyperglycemia in primary islets with a decrease in the expression of genes

vital in β cell function. Pancreatic islets from RCAN1 over expressing mice showed a decrease in the expression of four of the six MODY genes investigated (Hnf1α, Hnf1β, NeuroD1 and glucokinase). Furthermore, inhibition was seen in the gene expression of ARNT and its two protein partners, Hif1α and arylhydrocarbon receptor (AhR) along with inhibition in the expression of the Glut2 glucose transporter and Insulin receptor when measured in islet RNA samples (Peiris, 2011).

In β cells, the presence of stimulators such as glucose, promotes an increase in intracellular calcium concentrations and calcium acts as a second messenger in various biochemical pathways and plays an important role in the functioning of pancreatic β cells (Wollheim and Sharp, 1981). Interestingly, the expression of RCAN1 is regulated by the Calcineurin/NFAT pathway which is dependent on activation by calcium. Hence, the role of Calcineurin/NFAT pathway and the subsequent upregulation of RCAN1 may contribute to the understanding of hyperglycemia induced β cell dysfunction.

1.5 Calcineurin and NFAT pathway

1.5.1 Calcineurin

Calcineurin is a cytosolic calcium-calmodulin dependent serine/threonine phosphatase which is a downstream target of intracellular calcium signalling. The calcineurin protein is a heterodimer made up of two subunits; calcineurin A and calcineurin B; both of which are required for proper calcineurin function. The 57-71 kDa calcineurin A subunit is known as the catalytic subunit whereas the 18-20 kDa calcineurin B subunit serves as a regulatory subunit (Rusnak and Mertz, 2000). As seen in Figure 1-6, the primary sequence for the catalytic A subunit can be divided

into four domains: a catalytic domain at the N-terminus, the B-subunit binding domain, a calmodulin-binding domain and an auto-inhibitory domain at the C terminus (Liu, 2009a). Calcineurin is ubiquitously expressed and highly conserved in eukaryotes (Sieber and Baumgrass, 2009)

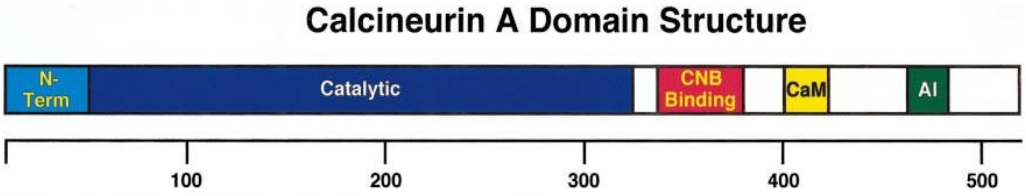

Figure 1-6: Domain structure of calcineurin A
Domains on Calcineurin which are involved in the regulation of its phosphatase activity. CaM, calmodulin; CNB, calcineurin B; AI, autoinhibitory (Rusnak and Mertz, 2000).

The calmodulin binding domain and the C-terminal autoinhibitory domain act together as a molecular switch for calcium sensing whereby the presence of calcium activates calcineurin activity. In the absence of calcium, the C-terminal autoinhibitory domain behaves as a pseudosubstrate and is bound to the active site ensuring inactivation of calcineurin. Increases in intracellular calcium promotes the binding of calcium both directly to calcineurin B (CnB) and as a calcium-calmodulin complex to the calmodulin-binding domain on calcineurin A (Rothermel et al., 2003a). This leads to a conformation change of the protein and the dissociation of the autoinhibitory domain from the active site of calcineurin. This then unmasks the active site of the catalytic domain, allowing the activation of calcineurin (Liu, 2009a).

Calcineurin is able to dephosphorylate a broad range of proteins amongst which are the cAMP-responsive element-binding protein (CREB) transcriptional co-activator, transducer of regulated CREB activity 2 (TORC2) and the nuclear factor

of activated T cells (NFAT) family of transcription factors (Lawrence et al., 2001). Through dephosphorylation-mediated nuclear localization of these proteins, calcineurin integrates calcium and cAMP signals generated by physiological stimuli such as glucose, to alter gene expression. In the current work, the NFAT family of transcription factors is the calcineurin target of interest.

1.5.2 Nuclear Factor of T-activated cells (NFAT)

The NFAT family of transcription factors are made up of NFATc1, NFATc2, NFATc3 and NFATc4 (Rao et al., 1997). All four NFATc proteins are expressed in β cells and calcineurin is required for the activation of each. In many tissues, both calcineurin and NFATc proteins are expressed and they function as signal integrators of calcium signalling to coordinate gene expression, growth and cellular responses to environmental cues (Heit, 2007). NFAT has a conserved ~300 amino acid region known as the NFAT regulatory domain which is located N-terminal to the DNA-binding domain with the major docking site of calcineurin on NFAT having the consensus sequence PxIxIT (Hogan et al., 2003). This domain is encoded in a single exon in all four NFAT proteins from all vertebrate species for which sequence data are available (Graef et al., 2001b). The NFAT regulatory domain is heavily phosphorylated with the phosphorylated serine residues distributed among four classes of conserved serine rich sequence motifs (Beals et al., 1997) and three out of these four motifs are dephosphorylated by calcineurin (Neal and Clipstone, 2001). Of interest is a second interacting sequence which is moderately conserved amongst the NFAT family which has been identified (Park et al., 2000) and this sequence resembles the highly conserved sequence in the calcineurin inhibitors RCAN1 (Fuentes et al., 2000, Rothermel et al., 2000) suggesting a possibility that NFAT and RCAN1 proteins compete for calcineurin binding in cells.

The heavily phosphorylated serines (phosphoserines) in the NFAT regulatory region masks the nuclear localization signals found at the C-terminal region of the NFATc protein. Hence, the dephosphorylation of NFATc proteins leads to the exposure of its nuclear localisation signal sequence which allows NFAT to rapidly translocate into the nucleus. (Liu, 2009a, Clipstone and Crabtree, 1992). The low affinity of individual NFAT proteins for calcineurin ensures sensitivity to environmental signals and prevents constitutive activation of NFAT.(Hogan et al., 2003) In resting cells, NFAT is actively phosphorylated and remains primarily in the cytoplasm as most of the NFAT kinases, such as protein kinase A and glycogen synthase kinase 3 (GSK3), are constitutively active. This ensures an extensive phosphorylation of NFAT and hence, a default cytosolic localisation of NFAT (Timmerman et al., 1996). This is confirmed in studies carried out in isolated rat islets which showed a cytosolic location for phosphorylated NFAT and also a lack of transcriptional activity (Demozay et al., 2011).

1.5.3 The calcineurin/NFAT pathway in β-cells

β cells express all four NFAT family members. Increase in intracellular Ca^{2+} activates the calcineurin phosphatase complex, leading to dephosphorylation of cytoplasmic subunits of NFAT transcription complexes (Figure 1-7). The unmasking of the nuclear localization signal by dephosphorylation allows NFAT to be rapidly translocated into the nucleus. In the nucleus $NFAT_c$ proteins assemble on DNA regulatory sequences with their nuclear partner proteins; known as $NFAT_n$. (Clipstone and Crabtree, 1992). The identity of NFATn varies between cell types , amongst which are API, GATA, MEF2 and cMAF (Rothermel et al., 2003b)-, Along with its nuclear partner proteins (NFATn), the dephosphorylated NFAT will then bind to consensus NFAT binding elements; GGAAA, on certain gene promoters to

specifically enhance their transcription leading to alteration in their gene expression. Upon cessation of the calcium signal, NFATc signalling is terminated through the rephosphorylation of NFAT by kinases such as Glycogen Synthase Kinase-3 (GSK-3) leading to the return of NFATc to the cytosol and the cessation of NFATc transcriptional activity (Graef et al., 2001a). Calcineurin is an important regulator of multiple biological functions in β cells. The calcineurin/NFAT signaling pathway have been shown to translates Ca^{2+} signals into amongst others insulin transcriptional activation (Heit, 2007) and to play a role in glucose homeostasis (Yang et al., 2006)

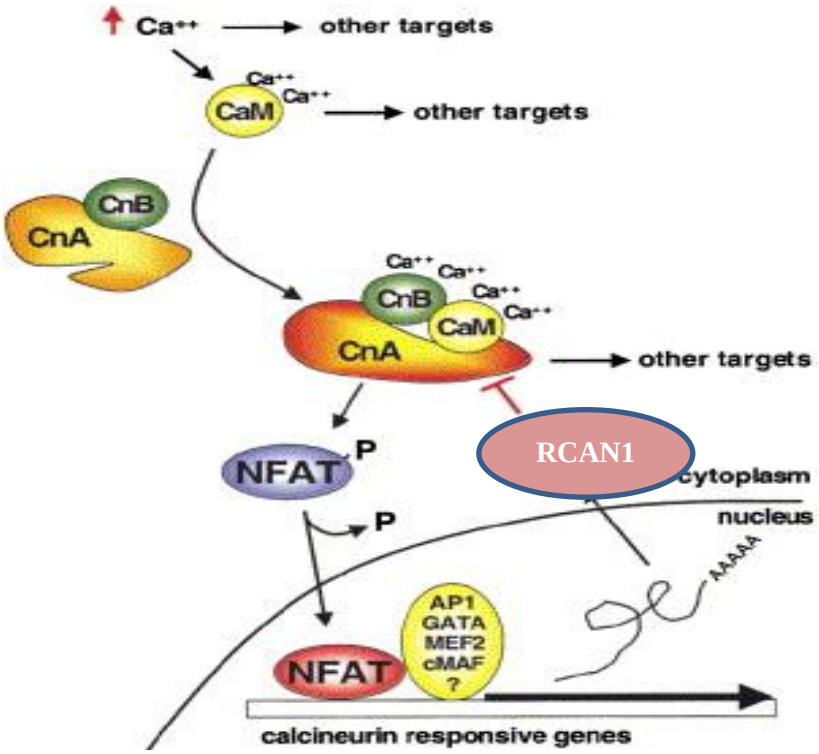

Figure 1-7: The calcineurin/NFAT signalling pathway
The calcineurin heterodimer is activated by the binding of calcium and calmodulin (CaM). The catalytic A subunit (CnA) contains an N-terminal catalytic domain and binding regions for both the regulatory B subunit (CnB) and CaM. The C terminus contains an autoinhibitory domain that folds to occlude the active site when CaM is not bound. Changes in intracellular calcium promote binding of Ca^{2+} both directly to CnB and as a Ca^{2+}/CaM complex to CnA, thereby displacing the autoinhibitory domain. Dephosphorylation of nuclear factor of activated T cells (NFATs) by activated calcineurin promotes its translocation from the cytoplasm to the nucleus, where NFAT binds DNA cooperatively with other transcription factors amongst which are AP1, cMAF, GATA, or MEF2 proteins. NFAT sites in the promoter of the regulator of calcineurin 1 (*RCAN1)* gene make it a calcineurin-responsive gene. When calcineurin is activated, RCAN1 is synthesized and binds directly to calcineurin and inhibits its activity, thereby establishing a negative feedback loop (**(Rothermel et al., 2003b)**.

Calcineurin/NFAT signalling controls the expression of other essential β cell genes such as insulin-receptor substrate 2 (IRS-2) which effects β cell survival ((Demozay et al., 2011). Experiments in rodents (Herold et al., 1993) using calcineurin inhibitors show that inhibiting calcineurin activity reduces insulin biosynthesis and secretion from β cells, resulting in hyperglycaemia and hypoinsulinemia (Lawrence et al., 2001). In addition to that, a mouse model,

βCnb1KO, with a β cell specific calcineurin inactivation of the calcineurin-b1 regulatory subunit has further enhanced the understanding of the calcineurin/NFAT pathway in β-cells (Heit et al., 2006). These mice develop hyperglycemia characterised by hypoinsulinemia. Inhibition of calcineurin resulted in changes in the expression of the MODY genes and impairment in β-cell function. via the NFAT proteins. The role of calcineurin/NFAT in β-cell proliferation was seen in this study with a decrease in β-cell mass and proliferation n these mice due to the inhibition of cyclin D1, cyclin D2 and cyclin-dependent kinase 4 (CDK4).Furthermore, this phenotype was associated with impairment in genes crucial to β cell development and function including Ins1, Ins2, Glut2 and Pdx. Expression of activated NFATc1 rescued this phenotype via increased expression of these cell cycle factors, confirming the role of NFAT in β-cell proliferation and mass. A number of other studies have now shown that the Calcineurin/NFAT pathway regulates insulin secretion (Heit et al., 2006, Rao et al., 1997, Rothermel et al., 2003a).

The inhibition of calcineurin has also been linked to protection against apoptosis via an inhibition of calcineurin-mediated dephosphorylation of pro-apoptotic proteins (Grunnet et al., 2009) Interestingly, transgenic mice overexpressing constitutively active calcineurin in β cells develop hyperglycemia and hypoinsulinemia as a result of decreased β cell mass and insulin secretion (Bernal-Mizrachi et al., 2010). These strongly suggests that Calcineurin-NFAT signalling must be tightly controlled in β cells since lack of activity compromises β cell survival whereas chronic uncontrolled activation leads to a decrease in β cell mass caused by increased apoptosis.

1.5.4 Calcineurin inhibitors

Despite the wide spectrum of physiological roles associated with calcineurin, the list of calcineurin modulators is short. These are broadly classified either as endogenous or synthetic inhibitors of calcineurin. Two synthetic inhibitors are Cyclosporine A (CsA) and tacrolimus (FK506) (Clipstone and Crabtree, 1992). Both these drugs have been extensively used as immunosuppressive agents in post-transplant patients while other topical uses have been suggested in dermatological complications (Al-Daraji et al., 2002, O'Keefe et al., 1992).

In β cells, such calcineurin inhibitors decrease insulin transcription and intracellular insulin content (Lawrence et al., 2002). CsA and FK506 do not directly bind calcineurin themselves but instead, bind to their endogenous partners, cyclophilin A and FK506 binding protein (FKBP), to limit the activity of these proteins (Liu et al., 1991). These immunophilins possess peptidyl-propyl cis-trans isomerase (PPI) activity, important in the folding of ribonuclease. The binding of CsA and FK506 inhibits the PPI activity of immunophilins (Takahashi et al., 1989). However this does not result in its immunosuppressive activity. Immunosuppression by these drugs-immunophilin complexes is via its association with calcineurin. Although there is no direct interaction between these immunophilin-drug complexes with the catalytic sites of calcineurin, they are able to block the binding of calcineurin substrates to the active site (Kissinger et al., 1995, Jin and Harrison, 2002). The drug-immunophilin complex formed is important in inhibiting calcineurin activity as neither the drugs nor are the immunophilins alone able to cause a significant decrease in calcineurin activity (Liu, 2009b). The complexes formed exert a non-competitive inhibition of calcineurin although the NFATc

binding motif on calcineurin is unmasked. This in turn will result in the inhibition of the dephosphorylation capacity of calcineurin for it physiological targets.

A large number of proteins have also been identified as inhibiting calcineurin activity and are classified as endogenous inhibitors of calcineurin. These proteins include Cabin 1, Carabin 1 and Regulator of Calcineurin 1 (RCAN1). The first two are expressed only in higher eukaryotes whereas the RCAN family of protein is conserved from human to yeast (Vega et al., 2003) and inhibits calcineurin in yeast, mouse and human (Kingsbury and Cunningham, 2000). There are at least three RCAN proteins in mammals, including RCAN1, RCAN2 and RCAN3. Interestingly, the expression of RCAN1 is induced by Ca^{2+} through a calcineurin-dependent mechanism. This inhibitory feedback loop may be important to avoid sustained calcineurin activity in situations of prolonged Ca^{2+} stimulus. As RCAN1 is a potent inhibitor of calcineurin *in vitro* and *in vivo* and as it is upregulated during hyperglycemia in β cells (Pieris and Keating unpublished data), the main focus of the current work is on RCAN1 expression in β cells and the mechanisms regulating his expression in conditions of hyperglycemia.

1.6 Regulator of Calcineurin 1 (RCAN1)

1.6.1 Structure and Location

RCAN1 also known as DSCR1, MCIP1, Adapt-78, calcipressin-1 or CALP-1 is located on chromosome 21 at 21q22.12 (Fuentes et al., 1997). The RCAN1 (regulator of Calcineurin-1) gene was first discovered as a chromosome 21 Down Syndrome Critical Region-1 (DSCR1) gene and was named DSCR1 (Fuentes et al., 1995). Later work identified this same gene as being transiently induced during cellular adaptation to oxidative stress, hence named Adapt78 (Crawford et al., 1997,

Fuentes et al., 1995). It has also been known as MCIP1 in many muscle-related studies on RCAN1 function. The gene was finally renamed RCAN1, reflecting its most well-characterised function as a regulator of the serine/threonine phosphatase calcineurin (Davies et al., 2007)

The RCAN1 gene consists of seven exons separated by six introns which are alternatively spliced to produce different mRNA isoforms (Figure 1-8). All the isoforms vary in their 5' exon (exon 1 or exon 4) but contain a similar 3' end comprising of exon 5, 6 and 7. Amongst the four possible transcripts of RCAN1, RCAN1-2 may not be synthesized due to a lack of a start codon and RCAN1-3, comprising of exon 3 which encodes for three amino acids has not been detected in any tissues so far by RT-PCR ((Fuentes et al., 1997, Park et al., 2009). To date, the major isoforms of the proteins are RCAN1-1 with the N-terminal encoded by exon 1 (252 amino acids), and RCAN1-4 (197 amino acids), with the N terminal amino acids encoded by exon 4. RCAN 1-1 protein can be classified as RCAN1-1S encoding a protein of 197 amino acids and a long protein RCAN1-1L with 252 amino acids. This is due to the different initiation sites in the RCAN1-1 transcript with RCAN1-1L promoter being further upstream of exon 1 than RCAN1-1S (Davies et al., 2007). There is a cluster of 15 NFAT binding sites on the RCAN1 gene, between exon 3 and 4, where an internal promoter for RCAN1-4 is located (Yang et al., 2000b, Harris et al., 2005).

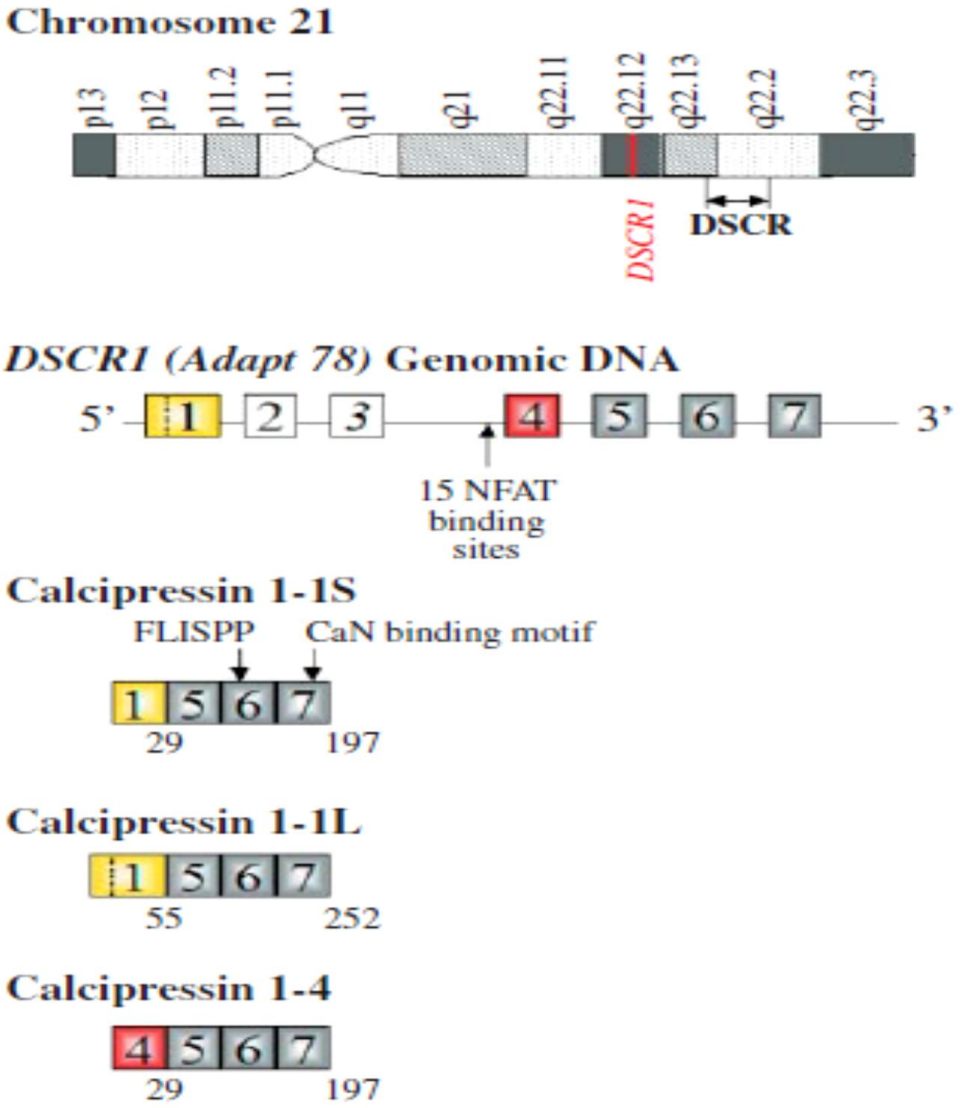

Figure 1-8: Chromosome 21: DSCR1 (Adapt78) is located on chromosome 21 in the region q22.12

The DSCR1 consists of seven exons separated by six introns that are alternatively spliced and vary in their 5' exon, but all contain exons 5,6 and 7. All RCAN1 isoforms share 168 amino acids encoded by exons 5, 6 and 7, as well as the FLISSP sequence found in all RCAN1 family members (Harris et al., 2005)

The induction for both the RCAN1 transcripts is different. The expression of RCAN1-1 is enhanced through the binding of transcription enhancer factor 3 (TEF-3) to the muscle specific-CAT element (M-CAT) site and by glucocorticoids (Liu et al., 2008). The expression of RCAN1-1 has been suggested to be down-regulated by Notch signaling (Mammucari et al., 2005). Constitutive levels of Notch activity are essential in maintaining numerous cellular events such as proliferation, differentiation and apoptosis (Greenwald, 1998, Bigas et al., 1998) via its activation or suppression which is dependent on its interaction with other signaling pathways (Artavanis-Tsakonas et al., 1999). Notch is cleaved upon activation, releasing intracellular Notch which translocates into the nucleus. The intracellular Notch associates with transcriptional factors which regulate the expression of its downstream target genes (Osborne and Miele, 1999, Yanagawa et al., 2000); amongst which is the Hairy/enhancer of split 1 (Hes-1), a repressor type basic helix-loop-helix transcriptional factor (Hisahara et al., 2008). The upstream region of RCAN1-1 promoter contains 4 high-affinities and one low-affinity Hes-1 binding site; in contrast to RCAN1-4 which contains only one low-affinity Hes-1 binding site (Iso et al., 2003). Activated Notch-1 expression has been shown to stably down-regulate the expression of RCAN1-1 via Hes-1 activity. (Mammucari et al., 2005)

On the other hand, the induction of RCAN1-4 expression is via the binding of NFAT (Yang et al., 2000b) and AP-1 (Zhao et al., 2008) to its promoter region or via induction by many other cell or tissue specific factors such as VEGF, β-amyloid fragments, thapsigargin, TNFα and IL-1β (Park et al., 2009). The promoter region of RCAN1-4 contains 15 NFAT binding site. Upon NFAT dephosphorylation and its move to the nucleus, RCAN1-4 expression increases. Interestingly, the increase in RCAN1-4 expression results in the inhibition of calcineurin; hence; down regulating

the expression of RCAN1-4 via a negative-feedback loop. Expression of the RCAN1 isoform, however, is differentially regulated. RCAN1-1 is constitutively expressed whereas expression of RCAN 1-4 is induced by various mitogens and inflammatory cytokines amongst which are ROS (Crawford et al., 1997).

RCAN1-1 and 1-4, contain the 168 amino acids encoded by exons 5, 6 and 7 as well as the conserved central region containing a novel consensus motif Phe-Leu-Ile-Ser-Pro-Pro-Xaa-Ser-Pro-Pro (the FLISPP motif) found in all the RCAN family members (Genesca et al., 2003). This conserved region is important for RCAN1 modulation of calcineurin function as well as in integrating calcineurin signal transduction pathways with other stress-activated signalling networks (Stie and Fox, 2008). This conserved sequence shares homology with the serine proline (SP) boxes found in NFAT protein family members and which is required on NFAT for its optimal dephosphorylation by calcineurin (Im and Rao, 2004) This suggests that the binding of RCAN1 to calcineurin via this sequence may hinder the binding of calcineurin to NFAT. This results in NFAT not being dephosphorylated and unable to relocate to the nucleus. The primary calcineurin binding motif, PKIIQT, of the RCAN1 protein is situated at its C-terminal encoded by exon 7 (Chan et al., 2005). Additional sites for calcineurin interaction have been identified and one is specific to the N-terminal region of RCAN1.4 (Vega et al., 2002).

The RCAN1 gene is inducible not only by oxidative stress but also by calcium and agents that alter calcium distribution (Davies et al., 2001b, Leahy et al., 1999). RCAN1 expression is primarily in the cytoplasm, although it is also found in the nucleus when bound to calcineurin (Leahy and Crawford, 2000). Both RCAN1 isoforms are expressed in a myriad of tissue with RCAN 1-1 most highly expressed in the heart, brain, skeletal muscle and pancreas and RCAN 1-4 in the heart, kidney,

liver and pancreas (Fuentes et al., 1997). RCAN1 is expressed in human pancreatic islets (Su et al., 2004) and RCAN1 expression is also seen in adrenal chromaffin cells (Keating et al., 2008a), neurons (Mitchell et al., 2007b) and pancreatic acinar cells (Gurda et al., 2010).

1.6.2 Interaction between RCAN1 and Calcineurin

Inhibition of calcineurin activity by RCAN1 occurs via physical and functional interaction with calcineurin. As RCAN1-4 expression is induced by the calcineurin/NFAT pathway and it is also able to inhibit calcineurin activity, a negative feedback loop is formed in the interaction between RCAN1-4 and the calcineurin/NFAT pathway (Yang et al., 2000b).

Studies in a mammalian two-hybrid assay and by co-immunoprecipitation of endogenous calcineurin subunit A (CnA) suggested an interaction between RCAN1 and CnA occurring independently of calcineurin activation or Ca^{2+}-calmodulin binding (Fuentes et al., 2000). Instead, RCAN1 preferentially binds to the activated form of calcineurin. A possibility is the binding of calcium/calmodulin and the removal of the autoinhibitory domain from the active site may help the binding of RCAN1 to calcineurin due to the availability of the active site for the binding of RCAN1 (Davies et al., 2007). This suggests that binding of RCAN1 to calcineurin does not disturb the interaction between calcium/calmodulin or the regulatory B subunit (CnB) to the catalytic A subunit of calcineurin. Fuentes et al (2000) used a yeast two-hybrid system to map the binding region of RCAN1 to the linker region between the catalytic domain and the CnB binding domain which encompasses residues 338-352 on CnA (Figure 1-6).

The induction of RCAN1 expression could lead to the inhibition of calcineurin and activation of GSK3β, both of which are key regulators of NFAT. The former is involved in the dephosphorylation of NFAT and the latter in the phosphorylation of NFAT. A unique feature of the RCAN1-calcineurin interaction was suggested by Vega et al (2003) where RCAN1 was identified as a dual regulator of calcineurin as both the overexpression and deletion of RCAN1 impairs the activity of calcineurin. This suggests an intricate regulatory mechanism controlling the activity of calcineurin.

1.6.3 Regulation of RCAN1 via phosphorylation

Post-translational modification of RCAN1 such as phosphorylation has been suggested to have different effect on its calcineurin inhibitory properties either by phosphorylation causing an increase in calcineurin inhibition or phosphorylation removing the inhibitory capabilities of calcineurin by RCAN1 (Liu, 2009a)

Phosphorylation of RCAN1-4 by Mitogen Activated Protein Kinase-1 (MAPK1) at Ser-112 followed by a subsequent phosphorylation at Ser-108 by GSK-3β increases the inhibition of calcineurin by RCAN1-4 (Genesca et al., 2003). This is similar to the observation that phosphorylation of RCAN1 by Protein Kinase A enhances the inhibitory function of RCAN1 on Calcineurin (Kim et al., 2012), although this group did not identify the site on RCAN1 which was phosphorylated.

On the other hand, phosphorylation of RCAN1 by Big MAPK (BMAK1) results in an activation of calcineurin by the dissociation of RCAN1 from calcineurin followed by its ubiquitination by the 14-3-3 protein (Abbasi et al., 2006). Similarly studies done in addressing the interaction between RCAN1 and TAK1(TGF-β-activated kinase 1)-TAB1(TAK-1 binding protein 1)-TAB2 (TAK-1 binding protein

2) suggested a similar removal of calcineurin inhibition by RCAN1 phosphorylation (Liu et al., 2009). However, the effect of calcineurin inhibition by RCAN1 was suggested to be dependent on the level of TAK1 activity. At low TAK-1 activity, RCAN1 is dephosphorylated and inhibits calcineurin activity by binding to the calcineurin catalytic site thus blocking NFAT activation. This group further illustrated that when TAK-1 activity is high, RCAN1 is predominantly phosphorylated and functions to facilitate calcineurin activity (Liu et al., 2009)

Different phosphorylation sites on RCAN1 suggested by various groups could confer different effects on the calcineurin inhibitory function of RCAN1. This was suggested by Shin et al (2011), where phosphorylation of RCAN1 was suggested to cause a differential effect in calcineurin inhibition dependent on the site of phosphorylation. The phosphorylation by TAK-1 at Ser-94 and Ser-136, converts the role of RCAN1 from an inhibitor of calcineurin activity to that of a facilitator. On the other hand, the phosphorylation by MAPK and GSK3β at serine-108 and serine-112 respectively, increases the inhibition of calcineurin by RCAN1. Interestingly, studies by (Hilioti et al., 2004) suggest that the different effect seen could be also be dependent on the concentration of the phosphorylated versus non-phosphorylated form of RCAN1. They suggested that low concentration of phosphorylated RCAN1 stimulates the activity of calcineurin where as a high concentration of either the phosphorylated or non-phosphorylated form causes an inhibition of calcineurin. Shin et al (2011) suggest the role of RCAN1 changes in a dose dependent manner producing a biphasic response; whereby RCAN1 functions as an inhibitor of calcineurin when RCAN1 levels are low but as a facilitator when RCAN1 levels are high. This may be due to the presence of a regulatory switch which regulates RCAN1 in the calcineurin-NFAT signalling network balancing between positive

(sequential phosphorylation of RCAN1) and negative (RCAN1 binding to calcineurin) regulation of calcineurin (Shin et al., 2011)

Hence, the different effect of RCAN1 on its calcineurin inhibitory function could be due to the different sites of phosphorylation, the level of phosphorylation, the amount of RCAN1 in the cell and the role of other signaling and degradation pathways.

1.7 RCAN1 and diseases

.Although RCAN1 has been shown to protect cells during oxidative stress, chronic expression of RCAN1 has been implicated in several disease pathways. RCAN1 first seen as being involved in diseases due to common clinical features associated with Down Syndrome such as immune system defects and Alzheimer's disease. was suggested to be possibly due to the extra copies of resident genes located on Chromosome 21, one of which is RCAN1

The transient expression of RCAN1 confers cells with a transient adaptation to oxidative stress (Crawford et al., 1997). This is important as many human diseases are linked to increased oxidative stress. The induction of RCAN1-1 by glucocorticoids which are increased during biomechanical stress and the predominant expression of this isoform in the brain, suggested a link between RCAN1-1 expression with psychosocial and emotional stress (Ermak et al., 2011). Studies in *Drosophila* have indicated that disruption and overexpression of *nebula* (RCAN1 ortholog) leads to learning and memory deficits which suggests a close link between RCAN1 and neuronal function (Chang and Min, 2005b) Various studies have also shown a role of RCAN1 in apoptosis (Sun et al., 2011), synaptic function (Chang and Min, 2009), stroke (Cho et al., 2008) and long term potentiation (Hoeffer

et al., 2007). In addition to this, RCAN1 is also linked to other brain diseases such as Alzheimer's and Huntington's disease.

The possible role between RCAN1 and Alzheimer was first suggested due to its role as the inhibitor of calcineurin. As an inhibitor of calcineurin and calcineurin representing a large portion of total brain protein (Klee et al., 1988), changes in the expression of RCAN1 would be expected to have a profound effect in the brain. This was further supported by studies showing that calcineurin activity levels decrease in Alzheimer's disease ((Ladner et al., 1996). Alzheimer's disease is characterized by neurodegeneration involving the accumulation of hyperphosphorylated tau protein which results in the formation of neurofibrillary tangles. Two possible mechanisms suggested in bringing about the accumulation of the hyperphosphorylated tau protein is either via RCAN1's inhibition of calcineurin (Ladner et al., 1996) or by the induction of GSK-3β (Ermak et al., 2006). The former would decrease the phosphatase activity of calcineurin; hence the accumulation of a hyperphosphorylated tau protein whereas the latter, would result in an increase in tau phosphorylation. RCAN1 has also been linked to Huntington's disease with its "deficiency" suggested to play a role in the etiology of Huntington disease. In Huntington disease, the expression of RCAN1 is depressed and its overexpression protects against huntingtin toxicity in a cell culture model of Huntington disease toxicity. Furthermore, the increased phosphorylation of huntingtin (via calcineurin inhibition) has been suggested to be the likely mechanism by which RCAN1-1 may be protective against mutant huntingtin (Ermak et al., 2009).

RCAN1 has is essential for valve formation in the developing heart (Lange et al., 2004, Wu et al., 2007) and cardiac hypertrophy as well as skeletal muscle hypertrophy (Yang et al., 2000a, Casas et al., 2001). This is again via its role as

calcineurin inhibitors as active calcineurin leads to hypertrophic growth which is decreased by RCAN1. This is by the prevention of NFAT from translocating to the nucleus and binding to the GATA4 and MEF-2 (myocyte enhancer factor-2) promoters (Vega et al., 2002), thus preventing hypertrophy. RCAN1 and NFAT function and RCAN1 overexpression in mice inhibits melanoma growth and metastasis (Hampton, 2005). RCAN1 has also been suggested to potentially have a role in the treatment of the dermatological condition, psoriasis, as calcineurin inhibitors have been shown to repair lesions and reduce inflammation in affected areas (Jegasothy et al., 1992).

The involvement of RCAN1 in the regulation of several disease pathways via its role as calcineurin inhibitors and the association between calcineurin-NFAT pathway with β-cell function as discussed earlier, suggests a need to understand the role of RCAN1 in β-cells and the mechanisms underlying its expression.

1.8 RCAN1 and β cells

Understanding the role of RCAN1 in β cells is necessary in order to obtain the effect of increased RCAN1 expression on β cell function. RCAN1 regulates exocytosis (Keating et al., 2008b), mitochondrial function (Chang and Min, 2005b) and oxidative stress (Porta et al., 2007b). These functions are relevant to the function of β cells; hence each will be discussed in detail.

1.8.1 RCAN1 and mitochondrial function

Mitochondrial function is important for normal cell function especially for cells with a high energy demand such as β cells. Mitochondrial function is closely linked to β cell function in glucose homeostasis as an increase in the ATP/ADP ratio through mitochondrial oxidative phosphorylation culminates in the release of insulin.

Mitochondria have been implicated as the main source of ROS which is a cause of oxidative stress.

Interestingly, in Drosophila the overexpression of RCAN1 contributes to ROS accumulation in neurons (Chang and Min, 2005a) via its role in the regulation of mitochondrial function. The correct dosage of Nebula, the Drosophila ortholog of RCAN1, was required for the maintenance of mitochondrial function along with the number and size of mitochondria (Chang and Min, 2005a).In this study the presence of *nebula* in mitochondria was confirmed along with the effect of nebula expression on the adenine nucleotide translocator (ANT) activity. Loss-of-function or overexpression of nebula results in a decrease in ANT activity which then disrupts the cellular equilibrium of ADP/ATP, resulting in a block in the electron transport chain and a decrease in mitochondrial ATP synthesis. This then leads to an increase in ROS levels. ROS may subsequently result in increased mitochondrial DNA damage, and changes in the number and size of mitochondria. The negative effect on ATP production is of particular importance in β-cells, where mitochondria is the site of glucose metabolism and ATP production forms the basis of glucose-stimulated insulin secretion (Jensen et al., 2008).

Our laboratory has evaluated the effect of overexpression of RCAN1 ($RCAN1^{ox}$) in mice on β-cell mitochondrial function. Our group observe using electron microscopy that the $RCAN1^{ox}$ islets had smaller size mitochondria and increased ROS production in response to high glucose (Peiris and Keating, unpublished data). As high glucose also induces RCAN1 expression in islets (Peiris and Keating, unpublished data) this effect of RCAN1 on β-cell mitochondria suggests a need to understand the mechanism which regulates RCAN1 expression in conditions of high glucose.

1.8.2 RCAN1 and exocytosis

Exocytosis is important for β-cells to carry out one of its primary function; the release of insulin to correlate with the blood glucose level. A study by Keating et al (2008) using transgenic and knock-out mice identified the role of RCAN1 in the regulation of exocytosis. In the study carried out using adrenal chromaffin cells both the increase and decrease in the expression of RCAN1 negatively affects the number of vesicles undergoing exocytosis. A potential mechanism by which RCAN1 regulates exocytosis could involve the inhibition of calcineurin. The inhibition of calcineurin by RCAN1 may affect calcineurin-dependent dephosphorylation of various endocytotic and exocytotic proteins. Exocytosis protein such as Munc-18 bind with lower affinity in a phosphorylated state resulting in accelerated fusion pore kinetics (Fujita et al., 1996). Similarly, numerous studies have confirmed the role of Munc-18 in the exocytosis of insulin from β-cells (Zhang et al., 2000).

As chromaffin cells and β-cells share similar exocytosis mechanism, the role of RCAN1 in chromaffin cells may be similar to its role in β-cells. The possible role of RCAN1 in insulin secretion by β-cells further suggests the need to understand the mechanisms which could potentially regulate RCAN1 expression in β-cells during hyperglycemia.

The importance of mitochondrial activity in β-cell function and the effect of RCAN1 on exocytosis suggest that RCAN1 could potentially be essential for the maintenance of β-cell function.

1.8.3 RCAN1 and oxidative stress

RCAN1 has been identified as an oxidative stress adaptive factor and confers a protective effect against oxidative stress (Crawford et al., 1997, Ermak et al.,

2002). The expression of RCAN1 is induced by H_2O_2, a major component of ROS in cells (Lee et al., 2009). In a study done with Hamster HA-1 cells, RCAN1 expression increased 8-12 fold as a result of adaptation to either an oxidative stress challenge with H_2O_2 or the calcium ionophore A23187 (Ermak et al., 2002). In the same study, the group found that the overexpression of RCAN1 conferred a protective effect on PC12 cells from H_2O_2 damage. Interestingly a similar trend was seen in the study done by Leahy and Crawford (2000) which implied a protective role by RCAN1 against both oxidative and calcium stress.

The exposure of cells to oxidative stress will cause activation and/or inactivation of various signal transduction proteins such as the activation of MAP kinases JNK, p38 and ERK1/2 (Hannken et al., 2000, Zhang and Jope, 1999) and inactivation of protein tyrosine phosphatases (Meng et al., 2002). RCAN1 has been suggested to be rapidly phosphorylated in response to oxidative stress causing a decrease in RCAN1-associated calcineurin inhibition (Lin et al., 2003). Hence the removal of calcineurin inhibition by RCAN1 during oxidative stress may allow calcineurin activity to be restored (Rusnak and Mertz, 2000). This may be necessary as calcineurin regulates the transcription of various pro-survival genes. In brains of Down syndrome foetuses (Fuentes et al., 2000) and individuals with Alzheimer's disease (Ermak and Davies, 2001), RCAN1 transcripts are overexpressed. In both these neurodegenerative diseases, oxidative stress is identified as a common hallmark of progression towards the loss of neurons (Busciglio and Yankner, 1995).

Work carried out by Pieris (2011), showed a significantly higher level of ROS in $RCAN1^{ox}$ islets compared to wild type islets cultured in high glucose conditions. As ROS causes an increase in oxidative stress in β cells, the direct link

between increase RCAN1 expression and oxidative stress in β cells was thus shown. As hyperglycemia increases oxidative stress via an increase in the production of ROS in β-cells and as RCAN1 expression increases in condition of hyperglycemia in islets, it would be crucial to understand the mechanism causing the upregulation of RCAN1 expression in β-cells and to see if the increase in expression is due to an increase in ROS. This may provide a link between ROS, β-cells dysfunction and induction of RCAN1 by conditions of high glucose.

On a different tangent, as RCAN1 expression has been shown to be linked to oxidative stress; the possibility arises that other biological systems in β cells which may undergo oxidative stress, could potentially cause an effect on RCAN1 expression. One such system which is implicated with β cell function is hypoxia.

1.9 Hypoxia in β-cells and RCAN1

Oxygen is crucial in supporting multicellular life. The increased dependence in the high energy obtained from nutrient oxidation has resulted in the evolution of mechanisms to protect cells from a drop in ambient oxygen tension (hypoxia). Hypoxia can be defined as the lower level of oxygen than that normally experienced by a specific cell (Cantley et al., 2010) resulting in many cell types being equipped with basic molecular response mechanism to adapt to hypoxia. Central to hypoxic response are the hypoxia-inducible factors (HIF). HIF was first identified in connection with binding to the erythropoietin gene enhancer during hypoxia; hence increasing erythropoiesis during systemic hypoxia (Semenza and Wang, 1992) Subsequently HIF has been linked to regulation of systemic metabolism and also glucose metabolism in many cells and tissues amongst which is the pancreatic β cells (Gunton et al., 2005, Cantley et al., 2009)

β cells can be exposed to a variety of situations leading to hypoxic stress. One of these is during the onset of insulin resistance which is first compensated for by an increase in β cell size and number (Weir and Bonner-Weir, 2007). The increase in islet mass causes a possible inadequacy in vascular density; hence oxygen delivery to the islet is compromised resulting in regions of the islet undergoing hypoxia. This is supported by the observation that islets from Zucker diabetic fatty rats show insufficient vascular density relative to obese non-diabetic control animals and an increase in the expression of HIF target gene such as lactate dehydrogenase (Ldha) which is indicative of hypoxia (Li et al., 2006)

Another situation which could lead to β cell hypoxia is during hyperglycemia, as islets consume greater amounts of oxygen when exposed to high glucose. This will lead to a transient lowering of islet oxygen tension and HIF activation if oxygen demand is greater than supply. This is supported by the observation in rat insulinoma cells (INS1) cultured under hyperglycemic conditions show activation of HIF target genes. However, the hypoxia signal transduction pathway may or may not result in an increase in ROS generation. Some models have proposed an increase in ROS production (Chandel et al., 1998, Semenza, 1999) whereas alternative models have proposed a decrease in the production of ROS by nicotinamide adenine nucleoitide phosphate (NADPH) oxidase ((Fandrey et al., 1994, Ehleben et al., 1998)

One of the most relevant situations in which the islet is exposed to severe hypoxic stress is during the transplantation of islet. Pancreatic islets have a dense network of blood vessels which provides β cells with highly oxygenated blood (Moritz et al., 2002). During islet transplantation, the capillary network supplying

blood is destroyed; hence, islet grafts have insufficient blood supply after transplant. In addition to this, there is reduced oxygen tension before adequate revascularization is obtained which may take up to 10 – 24 days to start and up to 6 months for vasculature to resemble a normal *in situ* islet (Carlsson et al., 2001). Nutrient deprivation and lack of oxygen supply are conditions which the islets will have to undergo period. Unsurprisingly newly transplanted islets are under severe hypoxic stress (Li and Mahato, 2011). Further compounding the hypoxic stress is the typical islet transplantation site, the portal vein of the liver which is perfused with a relatively deoxygenated blood compared to the oxygen-rich arterial blood supply of the native pancreatic islets (Cantley et al., 2010). Miao et al (2006) illustrated the activation of HIF correlates with a decrease in graft function.

Hundreds of potential HIF target genes have been identified and most of these genes possess a functional hypoxia response element (HRE) capable of binding HIF. Furthermore, the influences on gene expression by HIF could occur indirectly via an increase in the expression of various activators or repressors and by interacting with other transcription complexes. This is necessary as the induction of a series of hypoxic genes allows the cells to adapt metabolically to low oxygen concentrations (Moritz et al., 2002, Kajimoto and Kaneto, 2004). Such studies have shown that majority of HIF target genes are involved in adapting the cell or tissue to the hypoxic environment.

One such target gene is Carbonic Anhydrase 9 (CA9) which is strongly induced by hypoxia to regulate the microenvironment pH of cells during hypoxia. The hypoxic induction is suggested to be possible through the hypoxic responsive element lying adjacent to the CA9 gene initiation site (Wykoff et al., 2000). In immunostaining work done by this group comparing CA9 expression pattern with

those of other hypoxia marker such as pimonidazole, an overlap of staining pattern was seen supporting CA9 expression in hypoxia regions. A tight regulation of CA9 by hypoxia suggested its usefulness as a hypoxic marker.

The gene of interest in the current work, RCAN1, has been shown in various studies to be involved in stress adaptation; suggesting a possible of RCAN1 in hypoxia. This could be due to a change in glucose uptake caused by a switch from aerobic glucose metabolism to anaerobic glycolysis, or a change in the glucose transporter expression which may increase oxidative stress in the islet. However, the role of RCAN1 in hypoxia could also be indirectly due to the effect of HIF on various other genes in β cells such as those involved in the adaptation of β cells to anaerobic fuel (such as lactate dehydrogenase and aldolase A) or via signalling elements which mediate cross-talk with other pathways (Cantley et al., 2010). Hence, it is crucial to identify if the increase expression of RCAN1 seen during oxidative stress would also be translated to an increase in its expression during β cell hypoxia.

1.10 Insulin producing cell lines

The usage of primary β cells in research is dependent on maintenance of the original characteristics of the cells along with its cellular and hormonal characteristics. The usage of cell line allows for an animal-free opportunity to investigate the physiology or biochemistry of cells, to test the effect of using various drugs and also to synthesise therapeutic proteins which are valuable biologically (Masa Skelin, 2010) One major advantage in using a clonal batch of cells such as a cell line is the consistency and reproducibility of results. However, changes in cell characteristics over a period of continuous growth and the tumorogenic origin of the

cells may result in different protein expression and changes in metabolism compared to primary cells. The genetic manipulation of the cells may also cause defects in native functions and responses such as defective secretory mechanisms and a decrease in glucose responsiveness at normal physiological range as seen in most pancreatic β cell lines.

Three main categories of β cell lines have been identified (Masa Skelin, 2010). The use of cultured β cell lines are important for research purposes, as they provide a "pure cell" population to work with and are ideal for studying islet cell biology and the transcriptional cascade of endocrine differentiation (Limbert et al., 2008). Although these cell lines originate from transformed cells, they have retained most of the normal β cell characteristic. In most of the β cell lines, hormone secretion and glucose responsiveness is higher at early passage numbers but decreases with culturing time (Ulrich et al., 2002)

The first type of β cell line is the insulin secreting β-cell line comprising of the Rat Insulinoma cell line (RIN) and the Insulinoma cell line (INS-1) (Halban et al., 1983, Asfari et al., 1992). The second group comprises of transformed β cell lines and insulin secreting β cell lines derived from transgenic mice amongst which are the transgenic C57BL/6 mouse insulinoma cell line (MIN), the hamster pancreatic β cells (HIT), β hyperplastic islet-derived cells (HC) and β tumor cells (βTC). The third category of β cell lines is the insulin secreting cells of non-islet cell origin, AtT-20 cells. This cell line is obtained via the usage of a viral promoter to direct the expression of human proinsulin cDNA in cells of the anterior pituitary (Newgard., 1994). The AtT-20 cells however have been shown to not respond to

glucose as a secretagogue and, although they express the glucokinase gene, glucokinase activity is extremely low or absent (McClenaghan and Flatt, 1999).

The choice of cell line to be used is dependent on the specific need of the study. In the current study the ability to respond to glucose was necessary in selecting an ideal β cell line to be used. The current study was conducted using the MIN6 cell line which were established from insulinomas obtained by targeted expression of the simian virus 40 T antigen genes in transgenic mice (Miyazaki et al., 1990). MIN6 cells produces insulin and have morphological characteristics of pancreatic β cells. MIN6 cells exhibit GSIS comparable with cultured normal mouse islet cells (Miyazaki et al., 1990) and have been considered an appropriate model for investigating the mechanism of GSIS. The metabolism of glucose and concentration-dependence of insulin secretion in response to glucose from MIN6 cells closely resembles those in normal β cells (Ishihara et al., 1993). In addition to these, MIN6 cells were ideal for this study as their cell-to-cell interaction closely depict the effects in a pancreatic islet with, pancreatic β cell-to- β cell interaction are required for an integrated β cell response to nutrient stimuli (Hauge-Evans et al., 1999). Furthermore, MIN6 cells express GLUT-2 and glucokinase which is important in glucose uptake and glucose sensing mechanisms in β cells and thirdly, this cell line responds to glucose within the physiological range (Miyazaki et al., 1990).

Although MIN6 cells compare well to other β cell lines in their glucose responsiveness after repeated cultures, differing levels of glucose-stimulated insulin secretion (GSIS) ranging from 1.2 to 30-fold have been reported for this MIN6 cells (O'Driscoll et al., 2004)). Hence, in using this cell line it is ideal to use cells in their

early passage number; before passage number 30 (O'Driscoll et al., 2006). Although the MIN6 cells have all the characteristics of pancreatic β cells, the expression of RCAN1 in these cells has not been confirmed. It is therefore crucial to conduct preliminary work confirming the expression of RCAN1 in this cell line before using them in the current study.

1.11 Conclusion

RCAN1 is involved in the regulation of calcineurin activity and calcineurin activity is essential for proper β cell function. RCAN1 may also be important in β cells via regulation of exocytosis, mitochondrial function, control of oxidative stress and ATP production. In studies carried out in our laboratory RCAN1 expression is induced during periods of chronic hyperglycemia in pancreatic islets. However, the mechanism which governs this increase in RCAN1 expression has not been studied however we do know that RCAN1 expression is regulated in other cell by factors such as oxidative stress, Ca^{2+} and calcineurin activity. Additionally, as there are various situations under which β-cells may be exposed to hypoxic stress and as hypoxia is linked to oxidative stress, it would be beneficial to see if hypoxia has any effect on RCAN1 expression also.

1.12 Aims and Significance

The overall aim of this project is to firstly confirm the induction of RCAN1 expression *in vitro* during hyperglycemia in MIN6 β cells and secondly, to identify the mechanisms responsible for the expression of RCAN1 during hyperglycemia. We thirdly identified whether hypoxia can effect RCAN1 expression in MIN6 β cells.

The specific aims of the project are:

1. To investigate the effect of hyperglycemia on RCAN1 expression in the MIN6 cell line.
2. To determine the mechanism of RCAN1 induction by high glucose in MIN6 cells.
3. To investigate the effect of hypoxia on the expression of RCAN1.

2 MATERIALS AND METHODS

2.1 Materials

Reagent	Supplier
Tissue culture	
DMEM	Gibco , Australia
Fetal bovine serum	
L-glutamine	
Penstrep	
dPBS	
Trypin/EDTA	
N-acetyl-cysteine	Sigma, Australia
14.3M β-mercaptoethanol	
FK506 and CyclosporineA	
Nifedipine	
T75 and T25 cell culture flasks	Iwaki
Cell Scrappers for T25 flasks	
Absolute Ethanol	
Trypan Blue Stain	Invitrogen, Australia

Immunohistochemistry	
Antibodies:	
Primary antibody :SIGMA anti-DSCR1 (C-terminal) produced in rabbit	Sigma, Australia
Primary antibody: Guinea pig monoclonal antibody against insulin	Abcam, USA
Secondary antibody : Donkey anti-rabbit IgG labelled with Cy3-conjugated Streptavidin	Jackson ImmunoResearch Laboratories, USA
	Invitrogen, Australia
Nuclear marker stain, 3μM 4',6-diamino-2-phenylindole,dihydrochloride (DAPI)	Invitrogen, Australia
SlowFade® Gold antifade reagent	
Protein assay	
EZQ Protein Quantification	Biorad, USA
Albumin	Sigma Aldrich, Australia
Western blot	
10X Running Buffer, 1XTransfer buffer10X TBS, 1X TBS with tween	Details in Appendix
Antibodies:	
Primary antibody :SIGMA anti-DSCR1 (C-terminal) produced in rabbit	Sigma-Aldrich, Australia

Secondary antibody : Donkey anti Rabbit HRP	Jackson, USA
ECL plus	GE healthcare Buckinghamshire, UK
PCR	
RNA extraction	Qiagen, USA
RNeasy® Mini Kit	Gibco, Austalia
14.3M β-mercaptoethanol	
RNA Quantification: Agilent RNA 6000 Pico Kit	Agilent Technologies, Germany
Reverse transcriptase dNTP 5X First strand buffer RNase-OUT Ribonuclease Inhibitor Random primers reverse transcriptase DTT	Invitrogen
Forward and Reverse Primers	GeneWorks, South Australia
SYBR green	Qiagen, USA

Agarose Gel electrophoresis Agarose	Bioline, Australia

2.2 Cell Culture

2.2.1 Culture of MIN6 cells

MIN6 cells used in the course of this study were a gift from Michael Jackson from the Department of Immunology at Flinders Medical Centre. Cell lines were generally maintained in vented 25cm^2 or 75cm^2 flasks and media was changed every three days. The cells were grown in DMEM containing 10%FBS, 1% Penicillin-Streptomycin, 1% L-glutamine and 5µl/L of β-mercaptoethanol.

Prior to subculture, cells were monitored for any contamination and were only subcultured when the cells were 70%-80% confluent. During routine subculturing or harvesting of MIN6 cells, cells were removed from their flasks by enzymatic detachment. MIN6 flasks were first emptied of culture medium. 2mls of pre warmed (37^{o}C) calcium and magnesium free ($Ca^{2+/}Mg^{2+}$-free) phosphate-buffered saline PBS, was added to flasks and washed back and forth to remove all traces of serum and dead cells and repeated. The wash solution was then removed and pre-warmed (37°C) 0.125% trypsin/EDTA solution in dPBS was then added onto the cells (1ml/25cm^2 flask or 2 ml/75cm^2 flask) and the flasks incubated at 37°C until the cells detached (3 minutes). The Trypsin/EDTA solution was deactivated by addition of an equal volume of DMEM (containing serum). The cell suspension was aspirated gently to avoid from damaging the cells. Following this the

entire solution was transferred to a 15ml sterile tube (Iwaki) and centrifuged at 400*g* for 5 minutes.

The resulting cell pellet was re-suspended in pre-warmed (37°C) DMEM, cells counted and re-seeded at a cell density of 2.3 x 10^5 cells per ml in T-25 flasks. Experiments began a day after seeding. The different treatments the cells were exposed to and the concentration used is as listed in the table below:

Treatments	Concentration used
DMEM media with glucose	5.5mM and 25mM
N-acetyl-cysteine	10mM
FK506 and Cyclosporine A	5µM
Nifedipine	10µM

In hypoxia experiments, flasks were transferred 1 day after seeding to hypoxic or normoxic incubators for the duration of the experiment. The hypoxic experiments were performed within a Hypoxic Glove Box (Coy Laboratory Products) at 1%, 2% or 5% O_2 in a 5% CO_2 humidified environment with N_2 replacing O_2. Before transferring, each flask was washed with dPBS and old media was replaced with fresh media. The control cells were kept in the normoxic incubator at 37°C with 5% CO_2.

2.2.2 Cell Counting

Cell counting and viability determinations were carried out using a trypan-blue dye exclusion technique (Gibco). An aliquot of trypan-blue was added to a sample from a single cell suspension at a ratio of 1:2. Mixture was homogenized by

pipetting and 10µl was applied to the chamber of a haemocytometer over which a glass cover slip had been placed. Trypan-blue only stains dead cells, whereas viable cells appear bright with a halo and remain unstained. Cells in the 16 squares of the four outer corner grids of the chamber were counted using a haemocytometer. An average per corner grid was calculated with the dilution factor being taken into account. Final cell numbers were multiplied by 10^4 to determine the number of cells per ml. Non-viable cells were those which stained blue while viable cells excluded the trypan-blue dye and remain unstained.

2.3 Calcium Imaging

For calcium imaging, cells were seeded on 35mm tissue culture dish and grown as monolayers to allow for single cell imaging (~24 hours). A few hours before imaging, culture medium was replaced with DMEM medium containing 5.5 mM glucose. In preparation for imaging, culture medium was removed and cells were incubated with basal Krebs solution (140mM NaCl, 5mM KCl, 2mM $CaCl_2$, 1mM $MgCl_2$, 5mM D-glucose, 10mM HEPES, pH 7.4) containing Fluo-4 (10µM) for 1 hour at 37°C with 5% CO_2 in plates which were wrapped with foil in order to protect the dye from bleaching.

Plates were then rinsed with Krebs solution and placed on a stage of a Cascade II fluorescent microscope (Photometrix, USA) and allowed to equilibrate for ~3 minutes. Cells were first stimulated for 1 minute with basal Krebs solution, followed by perfusion with Krebs with 30mM glucose (140mM NaCl, 5mM KCl, 2mM $CaCl_2$, 1mM $MgCl_2$, 30mM D-glucose, 10mM HEPES, pH 7.4) for 5 minutes followed by 4 minutes of perfusion with basal Krebs to return cells to the control conditions. This was then followed by another stimulation of cells for 1 minute with

Krebs containing 70mM K^+ (75mM NaCl, 70mM KCl, 2mM $CaCl_2$, 1mM $MgCl_2$, 5mM D-glucose, 10mM HEPES, pH 7.4). Calcium influx was imaged as increases in cell fluorescence on a Cascade II fluorescent microscope (Photometrix USA). Results were analysed on Imaging Workbench software (version 6.0.22) (INDEC Systems, Inc, USA). All experiments were carried out at 34–37°C.

2.4 RNA Extraction and Analysis

2.4.1 Preparation for RNA analysis

RNA is easily degraded by RNAse (ribonuclease) enzymes, which are ubiquitous, thus the following precautions were taken prior to RNA work. All eppendorfs, PCR (polymerase chain reaction) tubes etc. were RNAse-free and pre-autoclaved prior to use as were pipette tips. Disposable nitrile gloves were worn at all times during RNA work to prevent RNA degradation and were changed frequently.

2.4.2 RNA extraction using RNeasy® Mini Kit (Qiagen, Australia)

RNA was extracted using the RNeasy® Mini Kit (Qiagen, Australia) as per the manufacturer's guidelines for the extraction of RNA from animal cells using spin technology. Briefly, 350 µl of RLT buffer (supplement with 0.1% β-mercaptoethanol) was added to the MIN6 cell pellet obtained from 5 x 10^6 cells. This was then passed through a blunt 20g needle followed by the addition of 350µl of 70% ethanol to the homogenised lysate and transferred to an RNeasy spin column placed in a 2 ml collection tube. Sample was centrifuged at 8000g for 15 seconds and the flow through discarded. The column was subsequently washed with RW1 buffer and RPE buffer twice with the flow through being discarded after each spin. To completely dry the spin column, it was placed in a fresh collection tube and

centrifuged at 8000*g* for 1 minute. Finally, RNA was eluted by passing through 35µl of RNase-free water (supplied) through the column by centrifuging it at 8,000rpm for 1 minute. The RNA samples obtained were then quantified and stored at -80˚C until required.

2.4.3 Total RNA Analysis

The Agilent 2100 Bioanalyzer (Agilent Technologies, USA) was used to measure RNA concentration and quality following the manufacturer's instructions.

2.4.3.1 Reagent Preparation

The channels of the chips were filled with Gel-Dye Matrix and the sample wells filled with 1µl each of sample and fluorescent dye. An RNA ladder is loaded into another sample well for size comparison. RNA Gel Matrix was prepared fresh just before use by adding 550 µl of RNA Gel matrix into the top receptacle of the spin filter and spun at 1500*g* for 10 minutes. Gel-Dye Matrix was prepared using 65 µl of the filtered Gel Matrix and 1 µl of RNA Dye Concentrate was added followed by centrifugation for 10 minutes at 13,000*g*. RNA samples were diluted 1:200 with RNase-free water in an RNA-free eppendorf tube. Samples and ladder were heat denatured at 70°C for 2 minutes and then placed on ice.

2.4.3.2 Loading the Gel-Dye Matrix

New chip was taken out of its sealed bag and placed on the Chip Priming Station. Then 9 µl of the Gel-Dye Matrix was pipetted in each of the wells marked 'G'. The Chip Priming Station was closed and 9 µl of the Gel-Dye Matrix was pipetted into each of the other two wells marked G and the remaining Gel-Dye mix was discarded.

2.4.3.2.1 Loading a Primed Chip

5 µl of RNA 6000 Pico Marker was pipetted into each well, including the well-marked "ladder". This was followed by adding 1 µl of heat-denatured RNA samples into each well, one sample per well and in the well-marked as "ladder", 1 µl of ladder was added. Care was taken to fill the unused wells as well. The chip was then vortexed at 2400 rpm for 1 minute.

2.4.3.2.2 Running the Agilent 2100 Bioanalyzer

The chip was then placed onto the Bioanalyzer chip reader. The machine is fully automated and electrophoretically separates the samples by injecting the individual samples contained in the sample wells into a separate chamber. The resulting data was presented as an electropherogram. RNA samples were compared to the RNA Pico ladder allowing the measurement of the RNA concentration in each sample and the assessment of RNA quality.

The electropherogram and the virtual gel obtained were used to determine the quality of the RNA obtained. Samples showing RNA integrity number of more than 8, RNA concentration between 500 and 5000 pg/µl and clear distinct bands on the virtual gel for the ribosomal RNA; 5S, 18S and 28S,; were deemed suitable and used for downstream experiments.

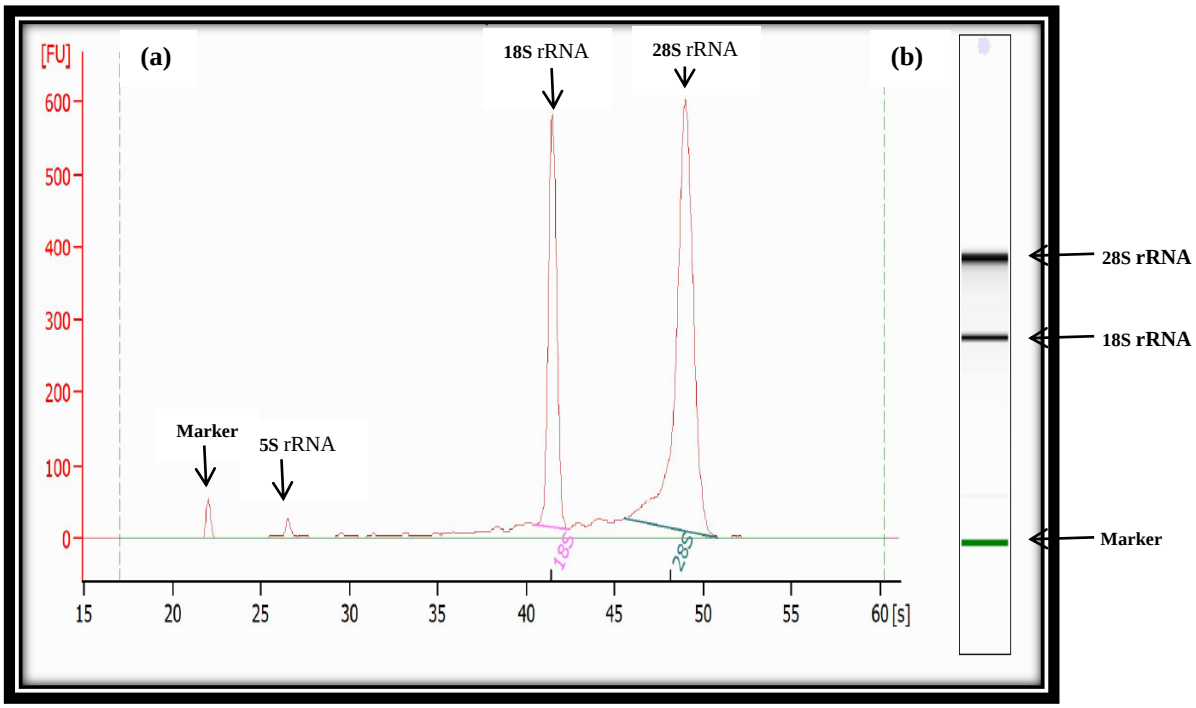

Figure 2-1: Electropherogram (a) and virtual gel (b) of RNA sample
(a) Electropherogram and virtual gel of RNA sample showing four distinct peaks for the marker, 5S rRNA, 18S rRNA and 28S rRNA on the electropherogram and two distinct bands on the virtual for 18S and 28S rRNA.

2.5 cDNA synthesis

cDNA synthesis was carried out using an M-MLV Reverse Transcriptase (M-MLV RT) kit (Invitrogen, Australia) based on the manufacturer's instructions. 1 µl of random hexamer primers (Geneworks, Australia) and 1 µl of 10 mM dNTP mix (Invitrogen, Australia) was added to 10ng of each RNA sample made up to 10µl in R6ase-free water. Samples were incubated at 65°C for 5 min and then placed on ice.

The PCR conditions for cDNA synthesis are shown below.

25 °C – 10 minutes

37 °C – 50 minutes

70 °C – 15 minutes

Following the completion of the reaction, the 20µl reaction was diluted 1 in 10 with RNase-free water and stored at 4°C until required for quantitative real-time PCR reaction.

2.6 Quantitative Real-Time PCR (qRT-PCR)

2.6.1 Real-Time PCR Primer Design

The PrimerQuestTM (Integrated DNA Technologies) program was used in designing the primers for qRT-PCR. The specificity of the designed primers were checked using the nucleotide BLAST function against sequence for mouse. Primers used were resuspended in RNase-free water to give a final concentration of 10 µM prior to usage in the qRT-PCR reactions. The sequences of primers used in the qRT-PCR reactions are described in Appendix 1.

2.6.2 Quantitative Real-Time PCR (qRT-PCR)

Real-time PCR was carried out using the Qiagen Quantitect® SYBR® Green PCR kit (Qiagen, US) and RotorGene 3000 thermocycler (Corbett Life Science, Australia). All real time runs were carried out using 3 µl of diluted cDNA as described above. 18S rRNA was used as the house keeping genes for real time runs and as a basis for normalisation and was compared with the genes of interest to evaluate changes in expression. All real time runs had a negative control of H_2O containing no cDNA template. All samples were run in triplicate to maximize accuracy.

Real Time Master Mix

2 X Quantitect SYBR Green Master Mix	- 12.5 µl
10 mM Forward Primer	- 0.5 µl
10 mM Reverse Primer	- 0.5 µl
RNase and DNase free water	- 8.5 µl
Template cDNA	- 3 µl

The following conditions were used to set the program for the RotorGene 3000:

Hold	- 95 °C (15 minutes)	
Cycling	- 94 °C (15 seconds)	50 cycles
	- 60 °C (20 seconds)	
	- 72 °C (25 seconds)	
Hold	- 72 °C (4 minutes)	
Hold	- 60 °C (1 minute)	
Melt	- 60 °C to 99 °C	

PCR products were stored at 4^{o}C until they were analysed by gel electrophoresis.

2.6.3 Validation of Quantitative Real-Time PCR primers

Real time PCR products were run on Ethidium Bromide-stained 1% agarose gels. 30ml of 10X Tris Borate EDTA (TBE) buffer (890mM Trizma Base, 890mM Boric Acid, 20mM Na_4EDTA) was diluted 1 in 10 to make 1X TBE buffer. Gels were prepared by mixing 65ml of 1X TBE buffer with 0.82g of agarose and melted in a laboratory microwave. Upon cooling, 3.25 µl of Ethidium Bromide (10mg/ml, Sigma) was added to the gel solution and mixed. Ethidium Bromide binds double stranded DNA by intercalating between base pairs and fluoresces when irradiated by UV light.

The gel solution was then poured into a gel tray with a 10-well comb and allowed to set for approximately 20 minutes. The comb was removed gently, followed by addition of 11.8 µl Ethidum Bromide to the remaining TBE. This was then poured into the electrophoresis tank holding the gel ensuring the gel was covered. 2 µl of gel loading solution (Sigma) was mixed with 10 µl of each qRT-PCR product and loaded into each well accompanied by the addition of 4 µl of the 1kB Plus DNA ladder (Invitrogen) into a ladder well. The gel was then allowed to run at 80V for approximately 90 minutes. Gel photographs were taken using the Gene Genius Bio Imaging System (Syngene, Synoptics Group, UK) and GeneSnap software (Syngene, Synoptics Group, UK).

2.6.4 Real Time PCR data analysis

Real-time PCR is a sensitive and reliable method for the quantitation of changes in cellular mRNA level in response to external stimuli. Coupled to the fluorescent dye SYBR Green 1, quantitative real-time PCR was used to evaluate the expression of a number of genes-of-interest throughout this project. Of the three phases of a PCR cycle (exponential phase, linear phase and plateau phase) the exponential phase is the earliest segment in the PCR, in which product increases exponentially as the reagents are not yet limiting. The linear phase is characterised by a linear increase in the product as PCR reagents become limiting. The PCR reaction eventually reaches the plateau phase during the latter cycles, the amount of product remains constant as the reagents have become limiting. Real-time PCR exploits the fact that the quantity of PCR products in the exponential phase is proportional to the quantity of the initial template. This increase in the PCR product is linked to a proportional increase in fluorescence by the ability of SYBR Green to

bind to double stranded DNA exclusively, causing the dye to fluoresce. This increase in fluorescence with time is quantitatively measured and is a sensitive indicator of the starting mRNA concentrations of specific genes.

Real-time PCR data can be quantified both absolutely and relatively. Absolute quantification employs an internal or external calibration curve to derive the input template copy number. Absolute quantification is important in situations where the exact transcript copy number needs to determine. However for most physiological and pathological studies relative quantification is the method of choice and was used for all experiments described here. Relative quantification requires the gene-of-interest to be compared to a house-keeping gene in each sample analysed. The selected house-keeping gene should ideally be constantly transcribed in all cell types and tissues, and its RNA transcription level should not be regulated by internal of external influences, at least no more than the general variation of mRNA synthesis (Radonic, et. al, 2004). Commonly used house-keeping genes include glyceraldehyde 3-phosphate dehydrogenase (GAPDH), β-actin, and 18S and 28S rRNAs. For the experiments in the current study, 18S rRNA was used as the reference gene.

Figure 2.4 shows a typical raw real-time PCR data set where normalised fluorescence has been plotted against cycle number. The genes of interest in this particular example were 18SrRNA (blue) and *Rcan1* (red). Due to the ability of SYBR Green 1 to bind to all double stranded DNA a melt curve analysis is carried out, where the temperature is progressively increased from 60-99°C at the end of the experiment and the change in fluorescence due to the dissociation of double stranded DNA is measured. When most of the fluorescent signal originates from the product

of interest during the amplification procedure, a single melting peak is obtained. In contrast, the amplification of secondary products, primer dimers of non-specific amplicons results in several melting peaks at temperatures lower than the expected melting point for the product of interest.

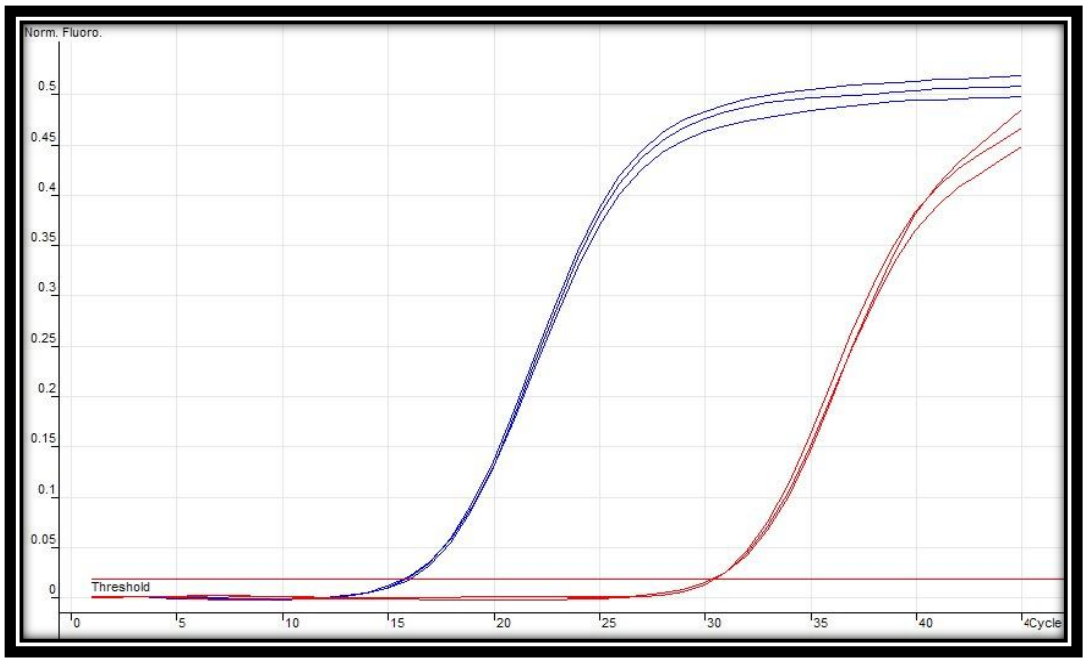

Figure 2-2: Raw real-time PCR fluorescence amplification plot
Raw quantitative real-time PCR data with the fluorescence amplification plot of 18S rRNA (blue) and *RCAN1* (red) with cycle number shows an increase in fluorescence as the cycle number increases.

In order to quantify changes in expression levels of the genes-of-interest the threshold cycle value (Ct) must be defined for each sample. The Ct value is the point at which the amount of amplified target cDNA reaches a fixed fluorescence threshold. The threshold is manually adjusted to the same value for all samples and must be within the exponential phase of the PCR reaction. This was easily distinguishable by plotting the log of fluorescence versus cycle number and setting the threshold in the linear portion of the curve (Figure 2.5).

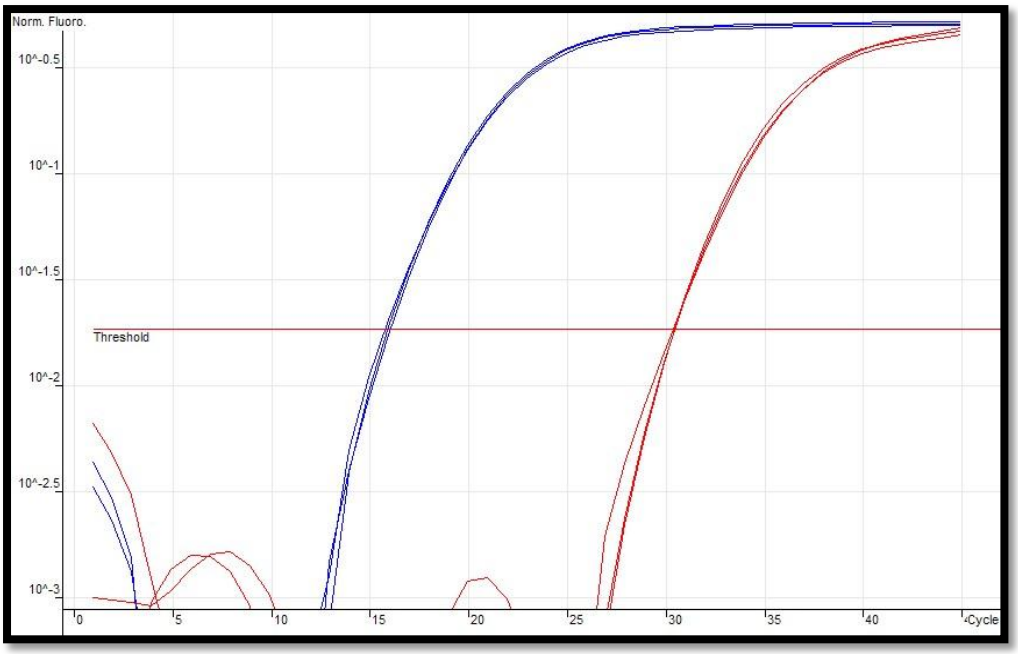

Figure 2-3: Location of the cycle threshold (Ct) with regard to log of normalised florescence versus cycle number.

Once the threshold value was set, the Ct values for each sample were generated by the Rotor-Gene 6 software (Corbett Research, Australia). As the samples were run in triplicate the average Ct value for each reaction set must be calculated. The ΔCt for the gene of interest is then calculated. This is obtained by subtracting the gene-of-interest Ct value from the Ct value of the house-keeping gene 18S rRNA as shown in equation 1.

$$\Delta Ct = Ct_{GOI} - Ct_{18SrRNA} \longrightarrow \qquad (1)$$

These ΔCt values were therefore normalised as each sample had the same starting template of the house-keeping gene. This calculation also eliminated any possible discrepancies due to variations in starting cDNA concentration from different samples and differences in RNA isolation, RNA degradation and efficiency of real-time PCR.

The ΔΔCt value was determined by subtracting the ΔCt of a control sample from that of an experimental sample (eg: MIN6 cells in 5.5mM DMEM vs MIN6 cells in 25mM DMEM) as shown in equation 2.

$$^{\Delta\Delta}Ct = {}^{\Delta}Ct_{\text{control}} - {}^{\Delta}Ct_{\text{experimental}} \longrightarrow \quad \textbf{(2)}$$

A positive $^{\Delta\Delta}Ct$ value was indicative of an increase in expression of the gene-of-interest while a negative $^{\Delta\Delta}Ct$ value indicated a reduction in expression. The $^{\Delta\Delta}Ct$ value obtained could then be converted to a fold difference in gene expression by using equation 3. This is based on the assumption that the PCR product doubles at every cycle and that primer binding to the template is optimal.

$$\text{Fold Increase} = 2^{-\Delta\Delta Ct} \longrightarrow \quad \textbf{(3)}$$

The control expression of each gene was normalised to 1 and the fold change in gene expression in the MIN6 treated and non-treated cells were compared to this.

2.7 Immunohistochemistry

2.7.1 Treatment for cover slips

13mm cover slips (Menzel_Glaser, Germany) were exposed to 0.2M HCL overnight before they were washed with autoclaved distilled water for 5 times. These was then stored in 100% ethanol until it was ready to be used.

2.7.2 Coating of coverslips with PDL and Laminin

Each coverslip was taken out of ethanol and passed through flame individually to dry them. Once dried, the coverslips were dropped into a solution of PDL (10 µg/ml) and this was kept overnight at 4°C or for a minimum of 2 hours. Coverslips were then placed in the wells of a 24-well plate, followed by washing

twice each time with dPBS and dH_20. The coverslips in the plate were then left to air dry in the laminar hood for 30 minutes before they were treated with laminin and allowed to air dry in the hood for 2 hours. Plates with coverslips were then sealed and stored at 4°C until needed if it wasn't being used immediately.

2.7.3 Preparation & Fixation of Cells on Coverslips

Cells were seeded by dropping 100 µl of cell suspension to the middle of each coverslip pre-coated with PDL/Laminin resulting in a density of 1.35×10^4 cells per ml per well. Plates were then incubated at 37°C with 5% CO_2 for 1 hour, after which the wells were topped up with media and plates kept for 24 hours in the incubator.

2.7.4 Treatment of cells for each individual experiment

Cells were then rinsed once with dPBS before the individual treatments were started. The plates were then kept in the incubator at 37°C with 5% CO_2 for 6 days. Plates were observed every day to ensure there was no contamination.

2.7.5 Fixation of cells onto coverslips

Media was removed from each well after 6 days and 500 µL of Zambonis Fixative Solution was added to each well. The plates were then stored at 4°C covered overnight.

2.7.6 Antibody treatment

Coverslips in each well were washed with various solutions as shown in Table 2, after which coverslips were blocked with 10% normal donkey serum ((Sigma-Aldrich, Australia) diluted in antibody diluent for 30 minutes.

Solution	Number of washes
80% ethanol	4 x 5 minutes
100% ethanol	2 x 5 minutes
DMSO	3 x 5 minutes
dPBS	4 x 5 minutes

Next, plates containing coverslips were incubated overnight in a humidified chamber at room temperature with unconjugated primary antibody diluted in antibody diluent at a dilution of 1:25. Control wells were incubated with antibody diluent without any primary antibody. The next day, plates were washed in dPBS for 3 times each for 10 minutes and then incubated with secondary antibody and DAPI, both diluted in antibody diluent at 1:200 and 1:500 dilutions respectively. Plates were then kept in a humidified chamber for a minimum of 2 hours in the dark at Room Temperature. DAPI is a nuclear counterstain that binds to DNA and has an absorption maximum at 358 nm and fluoresces blue at an emission maximum of 461 nm. Coverslips were then washed with dPBS twice for 5 minutes each; taking care at all times not to overexpose the coverslips to light. Coverslips were carefully removed from the wells and excess liquid was allowed to drain out onto a dry blotting paper. A drop per cover slip of anti-fade mounting medium, SlowFade® Gold antifade reagent, was first placed on a microscope slide. Coverslips were then mounted with the cells facing towards the microscope slide and covered with coverslips, after which these were allowed to air dry. Slides were then kept in the dark at 4°C for 3 days before visualising on a BX-50 Fluorescent Microscope (Olympus, Japan).

2.7.7 Antibodies used for Immunohistochemistry

Primary antibody, affinity isolated antibody anti-DSCR1 C-terminal antibody produced in rabbit was used at a dilution of 1:25

- Primary antibody: Guinea pig monoclonal antibody against insulin at a dilution of 1:3200.
- Secondary antibody, Donkey anti-rabbit IgG labelled with Cy3-conjugated Streptavidin was used at a dilution of 1:200.
- Nuclear marker stain, 3µM 4',6-diamino-2-phenylindole,dihydrochloride (DAPI) was used at a dilution of 1:500.

2.8 Western blotting

2.8.1 Preparation of protein samples from MIN6 cells

MIN6 cells from each T75 flask undergoing the respective treatments were lysed in RIPA Buffer (150mM NaCl, 50mM Tris, 0.5% sodium deoxycholate, 1% Triton X-100, 1mM EDTA, pH 7.4) with 1:100 dilution of PMSF. 650µl of the ice-cold RIPA buffer + PMSF were added to each flask and cells were scraped off using a cell scraper (Iwaki). The lysate was then transferred into a cold eppendorf tube and underwent further lysis using an automated tissue-lyser (Qiagen, Australia). Cells were lysed at a frequency of 30 rotations per second for 3 minutes. Samples were then centrifuged at 14,000g for 20 minutes at 4^{o}C. The supernatant was collected and aliquots were prepared for protein quantification and Immunoblotting. The aliquots were then stored at -80°C until required.

2.8.2 Protein Quantification of protein lysates

Protein concentration in each sample was determined using the EZQ Protein quantification kit (Invitrogen, Australia) according to the manufacturer's instructions. RIPA Buffer + PMSF were used to dilute the protein samples at 1:100 dilutions and as blank for the analysis. 1 µl of each sample was placed onto the assay paper in triplicate and destaining was then performed using 10% methanol and 7% acetic acid. The assay was then imaged using the GE Typhoon 9400 Fluorescence Imager (Amersham Biosciences, USA) with excitation and emission wavelengths of 450 nm and 618 nm respectively. Carestream Molecular Imaging software (Carestream Health Inc) was used to generate mass curves and to calculate sample protein concentrations via a standard curve generated from known concentrations of ovalbumin.

2.8.3 Immunoblotting

50 µg of protein extracts were prepared for loading in equal volumes of 20 µl with 1x sample buffer (5µl) containing mercaptoethanol (50µl) and lamelli buffer (950µl). Samples were incubated at 100°C for 3 min, cooled down to room temperature, spun down shortly. All samples were then run on 4-20% Tris-HCL Criterion Stain Free gels using a Criterion electrophoresis cell (Bio-Rad, Australia) and loaded directly onto Criterion TGX-stain free precast gels (Bio-Rad, USA). 5µl of BioRad Precision Plus Dual-Colour Marker was also loaded which did not contain the loading buffer and was not heated.

Gel was allowed to run for 21 minutes at a steady current of 200V in a 1X Running Buffer (diluted from 20x Running Buffer – Appendix 3) after which the gel was viewed using the Criterion Stain Free Gel Imaging System (Bio-Rad, USA) which comprises of an imaging system with a transilluminator for UV activation and visualisation of protein samples that have been separated. Gels were then transferred to a positively charged PVDF membrane (Millipore, USA) using a Trans-Blot Semi-Dry Electrophoretic Transfer Cell (BioRad, Australia) for 30 minutes using the Standard Molecular Weight Transfer program. After this, the blot was viewed using the Stain Free Imaging System and Image Lab software to confirm the transfer of proteins from the gel to the blot was successful. The blots were then probed and processed using a Millipore SNAPi.d Western blotting system according to the manufacturer's instructions. The antibodies used and their working concentrations are shown below:

Antibody used	Antibody concentration
Primary antibody SIGMA anti-DSCR1 (C-terminal) produced in rabbit	1:1000
Secondary antibody (Jackson donkey anti Rabbit HRP)	1:10000

Protein bands were developed using the Enhanced Chemiluminescence Kit (ECL) (Amersham, RPN2109) according to the manufacturer's instructions. The blot was removed and kept in the dark for all subsequent steps. A sheet of thick transparency paper was flattened over a smooth surface such as a glass plate.

The membrane was placed on the glass surface with the protein side facing up. 1ml each of ECL detection reagent 1 and ECL detection reagent 2 were mixed in a tube which was wrapped with a foil to protect from light. This solution was then dispensed over the membrane ensuring the membrane was fully covered and then kept covered in the dark. The solution was removed from the membrane after 5 minutes by allowing it to drip off the membrane and washing the membrane in a TBS-T washing solution one time. Membrane was visualised on a Fujifilm LAS4000 Luminescent Image Analyser (Fujifilm, Australia) and recorded using FujiFilm Global MultiGauge® electrophoretic software while densitometry analysis was performed using Carestream Molecular Imaging Software (Carestream Health Inc., USA)

2.9 Statistical Analysis

For individual comparisons, statistical analysis of data was carried out using the t-test: two sample assuming equal variances. For multiple comparisons, statistical analysis was performed using an ANOVA followed by Bonferroni's multiple comparison tests. All data are expressed as mean ± SEM. *P*-values less than 0.05 were considered significant

3 RESULTS

3.1 RCAN1 is expressed in MIN6 cells

This project was carried out to investigate the mechanisms regulating RCAN1 expression in MIN6 cells. Hence, it was necessary to first determine the expression of RCAN1 in this cell line. This was done by staining the MIN6 cells with anti-RCAN1 and anti-insulin antibodies and the nuclear marker DAPI. The results confirmed the presence of RCAN1 in insulin producing MIN6 β-cells (Figure 3-1). The expression of RCAN1 is primarily in the cytosol with very little expression seen in the nucleus.

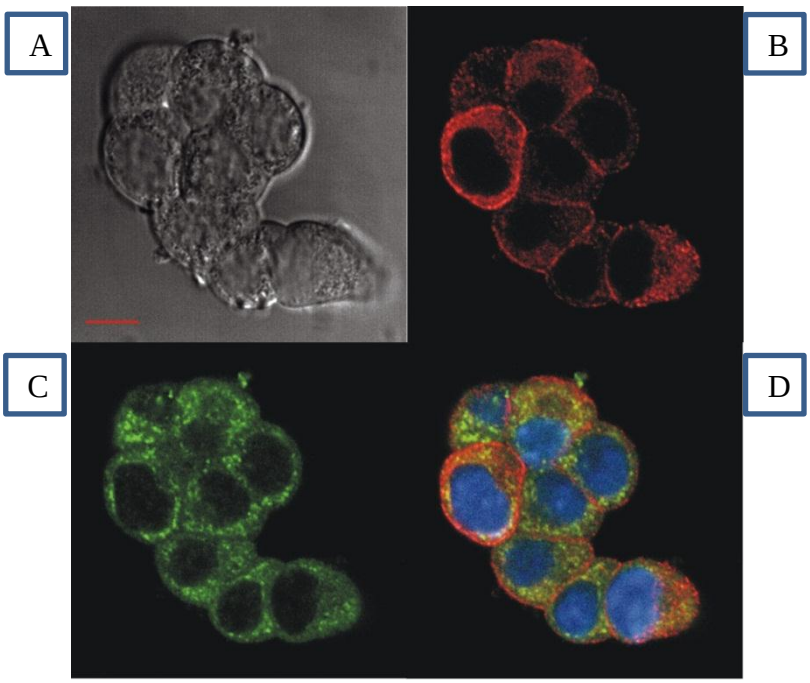

Figure 3-1: RCAN1 is expressed in insulin producing Min6 β-cells.
A: bright field image; B; insulin indicated by the red staining; C: RCAN1 indicated by green staining and D; merged image. Scale bar: 0.20µm

3.2 MIN6 cells are responsive to glucose

Pancreatic β-cells secrete insulin in response to increases in extracellular glucose concentrations. This occurs by the metabolism of glucose and a resulting increase in the ATP/ADP ratio in the cell, subsequent depolarization of the cell membrane, influx of Ca^{2+} through voltage-dependent calcium channels and triggering of vesicle fusion. In the current work, it was necessary to confirm the responsiveness of MIN6 cells to glucose as the previous work with expression of RCAN1 was carried out showing glucose-induction of RCAN1 in pancreatic islets. One of the methods to determine glucose responsiveness in MIN6 cells is via the measurement of Ca^{2+} during exposure to high concentrations of glucose. In the current work this was done using Calcium Imaging by loading cells with the fluorescence Ca^{2+} indicator, Fluo-4 (Section 2.3)

In response to Krebs + 30mM glucose, the fluorescence signal emitted by the cell steadily increases in a sequential manner (Figure 3.2). The fluorescence Ca^{2+} indicator, Fluo-4 dye binds to intracellular Ca^{2+} and fluoresces; hence, the fluorescence signal correlates to the amount of intracellular Ca^{2+}. As soon as the stimulation with Krebs with glucose was stopped, the fluorescence signal emitted returned to basal levels. The cells were then challenged with a Krebs solution with high potassium concentration (Krebs + 75mM K^{+}). Again, an increase in calcium signal was seen. Cells were deemed to be glucose responsive or non-responsive based on the trace generated as shown in :. Cells which were glucose responsive showed increase in fluorescence signal after perfusion with Krebs + 30mM glucose, whereas cells which were not glucose responsive did not show any response to this.

Out of the 43 MIN6 cells tested for glucose responsiveness, 43 (88%) of these cells were identified as glucose responsive (Table 3.1). It was interesting to note that all cells which were glucose responsive were responsive to potassium and all cells that were unresponsive to glucose were also unresponsive to high K^+ and vice versa. Non-glucose responsive cells may have been either unhealthy or dead. 100% of healthy cells were therefore glucose responsive. Hence, this cell line was ideal for use in the following experiments.

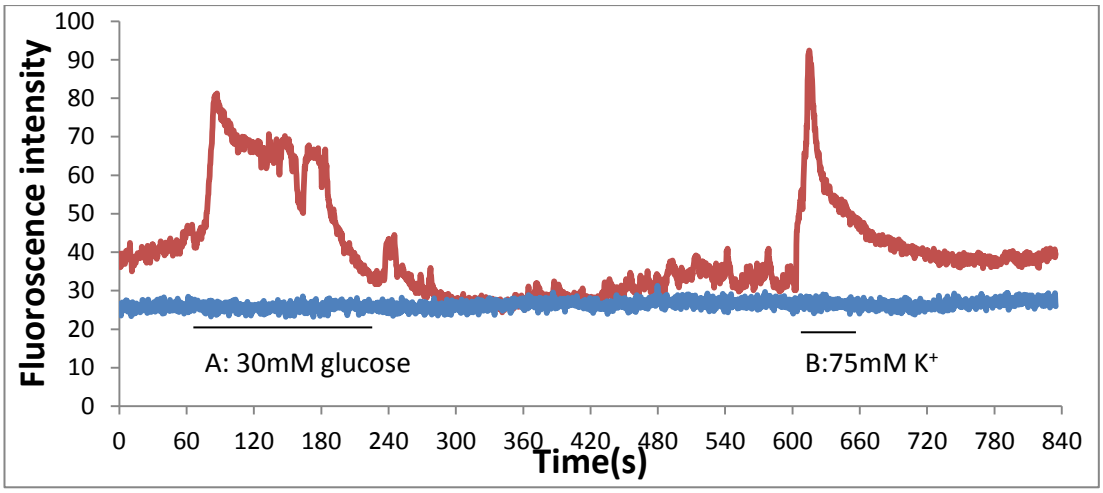

Figure 3-2: Ca^{2+} response to stimulation with high glucose and high K^+ in MIN6 cells.
Cells first perfused with basal Krebs were perfused with Krebs + 30mM glucose at 60 seconds for 3 minutes; followed by perfussion with basal Krebs. At 600 seconds, cells were perfused with Krebs + 75mM K^+ for 1 minute. Calcium influx into the cell was reflected by an increase in cell fluorescence observed on a Cascade II fluorescent microscope (Photometrix USA) and results were analysed on Imaging Workbench software (version 6.0.22) (INDEC Systems, Inc, USA).

	Responsive cells	Non-responsive cells	Responsive: 43 Non-responsive: 6 Percentage responsiveness: 89%
Plate 1	12	2	
Plate 2	9	3	
Plate 3	22	1	

Table 3-1: Number of MIN6 cells identified as glucose responsive and non-responsive.
Calcium trace in Figure 3-2 was used to classify cells as glucose responsive or non-responsive after perfusion with Krebs+ 30mM glucose followed by perfussion with basal Krebs and perfussion with Krebs + 75mM K^+ (*n= 43*).

3.3 High glucose increases the expression of RCAN1 in MIN6 cells

3.3.1 Quantification of RNA using Real-Time PCR

RCAN1 expression is increased in mouse pancreatic islets in response to chronic hyperglycemia in work carried out in our laboratory (Pieris & Keating, unpublished data). Therefore, it was necessary to determine if RCAN1's expression is similarly increased during exposure to conditions of high glucose (25mM) in MIN6 cells.

Therefore, we investigated whether exposure of MIN6 β-cells to hyperglycemia up- regulates RCAN1 expression. The primers used were specific to exon 1 to identify RCAN1-1, to exon 4 to identify RCAN1-4 and to exon 7, to detect the presence of both the transcripts, RCAN1-1 and RCAN1-4. The last group was designated RCAN1 NS (non-specific) or total RCAN1 in MIN6 β-cells. Primers were designed as described in Section 2.3 and primer sequences are shown in Appendix 1.

3.3.1.1 Assessment of RNA Quality

The electropherogram and the virtual gel obtained from Agilent 2100 Bioanalyzer were used to determine the quality of the RNA obtained. Samples showing RNA integrity number (RIN) of more than 8, concentrations greater than 1000 pg/µl and clear distinct bands on the virtual gel for the ribosomal RNA; 5S, 18S and 28S were deemed suitable and used for RT-PCR (Figure 2.1)

3.3.1.2 Confirmation of Primer Amplification Specificity

The amplification products obtained from each of the primer pairs used in real time PCR were checked for specificity of amplification by performing an agarose gel electrophoresis and a melt curve analysis. Results obtained from the gel showed that the product from each primer set comprised a single band of DNA and all bands were of expected size (Figure 3-3). The melt curve analysis showed a single peak for each primer set used (Figure 3-4). Each single peak is specific to one primer pair. Hence, obtaining a single peak for a specific primer is important in ensuring the products amplified are specific and that there are no primer-dimers. Primer-dimers are the ability of the primers to bind to each other forming double stranded DNA which would then be bound to by SYBR green. These two observations confirm we are amplifying a single gene product in these experiments.

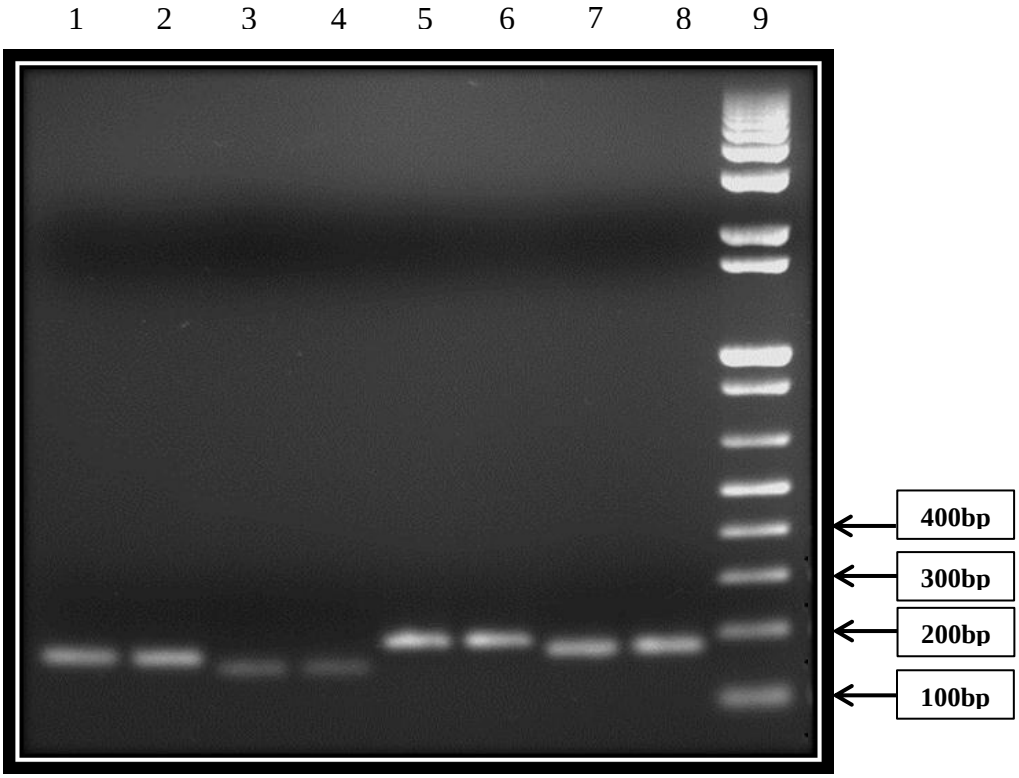

Figure 3-3: Agarose gel showing real time PCR products obtained in control and treated samples.

The agarose gel shows a single band of the expected band size for each primer set used in the study. The primers were loaded into each lane according to the order : Lane 1 and 2: RCAN1-1; Lane 3 and 4: RCAN 1-4; Lane 5 and 6: RCAN1 NS; Lane 7 and 8: CA9 and Lane 9: 1kb plus ladder. The expected sizes of each band is 169bp for RCAN1-1; 154bp for RCAN1-4, 196bp for RCAN1-NS an d 180bp for CA9

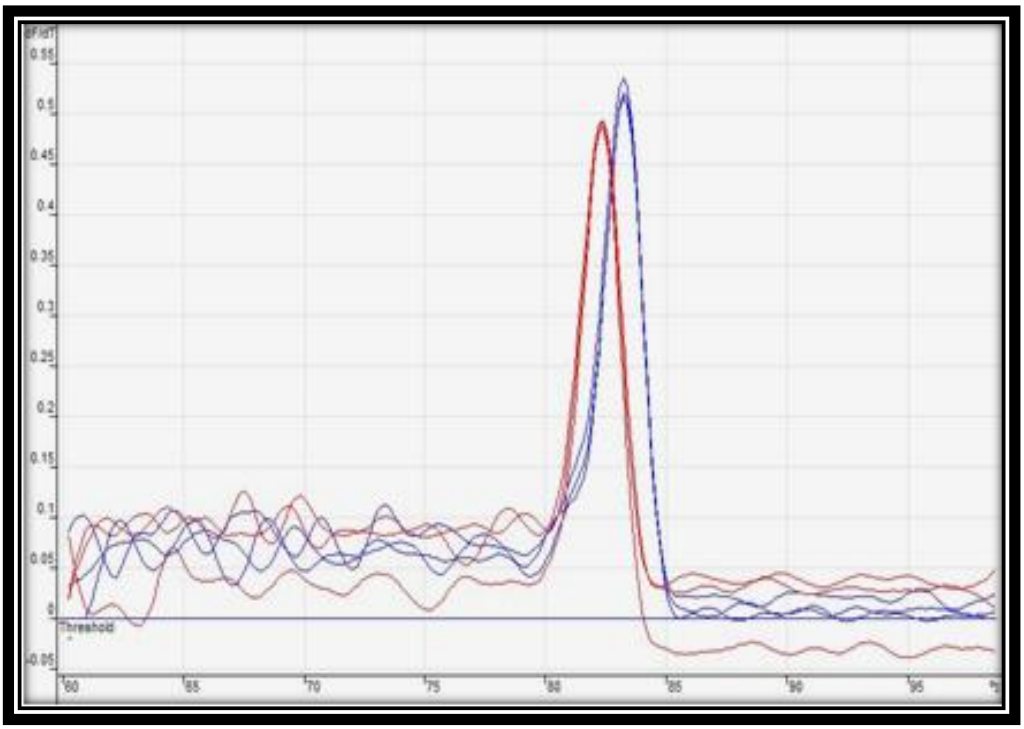

Figure 3-4: A representative melt curve of RCAN1-NS (red) and 18S RNA (blue).
The melting curve plot showing the specificity of the 18srRNA product (blue) and RCAN1 product (red) due to the single peak seen for each primer's product obtained from a triplicate sample.

3.4 Glucose-induced expression of RCAN1

3.4.1 Glucose-induced increase expression of RCAN1 seen via RT-PCR

Based on the time and concentrations used in the study with primary mouse islets, MIN6 cells were exposed to either 5.5mM or 25mM glucose for 6 days and the expression of RCAN1, RCAN1-1 and RCAN1-4 measured by real-time PCR. Expression was first normalised to that of the endogenous 18S ribosomal RNA housekeeping gene. Changes in the expression of RCAN1-1, RCAN1-4 and RCAN1-NS expression in MIN6 cells grown in 25mM glucose were calculated relative to that seen in cells grown in 5.5mM glucose.

No significant change in the expression of RCAN 1-1 mRNA was observed in MIN6 cells in high glucose. However, the expression of RCAN1-4 and RCAN1-

NS in treated MIN6 cells showed a significant increase of ~3.5 ($p<0.001$) and ~1.7 ($p<0.05$) fold, respectively, when compared to MIN6 cells exposed to 5.5mM glucose for 6 days (Figure 3-5). In the current study, only RCAN1-4 transcript was seen to be induced in MIN6 cells by high glucose. This is different to that observed in the study with pancreatic islets where the expressions of both the RCAN1-1 and RCAN1-4 transcripts were seen to be significantly increased in conditions of high glucose.

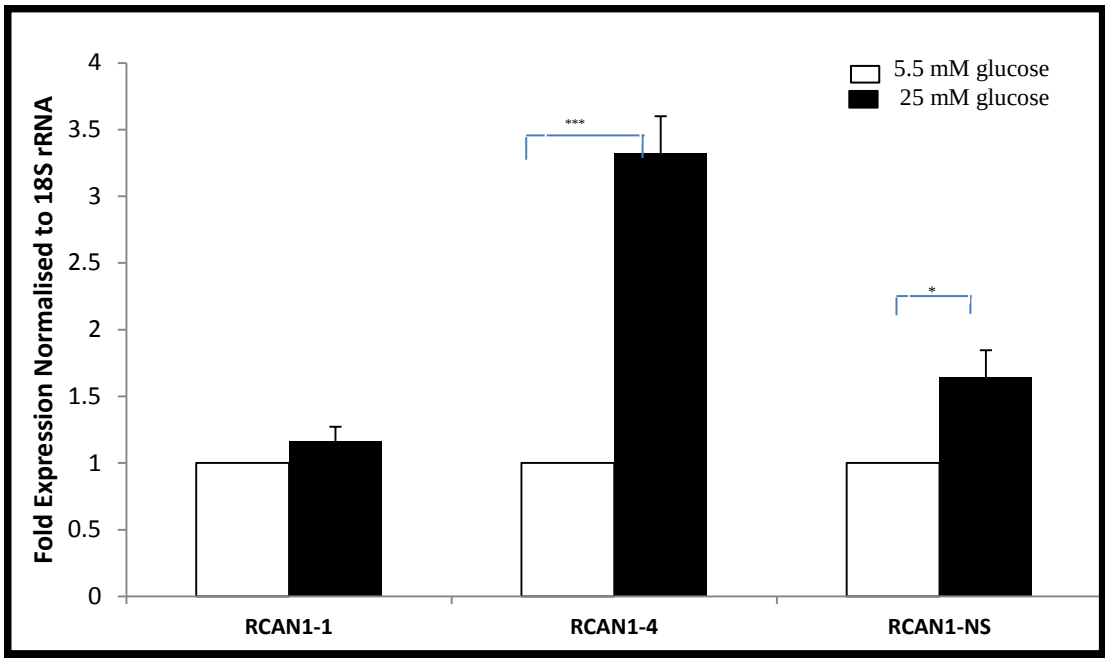

Figure 3-5: Increased expression of RCAN1-4 transcript in 5.5mM glucose compared to 25mM glucose after 6 days.
RCAN1 mRNA levels in MIN6 cells exposed to either 5.5mM (light bars) or 25mM glucose (dark bars). Changes in the expression of RCAN1-1, RCAN1-4 and RCAN1-NS expression in MIN6 cells grown in 25mM glucose were calculated relative to that seen in cells grown in5.5mM glucose. (n=4,* $p<0.05$ and ***, $p< 0.001$). Data shown is representative of four independent experiments and shown as mean ± SEM.

3.4.2 Glucose-induced expression of RCAN1 protein observed by Immunohistochemistry.

Having seen difference in the glucose-induced expression of RCAN1 at the RNA level, the next step was to see if this was translated at the protein level. Immunohistochemistry (Section 2.7.) was carried out to provide a preliminary qualitative indication of the expression of RCAN1 protein with high glucose

The results confirmed the expression of RCAN1 protein in MIN6 cells as shown in Section 3.1. They did not however show any clear increase in fluorescence intensity qualitatively in MIN6 cells exposed to high glucose (Figure 3.7). This result could be due to the fact that the RCAN1 antibody used in the staining of the samples identifies total RCAN1 in the MIN6 cells and cannot differentiate between the RCAN1-1 and RCAN1-4 transcripts. Hence, the staining intensity between the control and the treated samples may not show any significant difference.

Therefore, Western Blotting was carried out to done to identify the protein expression of RCAN1-1 and RCAN1-4 transcripts in conditions of high glucose. This technique not only allows the analysis of each transcript individually but also provides a quantitative analysis.

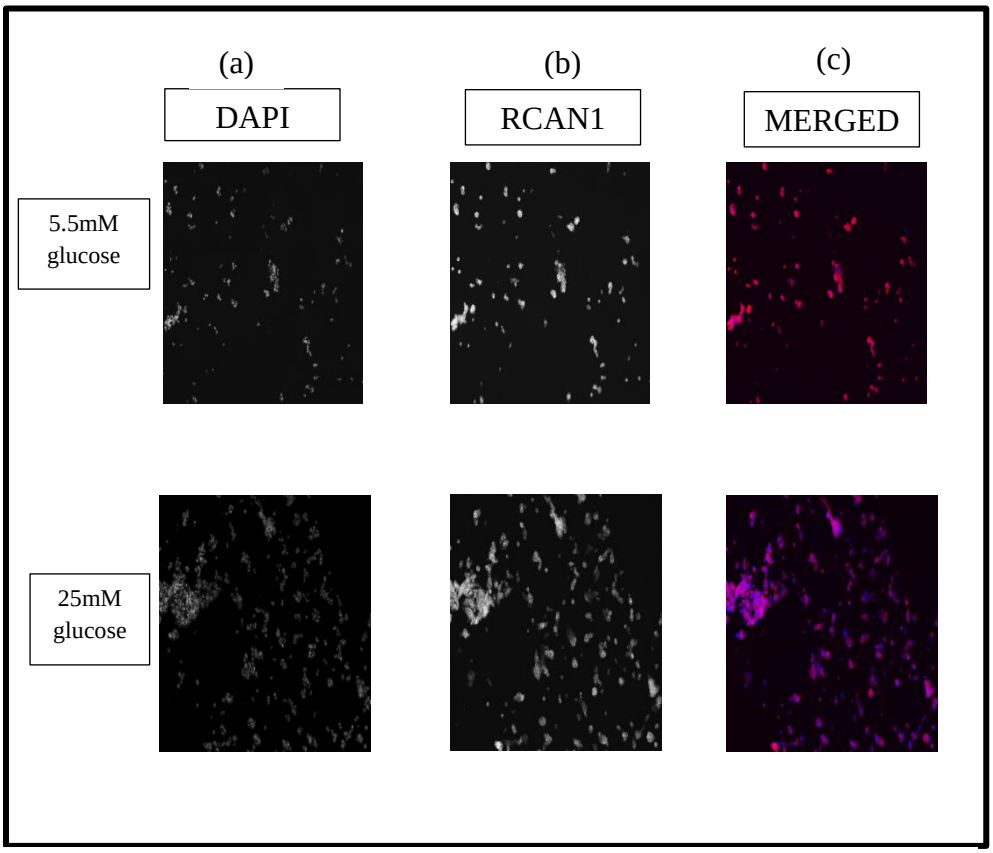

Figure 3-6: Staining of MIN6 cells cultured for 6 days in either 5.5mM glucose or 25mM glucose

MIN6 cells were cultured for 6 days in either 5.5mM glucose or 25mM glucose and were then labelled with antibodies for RCAN1 (red) and stained with DAPI (blue) as a nuclear marker. Panel (a) shows labelling for nuclear marker DAPI, (b) shows staining for RCAN1 protein and (c) shows the merged image of both (a) and (b) with RCAN1 protein seen as pink. MIN6 cells from both the group; control and treated, did not show any difference in staining intensity. (Magnification = 10X).

3.4.3 Glucose-induced increase in RCAN1 protein expression detected via Western Blotting

Western Blotting was done in order to identify the RCAN1 protein from each transcript present in MIN6 cells and to observe any glucose-induced differences at the protein level of expression as discussed in Section 2.8. The usage of TGX Stain Free Blot allowed the monitoring of the progress of Western Blotting through the stages of protein separation, protein transfer and finally probing and detection compared to the usage of other pre-cast gels which only allow the user to see the outcome of the technique after probing and detection are carried out.

The gel is first imaged after the samples were electrophoretically separated to ensure the protein obtained from each sample was not degraded (Figure 3-7). This was then followed by imaging the blot to ensure the transfer has been carried out successfully. Lastly, the gel was imaged after transfer was completed to ensure that the proteins of interest in the expected size range have been successfully transferred onto the blot. The proteins left behind on the gel are from the larger molecular weight category which transfers poorly.

The image of the blot after transfer which shows the total protein present in each lane is first used to obtain a normalising factor for each lane by comparing the total protein band intensity in each lane relative to a specific lane determine randomly. By doing this any error in loading of the protein onto the gel can be can be eliminated. The normalising factor for each lane is then used to obtain the relative optical density of the band of interest in each of the samples. The results were then expressed relative to those seen in the MIN6 cel cells grown in the presence of 5.5mM glucose.

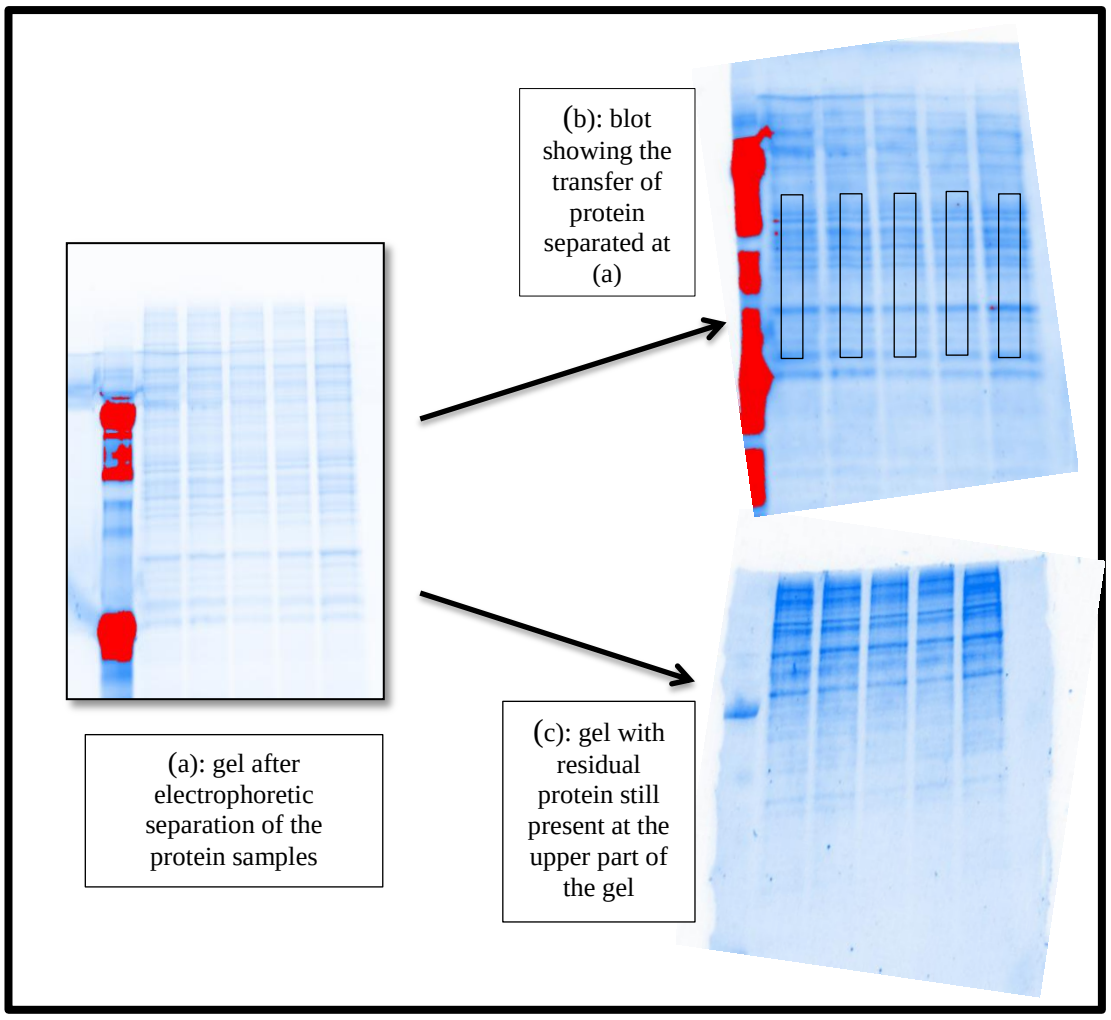

Figure 3-7: Image of the TGX Stain Free Gel before transfer, after transfer and an image of the blot obtained.
The images obtained from the Stain Free Imaging System and Image Lab software showing (a) Image of the gel before transfer showing the separation of the protein electrophoretically without any sample degradation; (b) image of the blot obtained immediately after transfer showing the successful transfer of separated proteins from the gel onto the blot and (c) image of the gel showing residual protein left which were not transferred to the blot being proteins of high molecular weight. The box shown in panel (b), indicates the identical sized box drawn to obtain the normalising factor for the total protein loaded into each lane

Western Blot analysis showed the two RCAN1 proteins at the desired band size (Figure 3-8). Protein samples obtained from MIN6 cells cultured in 5.5mM glucose or 25mM glucose showed two bands, one for RCAN1-1 at 35-36kDa and the other for RCAN1-4 at approximately 27-29kDa. It was also seen that the RCAN1-4 isoform comprises of a doublet band which was clearly observed in the samples obtained from 25mM glucose; whereas the samples in 5.5mM glucose showed a faint single band.

The band intensity in the two samples, however, was different for each of the RCAN1 isomers. The bands for RCAN1-1 and RCAN1-4 obtained in the protein samples from MIN6 cells grown in 25mM glucose was clearly more intense than that obtained from the samples grown at 5.5mM glucose.

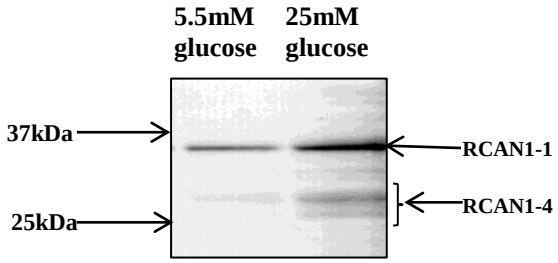

Figure 3-8: Western Blot of protein samples from MIN6 cells cultured in either 5.5mM glucose or 25mM glucose.
50µg of protein from MIN6 cells in 5.5mM glucose and 25mM glucose samples was separated on TGX Stain Free Gel and subjected to probing using anti-DSCR1 C-terminal antibody (primary antibody). RCAN1-1 band is of 35-36kDa and RCAN1-4 27-29kDa in size. The RCAN1-4 band is seen as a doublet

The intensity of each band was normalised to the total protein content, followed by the expression of this relative to the results seen in the control samples (Figure 3-9). Results showed that there was a significantly greater amount of RCAN1-1 ($p<0.05$) and RCAN1-4 ($p<0.01$) protein in MIN6 cells cultured in 25mM glucose with a ~2 fold increase in RCAN1-1 and ~4.5 fold increase for RCAN1-4.

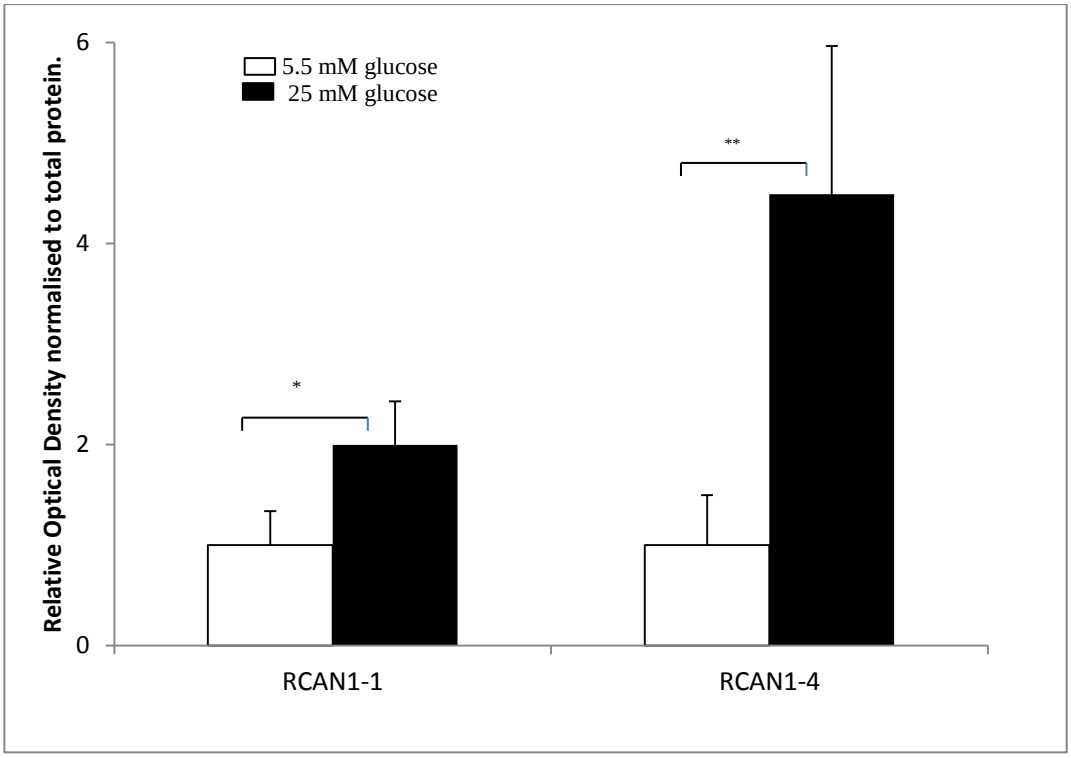

Figure 3-9: Quantification of RCAN1-1 and RCAN1-4 protein in MIN6 cells cultured for 6 days in 5.5mM or 25mM glucose

Relative band intensity of isoform 1 and 4 expression in MIN6 cells cultured in 5.5mM glucose or 25mM glucose. Results are representative of five experiments and average results are shown as mean ± SEM (n=5, *,$p<0.05$ and **,$p<0.01$

The expression of both RCAN1-1 and RCAN1-4 protein were also compared in 5.5mM glucose. The results showed a significant difference between the RCAN1-1 and RCAN1-4 protein. The RCAN1-1 protein was detected as the higher abundant protein by ~ 4 times (Figure 3-10).

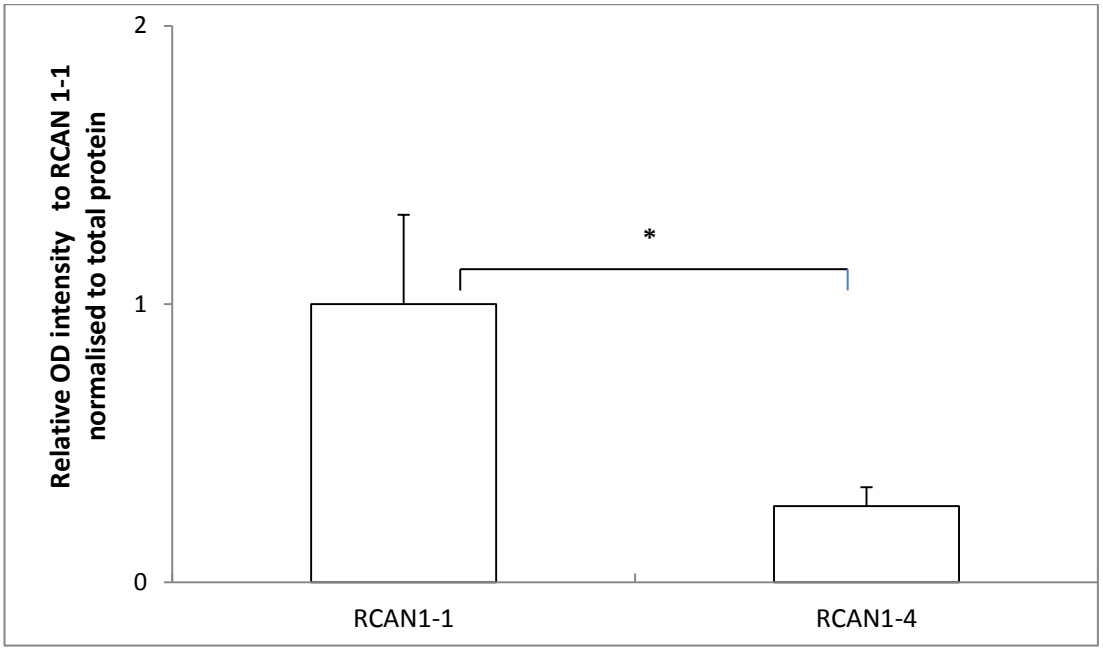

Figure 3-10: Comparison of RCAN1-1 and RCAN1-4 protein in MIN6 cells cultured for 6 days in 5.5mM glucose.
Relative band intensity of the two RCAN1 isoform, RCAN1-1 and RCAN1-4 protein in MIN6 cells cultured for 6 days in 5.5mM glucose. Results are representative of five experiments and results are shown as mean ± SED (n=5, *,$p<0.05$)

3.5 Mechanisms underlying the glucose-induced expression of RCAN1 in MIN6 cells.

The next part of our work was to understand the possible mechanisms underlying the glucose-induced increase in RCAN1 expression. Glucose induces oxidative stress in β cells (Ihara et al., 1999) and hyperglycemia is associated with ROS generation by β-cells (Laybutt et al., 2002, Tanaka et al., 1999, Mohanty et al., 2000). On the other hand, RCAN1 expression has been associated with oxidative stress in neuronal cells (Porta et al., 2007b). Taken together these observations suggested a possibility that ROS may have a role in the glucose-induced expression of RCAN1. In addition to this, the role of RCAN1 as a regulator of calcineurin also suggests a link between RCAN1 and the calcineurin/NFAT pathway in β cells. This suggests a need to dissect the calcineurin/NFAT pathway to understand its role in glucose-induced expression of RCAN1. Hence, three main factors were identified to potentially be involved in the mechanism behind the glucose-induced expression of RCAN1 in MIN6 cells. The first two were involved in the calcineurin/NFAT pathway; entry of calcium and calcineurin and the third was the glucose-induced increase in ROS. The role of each factor was evaluated at both gene and protein level.

3.5.1 Effect of each treatment on the glucose-induced expression of RCAN1 at the gene level

3.5.1.1 Oxidative stress underlies glucose-induced expression of RCAN1

We tested whether the increase in RCAN1 expression in conditions of high glucose could be reversed with antioxidant N-acetylcysteine (NAC). NAC, a thiol-containing radical scavenger and glutathione precursor, has been found to protect cells in culture from the effect of oxidants by decreasing the amount of ROS present

(Haber et al., 2003, Recchioni et al., 2002, Lin et al., 2005, Aruoma et al., 1989). Two groups of MIN6 cells were investigated; MIN6 cells growing in 25mM glucose + NAC for 6 days and MIN6 cells growing in 25mM glucose for 6 days.

We observe a significant decrease in the expression of all three targets amplified. RCAN1-1 ($p<0.01$), RCAN1-4 ($p<0.01$) and total RCAN1 ($p<0.05$) in MIN6 cells grown in 25mM glucose + NAC when compared to MIN6 cells grown in 25mM glucose alone have a decreased expression of ~0.2, 0.1 and 0.14, respectively (Figure 3-11).

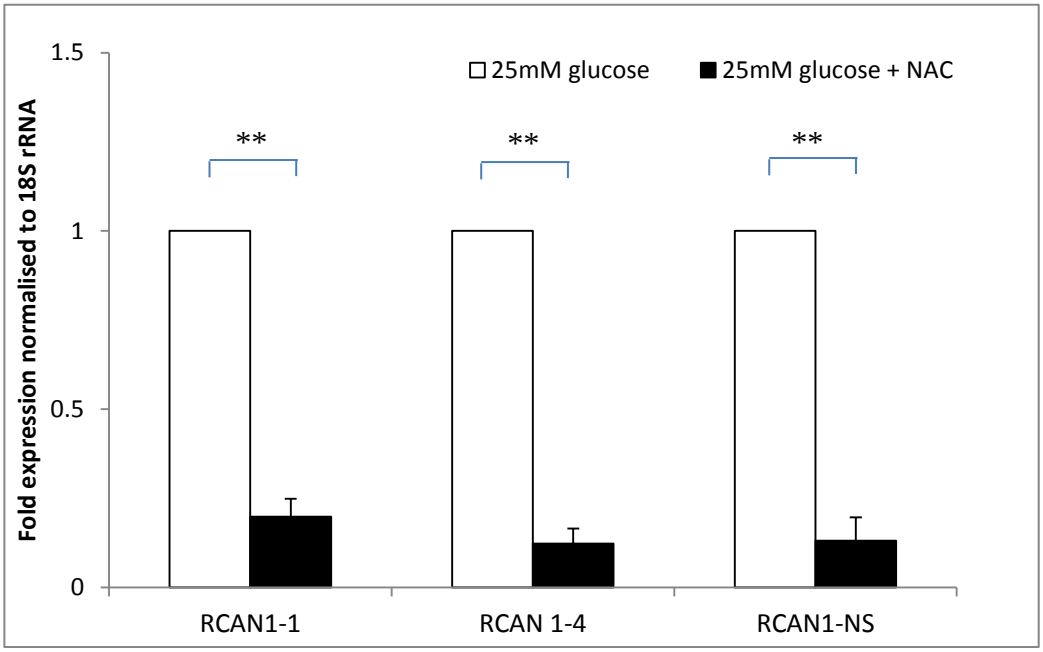

Figure 3-11: RCAN1 expression in MIN6 cells is reduced in the presence of the antioxidant, NAC
RCAN1 mRNA levels in MIN6 cells grown 25mM glucose alone (control, light bars) and MIN6 cells grown in 25mM glucose + NAC (treated, dark bars). (n=4 and **, $p<0.01$). Data shown is representative of four independent experiments and shown as mean ± SEM.

3.5.1.2 Glucose-induced expression of RCAN1 is Ca^{2+}-dependent

We next measured to see if the glucose-induced increase in RCAN1 expression is affected by blocking the entry of Ca^{2+} into MIN6 cells. There are four types of Ca^{2+} channels present in β- cells; however, the L-type channels are the predominant channel in MIN6 cells (Rutter et al., 1993). Nifedipine, a specific antagonist of L-type channels, has been used in other studies to similarly reduce the entry of Ca^{2+} (Shen et al., 2000, Schulla et al., 2003). Hence, in the current study Nifedipine was used to evaluate the effect of Ca^{2+} entry on the glucose induced expression of RCAN1. Two groups of MIN6 cells were investigated; MIN6 cells growing in 25mM glucose or cells in 25mM glucose + Nifedipine (10μM).

We observe a significant decrease in the expression of all three targets amplified. RCAN1-1 ($p<0.01$), RCAN1-4 ($p<0.01$) and total RCAN1 ($p<0.05$) in MIN6 cells grown in 25mM glucose + Nifedipine when compared to MIN6 cells grown in 25mM glucose alone show decreased expression of ~0.3, 0.15 and 0.3, respectively (Figure 3-12)

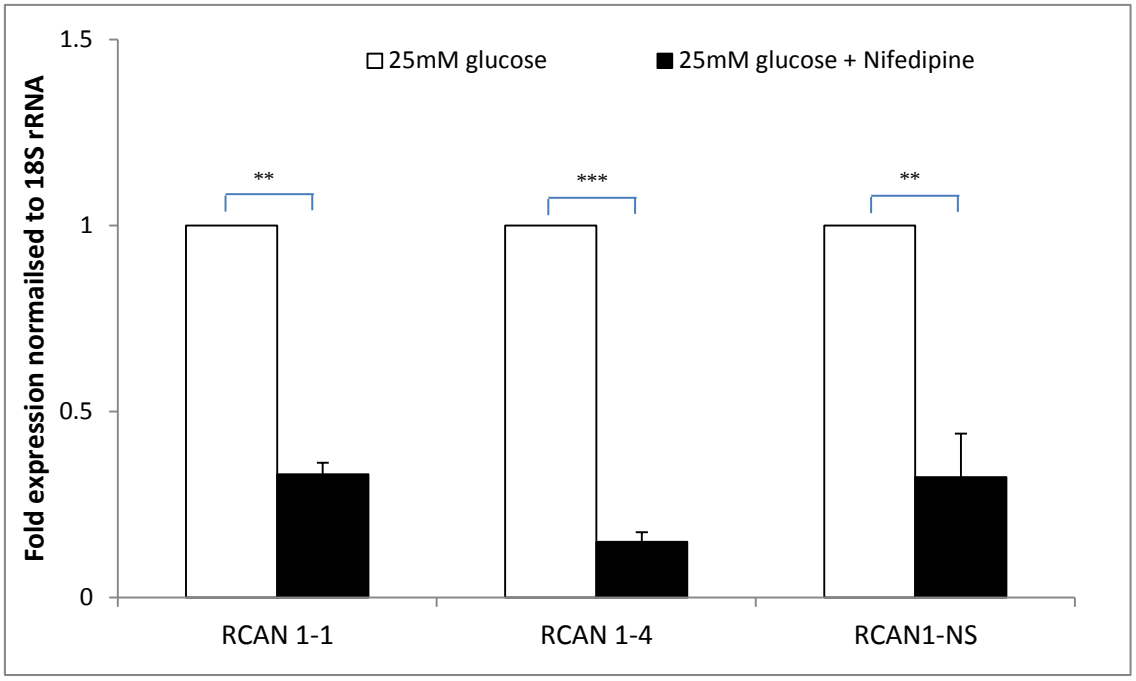

Figure 3-12: RCAN1 gene expression is reduced via blockade of L-type Ca^{2+} channels

RCAN1 mRNA levels in MIN6 cells grown 25mM glucose alone (control, light bars) and MIN6 cells grown in 25mM glucose + Nifedipine (treated, dark bars). (n=4 and **, $p< 0.01$, ***, $p< 0.001$). Data shown is representative of four independent experiments and shown as mean ± SEM

3.5.1.3 Calcineurin inhibition decreases glucose-induced expression of RCAN1-4, but not RCAN1-1.

The role of calcineurin in glucose-induced RCAN1 expression was next investigated. Two common calcineurin inhibitors, FK506 and cyclosporine A, were used in our study as these drugs inhibit calcineurin activity in β cells (Heit et al., 2006, Duan and Cobb, 2010). Two groups of MIN6 cells were investigated; cells cultured in 25mM glucose alone or in 25mM glucose + FK506 (10µM) + Cyclosporine A (10µM).

We observe a significant decrease in the expression of two of the targets amplified. RCAN1-4 ($p<0.005$) and total RCAN1 ($p<0.05$) in MIN6 cells grown in 25mM glucose + FK506 and cyclosporine A when compared to MIN6 cells grown in 25mM glucose alone show decreased expression of 0.1 and 0.5 fold, respectively (Figure 3-13). Although a decrease was seen in the expression of RCAN1-1 in the MIN6 cells cultured with the treatment (~0.75) , it was not significant.

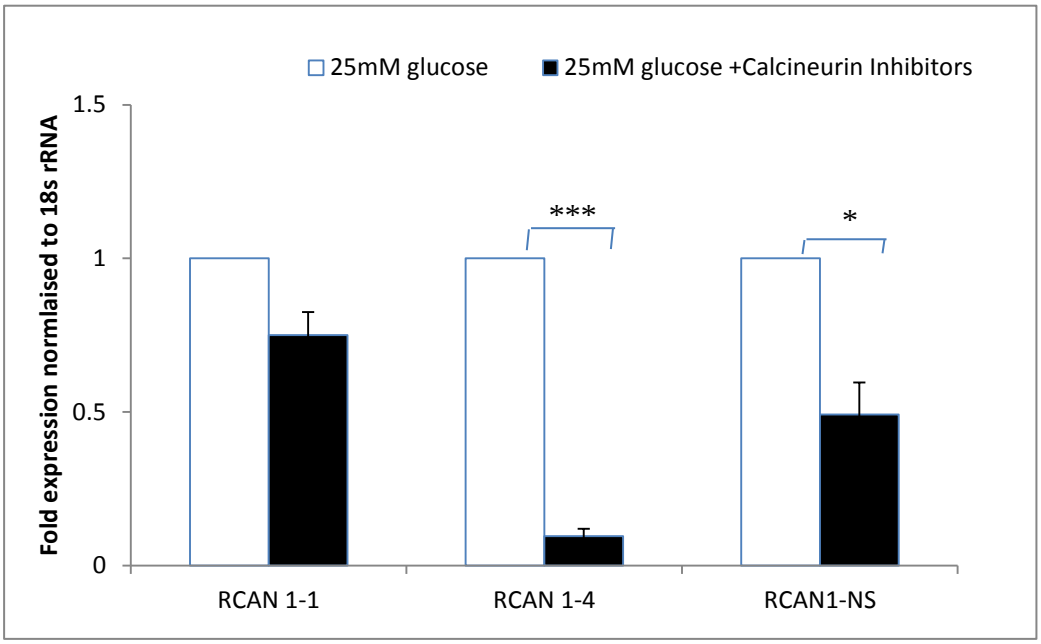

Figure 3-13: RCAN1 1-4 gene expression is reduced by inhibition of calcineurin activity.

RCAN1 mRNA levels in MIN6 cells cultured in 25mM glucose alone(control, light bars) or in 25mM glucose + calcineurin inhibitors (treated, dark bars). (n=4,* $p<0.05$ and ***, $p< 0.001$). Data shown is representative of four independent experiments and shown as mean ± SEM.

3.5.2 Oxidative stress, Ca^{2+} entry and activation of calcineurin decreased total RCAN1 protein in Immunohistochemistry.

Immunohistochemistry was carried out to understand the effect of antioxidant, Ca^{2+} entry and calcineurin on the glucose-induced expression of RCAN1 at the protein level. This was done to provide a qualitative indication on the changes of RCAN1 protein expression. Methods have been described in Section 2.7.

3.5.2.1 Antioxidants decrease the staining intensity for total RCAN1.

As an increase in the production of ROS was seen to have an effect on RCAN1 at the RNA level, we then tested if reducing ROS through the use of NAC would result in a decrease in RCAN1 protein. Immunohistochemistry (Figure 3-14) showed qualitatively that the total RCAN1 protein present in cells grown in 25mM glucose was much greater than that seen in cells in the added presence of NAC.

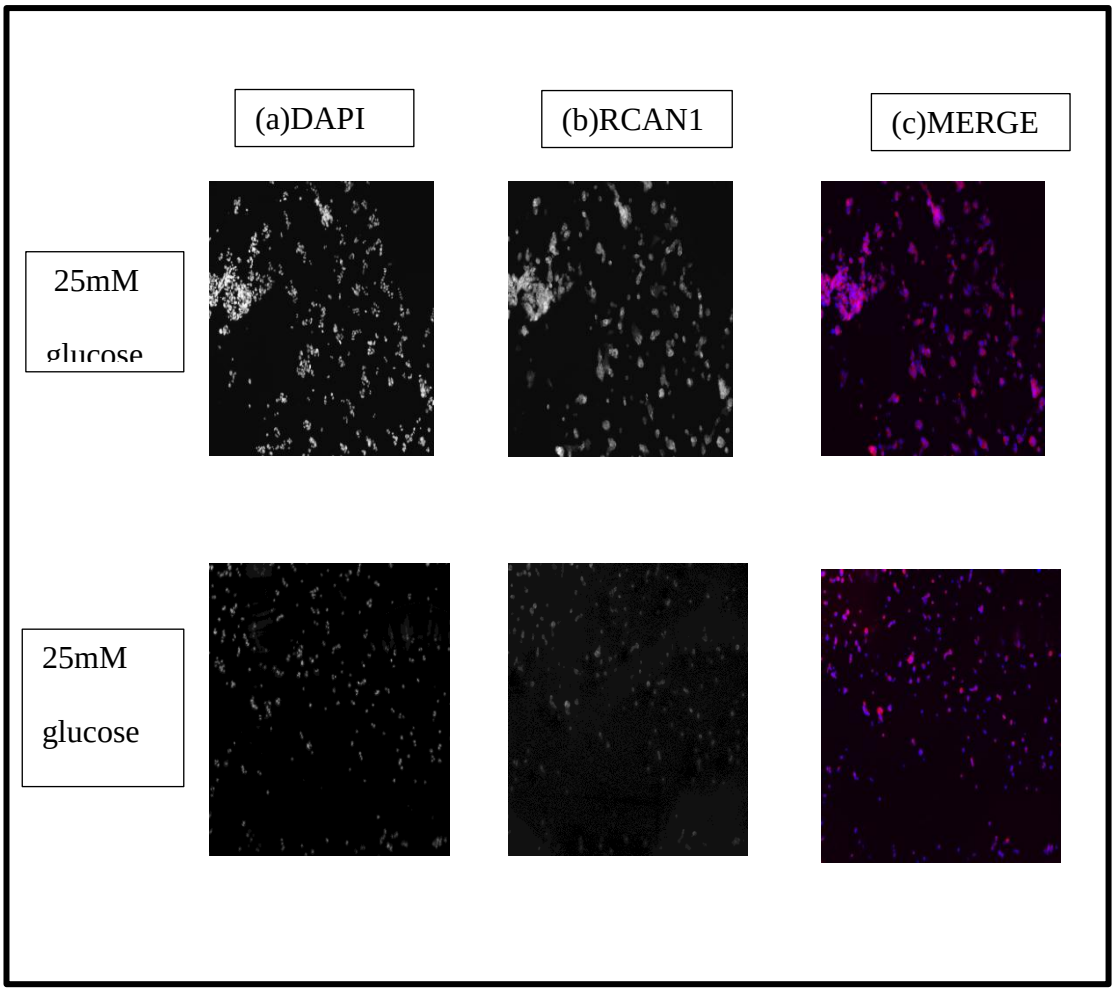

Figure 3-14: Immunohistochemistry staining of MIN6 cells cultured for 6 days in 25mM glucose or 25mM glucose with NAC

MIN6 cells cultured in 25mM glucose alone or 25mM glucose with NAC for 6 days were labeled for RCAN1 (red) detected with anti-DSCR1 C-terminal antibody and DAPI (blue). Panel (a) shows staining for the nuclear marker, (b) shows staining for RCAN1 protein and (c) shows the merged image of both (a) and (b), with RCAN1 protein seen as pink stain. Comparison of MIN6 cells staining from both the group showed difference in staining intensity with the MIN6 cells cultured without NAC showed greater staining intensity than the group with NAC (*n=6*, Magnification = 10X).

3.5.2.2 Blocking of Ca^{2+} entry into the cells resulted in a decrease in the immunolabelling of total RCAN1 protein

We next measured to see if the glucose-induced increase in RCAN1 expression would be affected at the protein level when the entry of Ca^{2+} into the cells is blocked. Nifedipine, an L-type calcium channel blocker was used to investigate this effect at the protein level. Immunohistochemistry showed qualitatively that the total RCAN1 protein present in cells cultured in 25mM glucose alone was much greater than that seen in cells cultured in 25mM glucose and Nifedipine. (Figure 3-15).

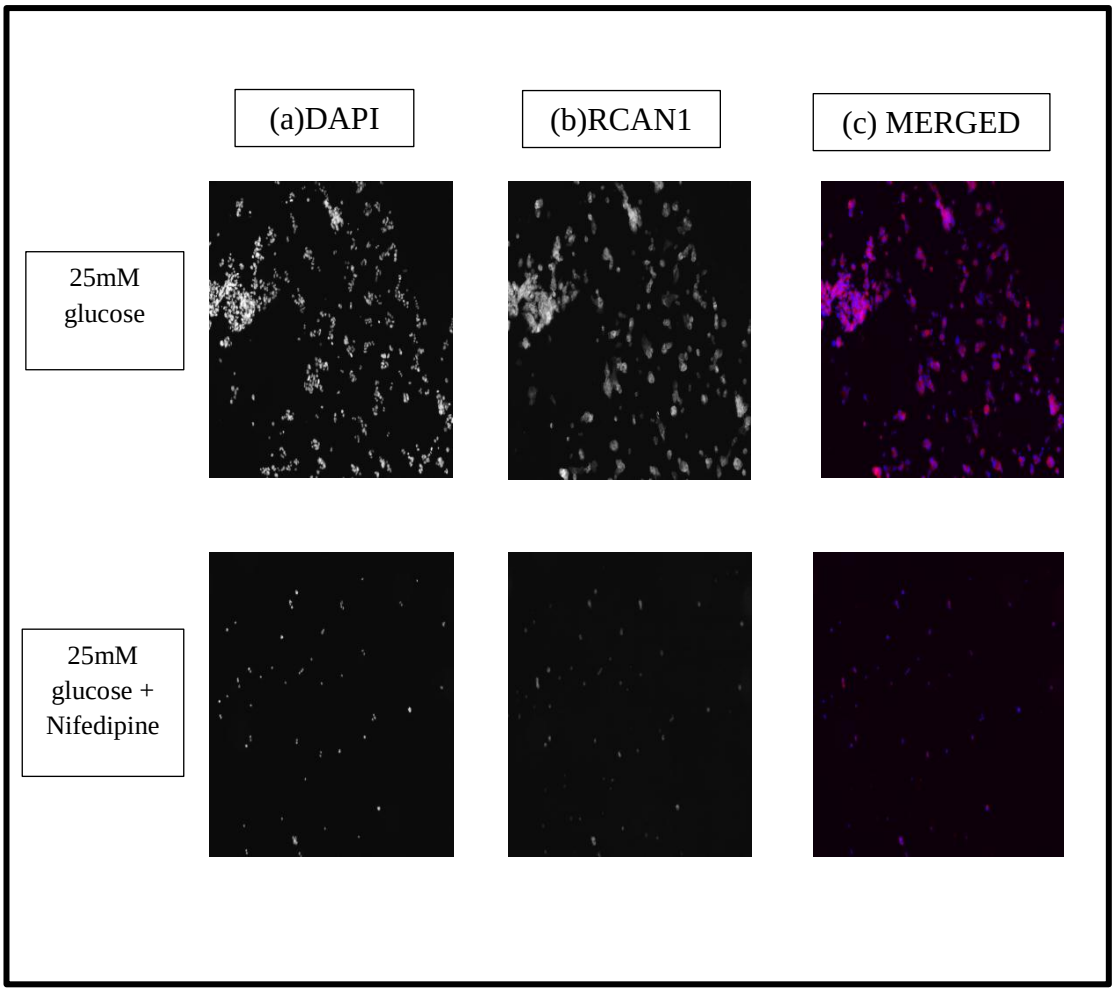

Figure 3-15: Immunohistochemistry staining of MIN6 cells cultured for 6 days in 25mM glucose or 25mM glucose with Nifedipine

MIN6 cells cultured in 25mM glucose alone or 25mM glucose with Nifedipine after 6 days were stained for RCAN1 (red) detected with anti-DSCR1 C-terminal antibody and DAPI (blue). Panel (a) shows staining for the nuclear marker, (b) shows staining for the RCAN1 protein and (c) shows the merged image of both (a) and (b) with RCAN1 protein seen as pink stain. Comparison of MIN6 cells staining from both the group showed difference in staining intensity with the MIN6 cells cultured without Nifedipine showed greater staining intensity than the group with Nifedipine (*n=6*, Magnification = 10x).

3.5.2.3 Inhibition of calcineurin resulted in a decrease in the immunolabelling for total RCAN1 protein

As we saw calcineurin inhibition at the gene level decreasing the glucose-induced expression of RCAN1, it was of interest to see the effect of calcineurin inhibition on RCAN1 at the protein level. As in the previous treatments, Immunohistochemistry showed qualitatively that the total RCAN1 protein present in cells cultured in 25mM glucose alone was much greater than that seen in cells cultured in 25mM glucose and calcineurin inhibitors (Figure 3-16).

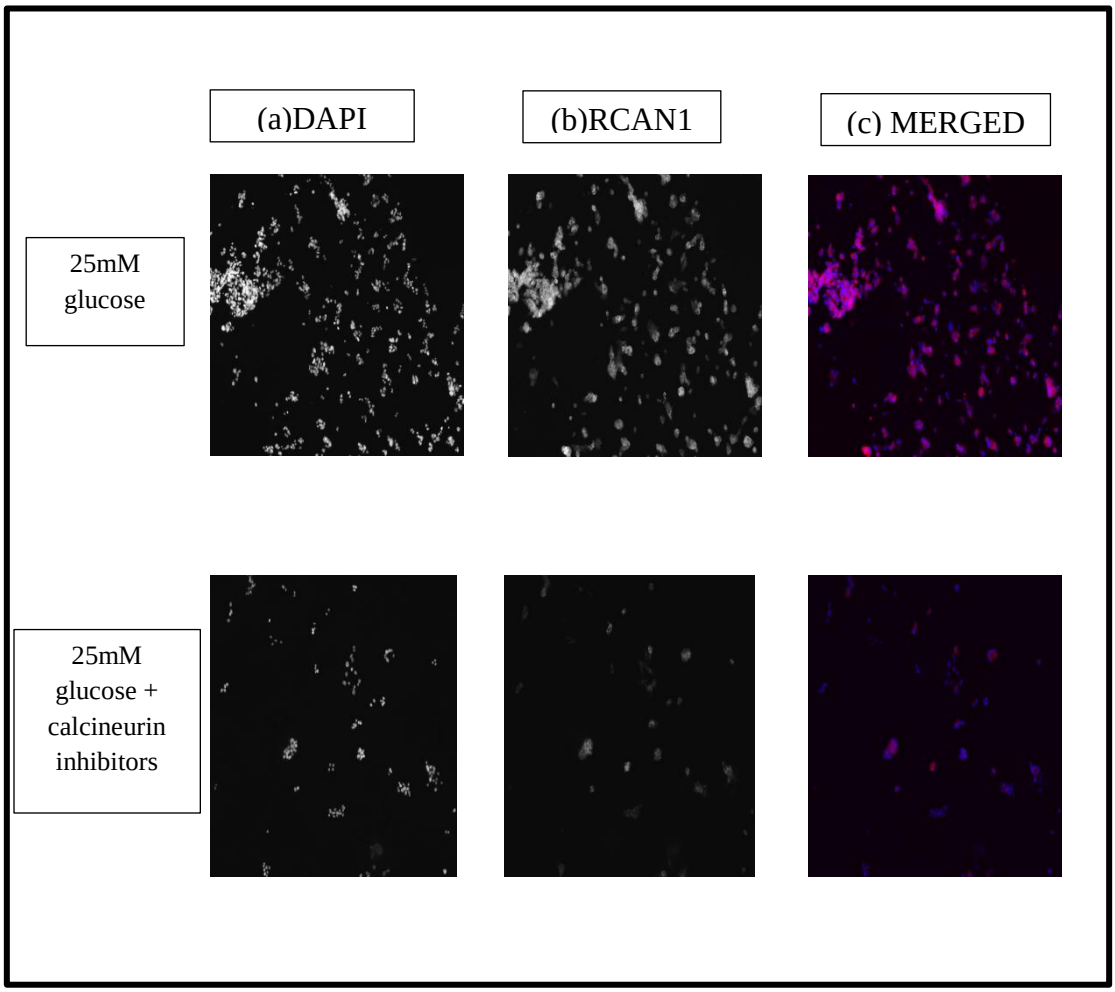

Figure 3-16: Immunohistochemistry staining of MIN6 cells cultured for 6 days in 25mM glucose or 25mM glucose with calcineurin inhibitors

MIN6 cells cultured in 25mM glucose alone or 25mM glucose with calcineurin inhibitors after 6 days were stained for RCAN1 (red) detected with anti-DSCR1 C-terminal antibody and DAPI (blue). Panel (a) shows staining for RCAN1 protein, (b) shows staining for the nuclear marker and (c) shows the merged image of both (a) and (b). Comparison of MIN6 cells staining from both the group showed difference in staining intensity with the MIN6 cells cultured without calcineurin inhibitors showed greater staining intensity than the group with calcineurin inhibitors (*n=6,* Magnification = 10X).

3.5.3 Oxidative stress, Ca^{2+} entry and calcineurin activation regulate glucose-induced expression of RCAN1-1 and RCAN1-4 protein.

Western blotting was performed as described in Section 2.8 to investigate whether the glucose-induced expression of RCAN1-1 and RCAN1-4 proteins was affected by antioxidants, Ca^{2+} channel blockers or calcineurin inhibition.

3.5.3.1 Glucose-induced RCAN1-1 protein induction is caused by oxidative stress and Ca^{2+} entry but not calcineurin activation.

All the samples obtained from MIN6 cells cultured in 5.5mM glucose, 25mM glucose alone and 25mM glucose with the treatments were quantified by normalising to the band intensity of samples from 5.5mM glucose. This was done to allow for the comparison of the glucose-induced RCAN1-1 protein expression alone and with treatment to that of RCAN1-1 at 5.5mM glucose. An example blot obtained for these experiments is shown in Figure 3-17 and the quantification of the band intensity is provided in Figure 3-18. The presence of antioxidants and the blocking of Ca^{2+} entry into MIN6 cells returned the glucose-induced increase of RCAN1-1 expression to that seen in MIN6 cells cultured in 5.5mM glucose.

The presence of antioxidants significantly decreased the glucose-induced RCAN1-1 protein intensity to ~0.73 compared to a glucose induced increase of ~2 seen in the 25mM group ($p< 0.01$). The blocking of Ca^{2+} entry saw glucose-induced RCAN1-1 expression significantly decreased to ~0.38, approximately an 80% decrease ($p< 0.01$). Although the treatment with calcineurin inhibitors decreased the glucose-induced expression of RCAN1-1 compared to that seen by glucose-induction alone, this reduction was not statistically significant. The inhibition of

calcineurin resulted in RCAN1-1 intensity decreasing to ~1.2 relative to that at the normal physiological level.

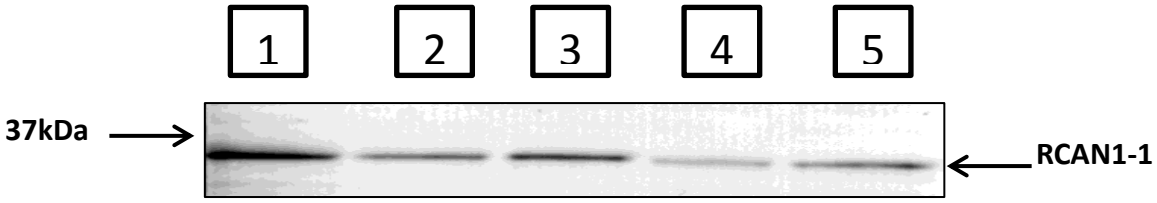

Figure 3-17: Western blot image of RCAN1-1 in various conditions
RCAN1-1 band is detected as 35-36 kDa in size. (1: 25mM glucose, 2: 5.5mM glucose, 3: 25mM glucose + calcineurin inhibitors, 4: 25mM glucose + Ca^{2+} channel blockers, 5: 25mM + NAC)

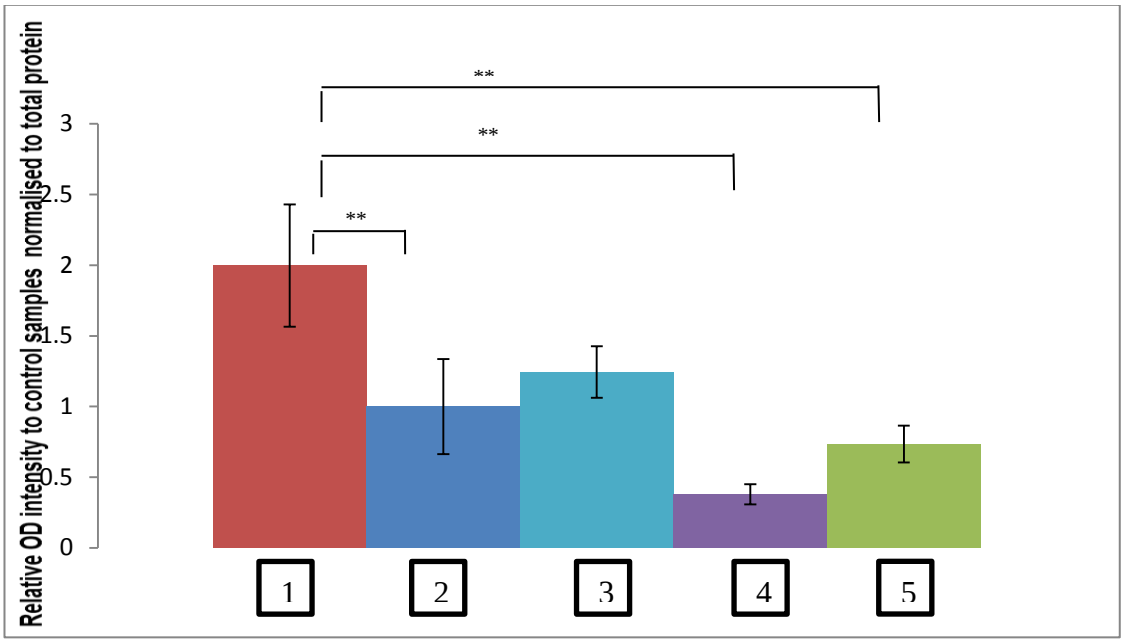

Figure 3-18: Optical density of RCAN1-1 in samples from various conditions
Band intensity of RCAN1-1 expressed relatively to the band intensity seen at 5.5mM glucose after normalising to total protein content in each lane. 1: 25mM glucose, 2: 5.5mM glucose, 3: 25mM glucose + calcineurin inhibitors, FK506 and cyclosporine A, 4: 25mM glucose + Ca^{2+} channel blockers, Nifedipine and 5: 25mM + NAC. Results are representative of five experiments and average results are shown as mean ± SEM (**, $p < 0.01$)

3.5.3.2 Glucose-induced RCAN1-4 induction is caused by oxidative stress, Ca^{2+} entry and calcineurin activation.

An example blot obtained for these experiments is shown in Figure 3-19and the quantification of the band intensity is shown in Figure 3-20. The RCAN1-4 band was detected as a doublet at a band size of 27-29 kDa. The doublet may represent the phosphorylated and unphosphorylated form of the RCAN1-4 protein as seen in previous studies (Mitchalik et al., 2004; Mitchell et al., 2007) (Figure 3-19). In doing the quantification, the doublets were used to quantify the optical density of the RCAN1-4 band.

The presence of antioxidants, the reduction of Ca^{2+} entry and the inhibition of calcineurin all reduced the glucose-induced increase of RCAN1-4 expression significantly. The presence of antioxidants decreased the glucose-induced RCAN1-1 protein intensity to ~1.14 compared to a glucose induced increase of ~4.5 seen in cells treated with 25mM glucose alone. The blocking of Ca^{2+} entry saw the glucose-induced expression decreased to ~0.34 while calcineurin inhibition saw a decrease in the band density to ~0.42.

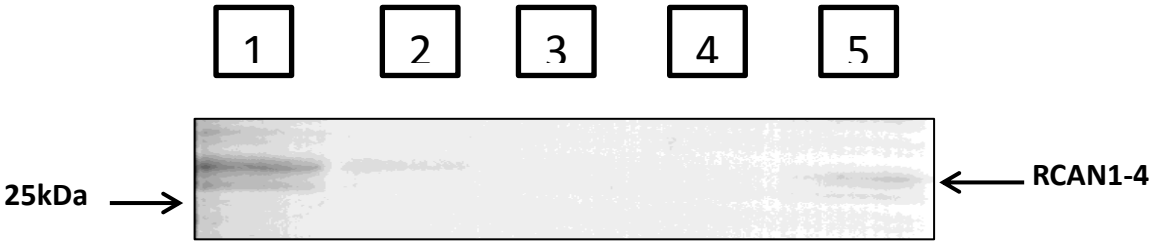

Figure 3-19: Western blot image of RCAN1-4 in various conditions
RCAN1-4 band is detected as 27-29 kDa in size and a doublet observed. (1: 25mM glucose, 2: 5.5mM glucose, 3: 25mM glucose + calcineurin inhibitors, 4: 25mM glucose + Calcium channel blockers, 5: 25mM + NAC)

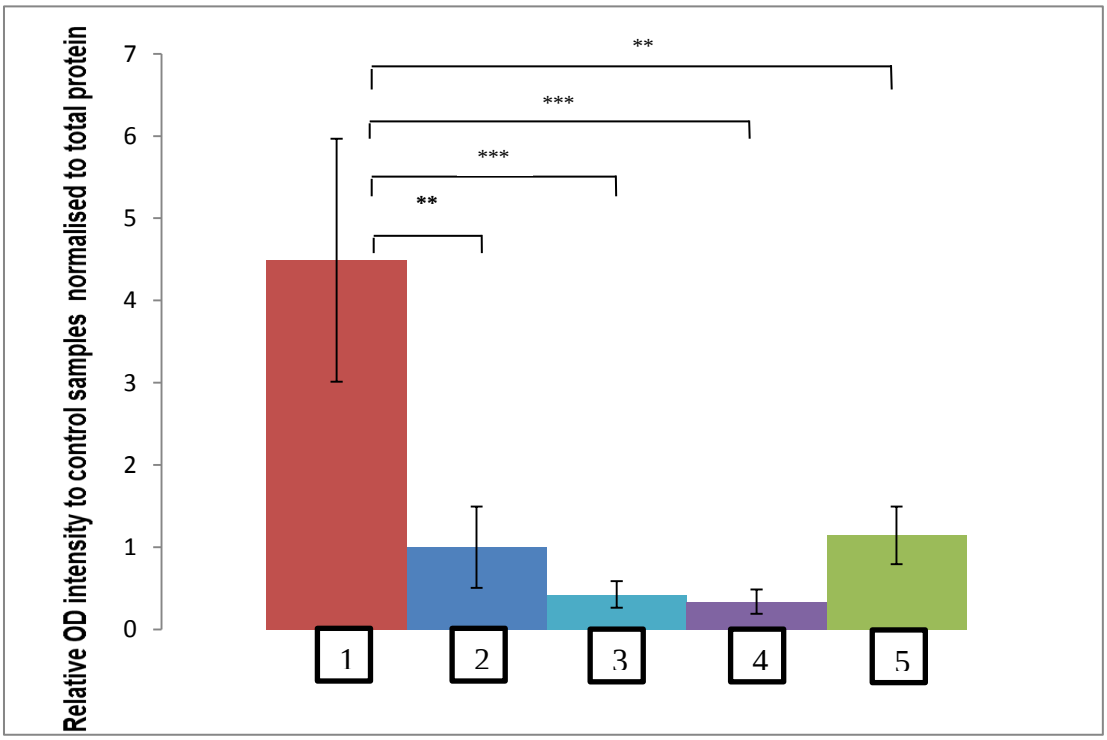

Figure 3-20: Optical density of RCAN1-4 in samples from various conditions
Relative band intensity of RCAN1-4 expressed relative to the band intensity seen at 5.5mM glucose after normalising to total protein content in each lane.1: 25mM glucose, 2: 5.5mM glucose, 3: 25mM glucose + calcineurin inhibitors, FK506 and Cyclosporine A, 4: 25mM glucose + Ca^{2+} channel blockers, Nifedipine and 5: 25mM + NAC. Results are representative of five experiments and average results are shown as mean ± SEM (**, $p < 0.01$ and ***, $p < 0.001$)

3.6 Hypoxia does not induce the expression of RCAN1 in MIN6 cells.

Hypoxia is defined as reduction in the partial pressure of oxygen. All eukaryote cells are equipped with basic molecular response mechanisms to adapt to hypoxia (Cantley et al., 2010). The role of ROS in hypoxia signaling pathway is debatable assome models have shown an increase in ROS generation during hypoxia (Chandel et al., 1998; Semenza., 1999) whereas other studies have proposed ahypoxia-induced decrease in the production of ROS (Fandrey et al., 1994; Ehleben et al., 1998). In the current study, the glucose-induced expression of RCAN1 is clearly regulated by increased ROS (Section 3.4.1). Hence, we wished to see whether hypoxia in MIN6 cells can have an effect on the expression of RCAN1.

The RNA extraction and quality assessment of RNA was carried out as described in Section 2.4 to 2.6. The primers used for RT-PCR were specific to exon 1 to identify RCAN1-1, to exon 4 to identify RCAN1-4 and to exon 7, to detect the presence of both the transcripts. The expression of an additional gene, CA9, was measured to confirm the induction of hypoxia in MIN6 cells. The primers were designed as outlined in Section 2.3 and the sequence of primers is shown in Appendix 1.

The MIN6 cells were cultured at different glucose concentrations and exposed to different hypoxic conditions as shown below:

a) *25mM glucose at 1% oxygen for 24 hours*
b) *5.5mM glucose at 1% oxygen for 24 hours and 48 hours*
c) *5.5mM glucose at 5% oxygen for 24 hours*
d) *5.5mM glucose at 2% oxygen for 4 days*

3.6.1 1% oxygen in 25mM glucose for 24 hours has no effect on the expression of RCAN1.

No significant change in the expression of any of the RCAN1 genes quantified was seen between the MIN6 cells cultured in hypoxic and normoxic conditions. However, the induction of hypoxia was confirmed as there was a significant increase ($p < 0.001$) in the expression of the hypoxic marker CA9 when compared between the normoxic and the hypoxic samples (Figure 3-21).

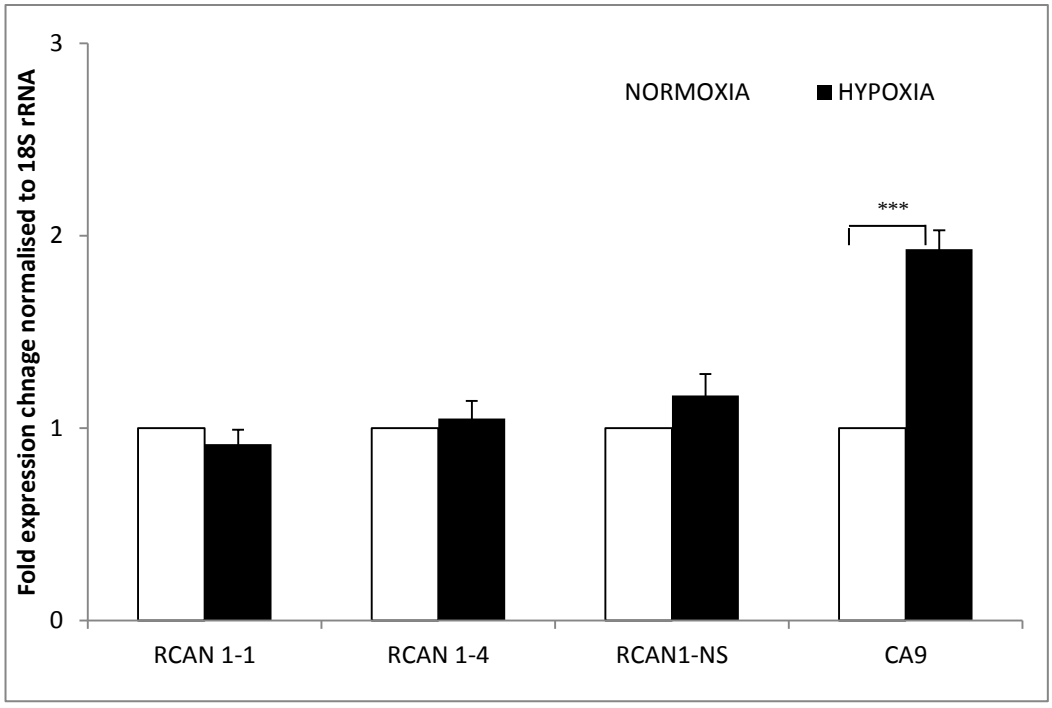

Figure 3-21: Expression of RCAN1 is unchanged in MIN6 cells after 24 hours in 1% oxygen and 25mM glucose
RCAN1 mRNA levels in MIN6 cells cultured in 25mM glucose either in normoxic conditions (light bars) or hypoxic (1% O_2) conditions (dark bars) for 24 hours (n=4, ***, $p < 0.001$). Data represented as mean ± SEM.

3.6.2 1% oxygen in 5.5mM glucose for 24 or 48 hours has no effect on the expression of RCAN1.

The RNA extracted at both time points showed severe degradation suggesting that the hypoxic conditions used at 5.5mM glucose was resulting in cell death. As there was no RNA of acceptable quality (RIN > 8), the downstream experiments with this samples were not carried out (Figure 3-22).

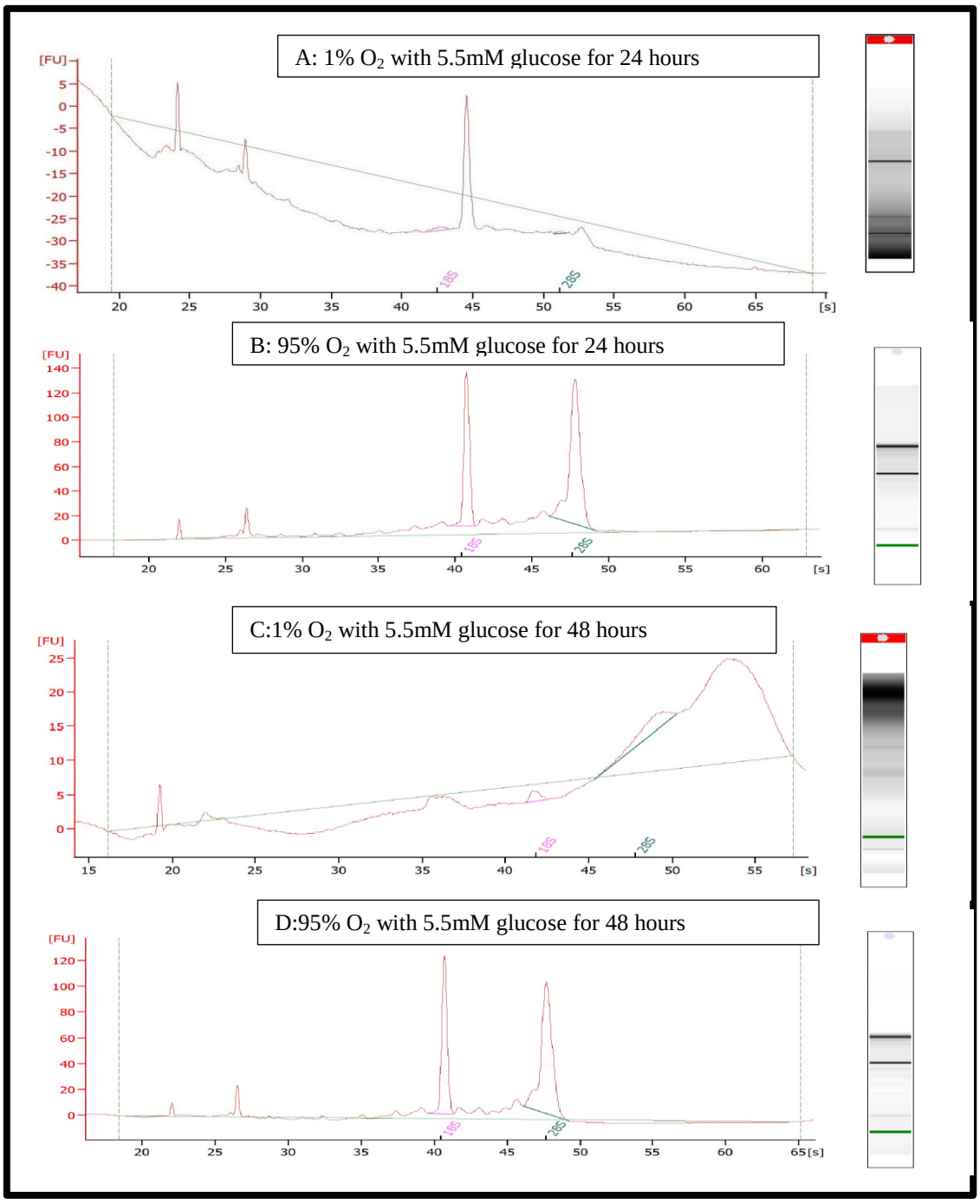

Figure 3-22: Electropherogram of RNA degradation in 1% oxygen and 5.5 mM glucose

Samples were quantified and assessed for quality with the Agilent 2100 Bioanalyzer. A: Hypoxic samples at 1% O_2 in 5.5mM glucose after 24 hours, B: Normoxic samples, 95% O_2 in 5.5mM glucose after 24 hours, C: Hypoxic samples at 1% O_2 in 5.5mM glucose after 48 hours and D: Normoxic samples, 95% O_2 in 5.5mM glucose after 48 hours.

3.6.3 5% oxygen in 5.5mM glucose for 24 hours has no effect on the expression of RCAN1.

No significant change in the expression of any of the RCAN1 genes was seen between the MIN6 cells cultured in hypoxic and normoxic conditions (Figure 3-23). Nor were there any significant changes in the expression of the hypoxic marker, CA9 between these two groups.

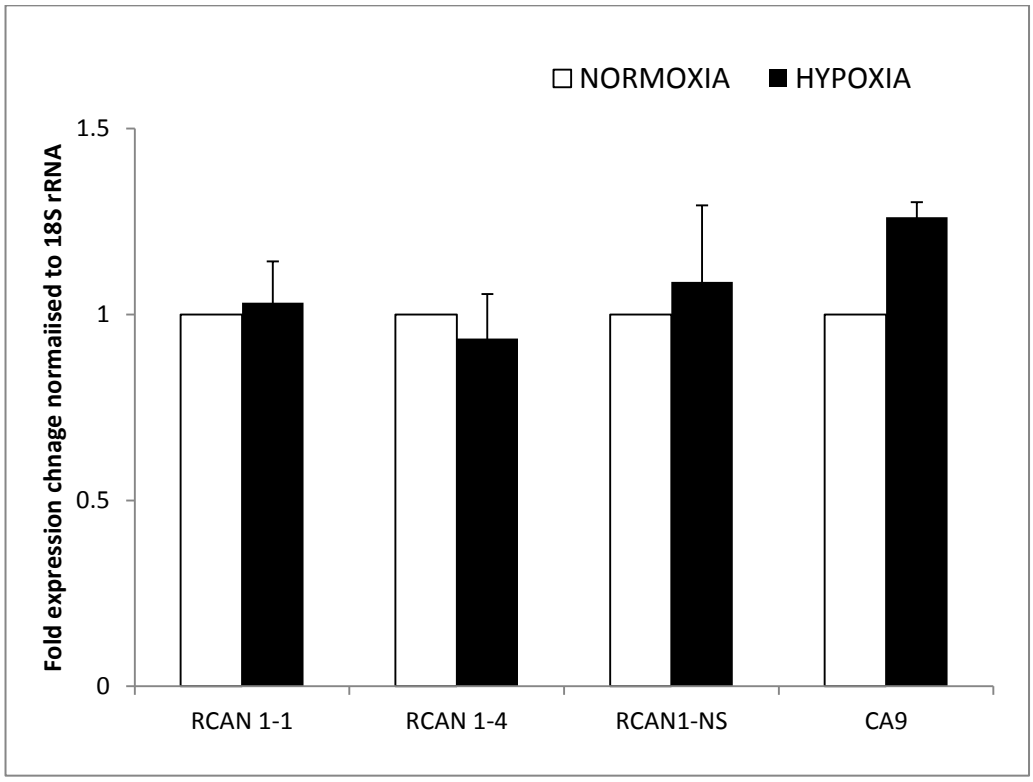

Figure 3-23: Expression of RCAN1 genes is unchanged in MIN6 cells after 24 hours in 5% oxygen and 5.5mM glucose
RCAN1 mRNA levels in MIN6 cells cultured in 5.5mM glucose either in normoxic conditions (light bars) or hypoxic (5% O_2) conditions (dark bars) for 24 hours (n=4). Data represented as mean ± SEM.

3.6.4 2% oxygen in 5.5mM glucose for 4 days has no effect on the expression of RCAN1.

We observe a significant induction of CA9 expression in the hypoxic samples compared to that in the normoxic samples which confirmed the induction of hypoxia.

However, no changes in the fold expression of any of the RCAN1 genes amplified was seen between the hypoxic and normoxic samples (Figure 3-24).

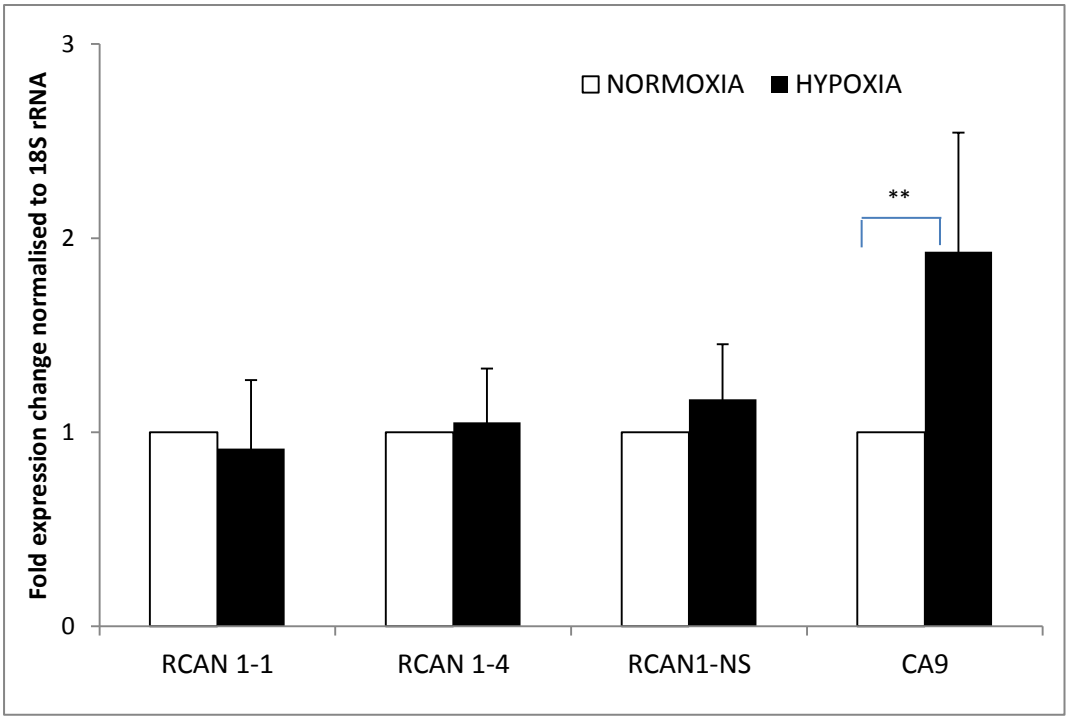

Figure 3-24: Expression of RCAN1 genes is unchanged in MIN6 cells after 4 days in 2% oxygen and 5.5mM glucose
RCAN1 mRNA levels in MIN6 cells cultured in 5.5mM glucose either in normoxic conditions (light bars) or hypoxic (2% O_2) conditions (dark bars) for 4 days (n=4, **, $p < 0.01$). Data represented as mean ± SEM.

4 DISCUSSION

Preceding any work to address the aims of the current study, preliminary work was first carried out confirming that the MIN6 cells used in the current study were glucose responsive and expressed the RCAN1 protein. The results obtained demonstrated the expression of RCAN1 by these MIN6 cells and the production of insulin in this cell line confirms the MIN6 cells as a β cell line. Glucose responsiveness of this cell line was confirmed by Ca^{2+} imaging which allowed the effect of high glucose concentration on the intracellular Ca^{2+} level to be measured. A high percentage of MIN6 cells were confirmed to be glucose responsive; hence these cells were deemed suitable for use in the current study. The first aim of the study was to investigate the effect of high glucose on the expression of RCAN1 in MIN6 cells. We saw that exposure of these cells to high-glucose led to an increase in the expression of RCAN1-4 but not that of RCAN1-1 at the mRNA level. However, at the protein level, both the isoforms showed a significant increase in the presence of high glucose concentration. Having seen this, we then proceeded to uncover the mechanisms underlying the glucose-induced expression of RCAN in the MIN6 β cell line. Three possible factors were identified to possibly play a role in the glucose-induction of RCAN1 expression; the production of ROS, the entry of Ca^{2+} into the cell and the activation of calcineurin. The contribution of ROS in the glucose induction was confirmed via the use of NAC, an antioxidant which is a ROS scavenger; hence removing ROS generated in conditions of high glucose. By using NAC, a reversal on the glucose-induction of RCAN1 was seen suggesting a role of ROS in the glucose-induced expression of RCAN1. In addition to that, we saw that the usage of Nifedipine, an L-type Ca^{2+} channel blocker, resulted in a similar reversal of the glucose-induced increase of RCAN1 expression. This suggested that the

increase in RCAN1 expression in conditions of high glucose was dependent on the entry of Ca^{2+} into the MIN6 β cells. The last factor examined was the role of calcineurin using two well-known calcineurin inhibitors, FK506 and Cyclosporine A. A reversal in the glucose-induced expression of RCAN1-4 was seen; however, a similar trend was not seen with the expression of RCAN1-1. This suggests a different pathway in regulating the glucose-induced expression of the two RCAN1 isoforms. This study also attempted to uncover the effect of hypoxia in MIN6 β cells on the expression of RCAN1. This was based on the premise that hypoxia will result in an increase in the generation of ROS by β cells. Interestingly, no difference in the expression of RCAN1 was seen in MIN6 β cells in hypoxic conditions suggesting that the hypoxia signaling cascade in MIN6 β cells might not result in an increase in the generation of ROS.

4.1 Expression of RCAN1 in MIN6 cells

Immunohistochemistry confirmed the expression of RCAN1 in the MIN6 β cell line. The expression of RCAN1 in the MIN6 cells was observed mainly in the cytosol, with low levels of expression observed in the nucleus. Studies carried out in neuronal cultures (Porta et al., 2007b) and kidney cells (Chan et al., 2005) have also reported a similar observation where high levels of RCAN1 expression were observed in the cytosol and low levels in the nucleus. As for the staining for insulin in MIN6 β cells, high levels of insulin were observed in the cytoplasm and these were mainly located near the plasma membrane of the MIN6 β cells. Although the expression of RCAN1 was observed to overlap with the synaptic vesicle protein synaptophysin (Ma et al., 2004), this was not seen in the current work. Instead, the merged images suggested that the cytosolic expression of RCAN1 is not correlated to areas where insulin staining is seen.

Pancreatic β cells act as glucose sensors and secrete insulin in response to increases in extracellular glucose concentration. MIN6 cells, being derived from β cells, should also share this inherent β cell characteristic; termed as "glucose responsiveness". However, to be considered as a suitable β cell source for the current study, the glucose responsiveness of this cell line was first confirmed by Ca^{2+}imaging. In β cells, entry of Ca^{2+} through L-type voltage-dependent Ca^{2+} channels (VDCC) in response to depolarization of the cell membrane is a well-established mechanism of increase in Ca^{2+} concentration in response to high extracellular glucose (Berggren and Larsson, 1994, Henquin, 2000). The observation that the MIN6 β cells were able to respond to high glucose concentration by an increase in intracellular Ca^{2+} confirmed the glucose responsiveness of this cell line. Thus, MIN6 cells appear to be a suitable replacement for primary β cells for the main purposes of this study.

4.2 RCAN1 expression is induced by high glucose in MIN6 cells.

The observation in the current study that RCAN1 expression increases in MIN6 cells in response to conditions of high glucose replicate results seen in mouse pancreatic islets (Keating and Peiris, unpublished data). The RCAN1 protein exists as two isoforms; RCAN1-1 and RCAN1-4 (Harris et al., 2005). This was confirmed in the current study as both the RCAN1 isoforms, RCAN1-1 and RCAN1-4, were detected in MIN6 β cells by the two distinct bands corresponding to each RCAN1 isoforms in the immunoblot. In addition to that, the band sizes of RCAN1 proteins detected in this study; RCAN1-1 at 35-36kDa and RCAN1-4 at 27-29kDa; is in agreement with that seen in other studies carried out in non-brain cells whereby RCAN1-1 has been sized at 36-41kDa and RCAN1-4 at 25-29kDa (Lin et al., 2003, Michtalik et al., 2004). The two RCAN1 isoforms have different levels of expression

in various cells. In hamster HA-1 cells, RCAN1-1 protein is the most abundant form of the two RCAN1 isoforms (Crawford et al., 1997) and similarly it was identified as the pre-dominant form in human brain with the level of RCAN1-1 about double that of RCAN1-4 (Ermak et al., 2002).

There were two main differences seen in the glucose-induced expression of RCAN1-1 and RCAN1-4. Firstly, the glucose-induction seen for both the isoforms was different with expression of RCAN1-1 being induced at the protein level and RCAN1-4 at the gene and protein level. This suggests a different mode of induction by glucose for these two isoforms. RCAN1-1 might be induced in the presence of glucose by an increase in the translation of its mRNA giving rise to an increase of RCAN1-1 protein whereas the increased expression of RCAN1-4 appears to be due to an induction by glucose at the gene level resulting in an increase of RCAN1-4 protein in the MIN6 cells. The alteration of gene expression in response to various stimuli has been suggested to be not just via an increase in the expression of gene; hence an increase detected at the mRNA level but could also be due to an increase in translation of pre-existing mRNA's; resulting in an increase at the protein level (Davies, 1999). Furthermore, although both isoforms have almost identical amino acid sequence at their N-terminal, their promoter regions are different (Park et al., 2009). Thus the transcriptional regulation for both isoforms is different with binding of different transcription factors driving the expression of its gene product. RCAN1-1 is induced through the binding of transcription enhancer factor 3 (TEF3) to a M-CAT (muscle specific-CAT element) site (Liu et al., 2008) whereas RCAN1-4 is induced via the binding of NFAT and AP-1 at its promoter site (Ermak et al., 2002, Fuentes et al., 1997). Differences in transcriptional regulation between RCAN1-1 and RCAN1-4 supports the possibility that both the isoforms are induced by glucose

at different level as their transcriptional machinery may operate differently due to the difference at their 5' promoter region. However, the observation made in the glucose-induction of both the RCAN1 isoforms at the gene level in the current study is different from that observed in the pancreatic islets where both the isoforms were seen to be significantly upregulated at the gene level in the presence of high glucose (Keating and Peiris, unpublished data). The second difference seen was in the phosphorylation state of the RCAN1 isoforms. The induction of RCAN1 expression in high glucose saw two bands for RCAN1-4 but only one band for RCAN1-1. The two bands of RCAN1-4 are suggested to be due to the phosphorylated and non-phosphorylated form (Mitchell et al., 2007a, Lin et al., 2003). This is in contrast to RCAN1-1 which only shows a single, presumably non-phosphorylated form (Hirakawa et al., 2009).

Having seen the glucose-induced expression of RCAN1 in MIN6 β cells, we next wished to understand the mechanism underlying this. The usage of MIN6 cells rather than pancreatic islets is beneficial as it allows observation of a pure β cell population. However, the MIN6 cell lines declining glucose responsiveness as the passage number increases is a major disadvantage. In the current study this is circumvented by using MIN6 cells from low passage numbers which have been identified to retain their glucose responsiveness (O'Driscoll et al., 2004, O'Driscoll et al., 2006).

4.3 Glucose-induced RCAN1 expression is ROS dependent.

N-acetyl cysteine (NAC), a scavenger of free radicals, interacts with ROS such as OH and H_2O_2 (Aruoma et al., 1989). Therefore, NAC was used in this study to reverse the effects of the increased production of ROS that may occur during

conditions of high glucose. The increase in RCAN1 expression by high glucose was reversed in MIN6 β cells in the presence of NAC. Interestingly this RCAN1 expression returned to the levels seen in low glucose conditions. This result suggests a role for ROS produced during conditions of high glucose in inducing the expression of RCAN1 in MIN6 β cells. In neurons, the induction of RCAN1, specifically RCAN1-4, is ROS-dependent (Porta et al., 2007b). This is similar to our observation in MIN6 cells that RCAN1-4 is primarily induced with exposure to high glucose.

Exposure to high glucose leads to an increase in peroxide (a type of ROS) in islets and when glucose metabolism is blocked, this increase in peroxide levels is also blocked (Robertson and Harmon, 2006). Under normal conditions, glucose enters the glycolytic pathway and undergoes oxidative phosphorylation. However, conditions of high glucose or hyperglycemia, inhibit glyceraldehyde catabolism resulting in glucose being metabolised via alternative pathways (Robertson, 2004). Glucose metabolism via glyceraldehyde-autoxidation (Wolff and Dean 1987), PKC activation, dicarbonyl formation, sorbitol metabolism and hexosamine metabolism lead to elevated ROS accumulation in β cells (Brownlee, 2005). The accumulation of ROS in β cells has been linked to diabetic complications such as decreased insulin secretion primarily due to low levels of the anti-oxidant enzymes catalase and glutathione peroxidase in β cells (Kaneto et al., 1999).

The glucose-induced increase in ROS could be linked to an activation of the calcineurin-NFAT pathway effecting the expression of RCAN1. This is very relevant to the expression of RCAN1-4 with its high dependency on NFAT binding to its promoter region comprising of 15 NFAT binding sites. Two potential mechanisms can account for this. First is the action of H_2O_2 in increasing intracellular Ca^{2+}

(Huang et al., 2001, Hoyal et al., 1996, Camello-Almaraz et al., 2006). The depolarization of the mitochondrial membrane by H_2O_2 leads to a change in the ability of mitochondria to take up and retain Ca^{2+} (Huang et al., 2001) resulting in an increase in intracellular Ca^{2+}. In addition to this, in exocrine and HeLa cells, mitochondria modulates the release of Ca^{2+} from the ER via the inositol 1, 4, 5 triphosphate-receptors (Rizzuto et al., 1993) and ryanodine-receptors (Camello-Almaraz et al., 2006). This increase in Ca^{2+} by ROS would lead to an increase in RCAN1 expression via the calcineurin-NFAT pathway. Second is via the induction of two major members of the AP-1 family of transcription factors, *c-fos* and *c-jun* by ROS (Li et al., 1998). The effect of ROS on *c-fos* and *c-jun* is directly linked to the expression of RCAN1-4 as the AP-1 family of transcription factors are co-transcription factors along with NFAT which bind to the promoter region of the RCAN1-4 transcript. Hence, induction of AP-1 along with NFAT activation would result in the increased expression of RCAN1-4.

An alternative mechanism explaining the ROS-induced expression of both RCAN1 isoforms could be via the activity of SIRT1. SIRT1 is a member of the Sirtuins, a conserved family of NAD+-dependent proteins (Frye, 1999, Frye, 2000). Neuronal progenitor cells (NPC) exposed to conditions allowing for the accumulation of ROS *in vitro* and *in vivo* showed an increase in the expression of SIRT1 (Prozorovski et al., 2008), an NAD^+ dependent Class III histone deacteylates which deacteylates lysine residue on histone and non-histone substrate (Imai et al., 2000, Haigis and Guarente, 2006, Longo and Kennedy, 2006). SIRT1 has been linked to various cellular processes such as energy metabolism, transcriptional silencing and DNA repair. One possible interaction partner of SIRT1 is a member of the Notch signaling pathway, Hes-1 (Hisahara et al., 2008). The upstream region of RCAN1-1 promoter

contains 4 high-affinities and one low-affinity Hes-1 binding site in contrast to one low affinity Hes-1 binding site on RCAN1-4 (Iso et al., 2003). Activated Notch-1 expression has been shown to stably down-regulate the expression of RCAN1-1 via the repression of RCAN1-1 expression by Hes-1 (Mammucari et al., 2005). The increase of Sirt1 expression will thus effect Hes-1 activity either via direct interaction with Hes-1 blocking its function or by translocating into the nucleus and supressing the expression of Hes-1 (Hisahara et al., 2008). The nett outcome from Sirt-1 and Hes-1 interaction is the removal of RCAN1-1 repression by Hes-1, leading to an increase in RCAN1-1 mRNA and protein in conditions of high glucose.

4.4 Glucose-induced RCAN1 expression is Ca^{2+}-dependent

Ca^{2+} channel blockers were used to block the entry of Ca^{2+} into the cell via L-type Ca^{2+} channels. This group of Ca^{2+} channels have been identified as the dominant form of Ca^{2+} channels in β cells (Rutter et al., 2006b, Rutter et al., 1993). Immunohistochemistry illustrated a reduced number of MIN6 cells cultured in the presence of Nifedipine. This could be due to inhibition in the proliferation of MIN6 cells via Ca^{2+} activation of calcineurin (Heit et al., 2006). Besides its role in the calcineurin-NFAT pathway, Ca^{2+} is also a key regulator of β cell function and survival (Ramadan et al., 2011).

Both RCAN1.1 and RCAN1.4 are regulated by oxidative stress and Ca^{2+} (Holmes et al., 2010, Porta et al., 2007a). β cells respond to increased nutrients such as glucose by increasing their uptake via the high K_m Glut2 glucose transporter. Increased glucose uptake results in depolarisation of the β cell via K_{ATP} channel closure resulting in Ca^{2+} entry via L-type Ca^{2+} channels triggering insulin exocytosis (Xu and Rothenberg, 1998). The glucose-induced increase of

RCAN1.1 and RCAN1.4 expression could potentially be following a similar pattern of induction, where increase glucose uptake into the MIN6 β cells results in Ca^{2+} entry followed by the induction of RCAN1 expression.

Although both the RCAN1 isoforms are differentially upregulated (Lin et al., 2003), Ca^{2+} has been implicated in both their regulation (Davies et al., 2001a, Ermak et al., 2002, Porta et al., 2007a). In human astrocytoma and neuroblastoma cells the expression of RCAN1 was induced by Ca^{2+} (Fuentes et al., 200). Similar to blocking the entry of Ca^{2+} into the cell, usage of intra-cellular Ca^{2+} chelators such as BAPTA-AM resulted in a reversal of RCAN1 induction due to oxidative stress by hydrogen peroxide in Chinese hamster ovary cells (Leahy et al., 1999). In astrocytes, RCAN1-4 mRNA expression was induced upon stimulation with agents that increase Ca^{2+} concentration in cells (Canellada et al., 2008). Taken together, the previous studies and the current study confirm the role of Ca^{2+} in the glucose-induced increase expression of RCAN1.

The relationship between Ca^{2+} and RCAN1 expression is based on the premise that Ca^{2+} indirectly induces RCAN1 expression via the calcineurin-NFAT pathway. In conditions of high glucose, there is an influx of Ca^{2+} into the cell due to the opening of VDCCs. Ca^{2+} is required for the activity of calcineurin and the activation of calcineurin results in dephosphorylation of NFAT and subsequently transcription of RCAN1. However, the blockage of Ca^{2+} entry into the MIN6 β cells may have resulted in the AID domain not being removed from calcineurin catalytic site; hence calcineurin was not able to carry out its phosphatase activity. Without the dephosphorylation of NFAT by calcineurin, the expression of RCAN1 would not occur.

Although the effect of Ca^{2+} entry on the calcineurin-NFAT pathway could be the underlying mechanism in the increase expression of RCAN1-4; this may not be true for the glucose-induced expression of RCAN1-1. The RCAN1-1 isoform does not have NFAT binding region, suggesting the involvement of a different pathway in the upregulation of RCAN1-1 expression induced by glucose. Interestingly, SIRT-1 which was suggested previously to play a role in ROS induced increase of RCAN1-1 expression can also be upregulated by Ca^{2+} (Mammucari et al., 2005). Hence, the increase in Ca^{2+} induced by glucose and the effect of this on the upregulation of SIRT1 activity would culminate in the removal of RCAN1-1 repression by Hes-1 (Hisahara et al., 2008). This, then further supports the initial suggestion by various groups that RCAN1-1 and RCAN1-4 are regulated via different pathways; the former via the Notch signaling pathway and the latter via the Calcineurin-NFAT pathway.

4.5 Glucose-induced RCAN1 expression is related to calcineurin activity

FK506 and cyclosporine A inhibit the catalytic activity of calcineurin by first forming a stable complex with their respective immunophilins (Kissinger et al., 1995, Jin and Harrison, 2002). These drug-immunophilin complexes then bind to calcineurin and inhibit its phosphatase activity (Griffith et al., 1995, Jin and Harrison, 2002). This inhibition results in the relocalization of NFAT to the cytoplasm and loss of NFAT DNA binding activity. The consequence of this is a decrease in the expression of genes under the control of the calcineurin-NFAT pathway, one of which is RCAN1 Immunohistochemistry suggested a decrease number of MIN6 cells in the presence of calcineurin inhibitors. This could be due to a decrease in calcineurin-associated β cell proliferation (Heit et al., 2006).

In the current work the expression of RCAN1 especially that of RCAN1-4 was greatly reduced in the presence of these calcineurin inhibitors. In their work with neurons, Porta et al (2007) demonstrated that the pre-incubation of neurons with FK506 and cyclosporine A resulted in the prevention of RCAN1-4 induction. Other reports have also shown that RCAN1-4 induction occurs via a calcineurin dependent mechanism involving RCAN1-4 promoter regions that contain NFAT transcription factor binding motifs (Fuentes et al., 2000, Yang et al., 2000a, Cano et al., 2005). In studies carried out to understand the transcriptional regulation of RCAN1 transcripts, 15 NFAT binding regions were discovered at the promoter region of the RCAN1-4 transcript (Ermak et al., 2002) suggesting a direct influence on RCAN1-4 expression by the inhibition of calcineurin.

As for RCAN1-1, the absence of NFAT binding region at its promoter site suggests a lack of effect in its glucose-induced expression by the Calcineurin-NFAT pathway. Interestingly, the expression of RCAN1-1 has been suggested to occur via the binding of transcription enhancer factor 3 (TEF3) to M-CAT (muscle specific-CAT element) site at its promoter site (Liu et al., 2008); hence, the inhibition of calcineurin would not have an effect on its glucose-induced expression.

4.6 Hypoxia does not effect RCAN1 gene expression

Hypoxic conditions in MIN6 β cells were confirmed by using CA9, a hypoxic marker which is upregulated by hypoxia in a broad range of cell types (Wykoff et al., 2000) and confers adaptation to hypoxia (Cantley et al., 2010). Hypoxic induction in MIN6 β cells was seen by the significant increase in CA9 expression at 1% and 2% oxygen; although at 5% oxygen, there was no significant increase in CA9 expression. This suggests that 5% oxygen was not sufficient to generate hypoxic conditions in the MIN6 β cells microenvironment. This is in

agreement with studies carried out in β cells and isolated islets from C57BL/6 mice where 1% oxygen caused changes in gene expression related to hypoxic stress whereas the usage of 5% oxygen did not result in any such changes (Cheng et al., 2010).

The study of hypoxia in MIN6 cells were based on the premise that hypoxia would result in an increase in the generation of ROS. Although the MIN6 β cells were undergoing hypoxia; no changes was seen in the expression of RCAN1. The lack of RCAN1 induction during hypoxia in MIN6 β cells along with the association showed earlier in our work between the expression of RCAN1 with an increase in ROS, suggests a signaling cascade during hypoxia that does not involve increases in ROS production. The hypoxia signal-transduction pathway has been suggested to be cell-type specific (Semenza et al., 2000); hence, the hypoxia pathway in MIN6 β cells may be different than that seen in other cells.

The lack of ROS production in MIN6 β cells during hypoxia could be explained by the following observation. Hypoxia in β cells lead to altered expression of genes involved in glucose uptake, glycolysis and pyruvate utilization such as Glut1, pyruvate dehydrogenase kinase 1, lactate dehydrogenase A and monocarboxylate transporter 4. This would result in the shuttling of pyruvate away from the mitochondrial oxidation and instead into the formation of lactate (Cantley et al., 2010). The expression of Glut1 rather than Glut2 by β cells in conditions of hypoxia results in no oxidative stress generated in β cells. This is due to Glut1 being a low Km glucose transporter (K_m = 2.3-2.6mmol/l in human) compared to Glut 2 (K_m = 17mmol/l), hence, the uptake of glucose into β cells would not be as high as in normoxic conditions. The decreased uptake of glucose into MIN6 cells would therefore not result in glucose being shuttled into other metabolic pathways such as

glyceraldehyde autooxdiatation through non-mitochondrial pathways, glucose enediolization and activation of PKC, glycation and hexosamine metabolism (Robertson and Harmon, 2006). To strengthen this premise, the depletion of oxygen during hypoxia has been suggested to be off-set by cells decreasing their cellular demand for oxygen (Hochachka et al., 1996). This is done by upregulating anaerobic ATP-producing pathways and downregulating ATP-consuming processes. Hence, a lack of ROS production in MIN6 cells during hypoxia (Michtalik et al., 2004) may explain the lack of increase in RCAN1 expression.

The ATP/ADP ratio in β cells has also been implicated to have a role in hypoxia. Firstly, the switch in β cells glucose metabolism from aerobic oxidative phosphorylation to anaerobic glycolysis may not result in an increase in the ATP/ADP ratio in β cells. Furthermore, it is suggested that hypoxia results in a decrease in K_{ATP} channel activity due to ubiquitin mediated degradation of the catalytic subunit of the channel by mitochondrially generated ROS (Comellas et al., 2006, Dada et al., 2003). The ATP/ADP ratio is necessary for membrane depolarization, Ca^{2+} influx into the cell via the VDCC followed by the downstream activation of calcineurin. Hence, another possible explanation for the lack of changes in RCAN1 gene expression during hypoxia could be due to there not being any increase in calcineurin activation beyond the basal level of activity seen in normoxic conditions.

4.7 Conclusion

The current study has identified the mechanisms underlying the glucose-induced expression of RCAN1 in MIN6 β cells. Interestingly, the induction of both the RCAN1 isoforms in the presence of high glucose concentrations may be different.

The addition of a ROS scavenger, NAC, suggested that the increase ROS production in conditions of high glucose leads to an increase in expression of both the RCAN1 isoforms. However, the downstream effect of an increase in ROS could suggest either an activation of Calcineurin-NFAT pathway which may be relevant to the expression of RCAN1-4 or via SIRT1 activation followed by Hes-1 repression which could play a role in the expression of RCAN1-1. The usage of L-type Ca^{2+} channel blocker, nifedipine, has linked Ca^{2+} entry to glucose-induced increase in expression of both the RCAN1 isoforms. The activation of the Calcineurin-NFAT expression requires the entry of Ca^{2+}; hence leading to an increase expression of RCAN1-4 expression. Interestingly, Ca^{2+} has also been linked to the increase in SIRT1 activity; hence possibly effecting the Notch signaling pathway which downregulates the expression of RCAN1-1 via the activity of Hes-1. The usage of Calcineurin inhibitors helped to dissect the mechanisms more precisely. With the addition of these inhibitors, a decrease is seen in the glucose-induced expression of RCAN1-4 but not RCAN1-1. This clearly suggests the role of calcineurin-NFAT pathway in the glucose induced increase expression of RCAN1-4 and an alternative pathway in the glucose-induced expression of RCAN1-1 which may involve SIRT-1 and Hes-1 via the Notch signaling pathway. These observations suggested that the increase in ROS during glucose metabolism in the cell led to an increase in cytoplasmic Ca^{2+}. This then led to the activation of calcineurin and consequently the upregulation of NFAT activity culminating in increase expression of RCAN1-4. However, the expression of RCAN1-1 could potentially be via the activation of SIRT1 by the increase in ROS production and intracellular Ca^{2+} during conditions of high glucose. The increase in SIRT1 results in the removal of the repression by Hes-1, a component of the Notch signaling pathway culminating in an increase expression of RCAN1-1.

The current study has also shown that the stress generated in β cells during hypoxia does not lead to a change in the expression of RCAN1. At this stage it is possible to speculate that firstly, the combination of markedly reduced glucose uptake by the switch from Glut2 to Glut1 and impaired glycolytic flux prevents the burst of mitochondrial oxidative phosphorylation required for downstream activation of calcineurin. Secondly, this could also suggest the possibility that the hypoxic signaling pathway in MIN6 β cells does not cause an increase in the generation of ROS.

4.8 Future Directions

Although the current study has laid the foundation for furthering our understanding of the mechanisms underlying glucose-induced increase in RCAN1 expression in β cells, there are still a few fundamental questions which are left unanswered. Firstly, it is important to note that this investigation was carried out in MIN6 cells cultured in 25mM glucose and all the treatments was carried out to see the if a reversal of this induction was seen. However, in order to have a more comprehensive understanding of this mechanism it would be necessary to also see the effect of antioxidants, Ca2+ channel blockers or inhibition of calcineurin on RCAN1 expression in MIN6 cells cultured at 5.5mM glucose. The current study has also suggested a different glucose-induction mechanism in the expression of RCAN1-1 from that of RCAN1-4; potentially via the interaction of Hes-1 and SIRT1. This needs to be further evaluated to help understand the possible difference in glucose-induction for both the RCAN1 isoforms.

It would also be interesting to understand the role of NFAT in the expression of RCAN1, particularly RCAN1-4, as we did not look directly at the effect of NFAT inhibition on the expression of this isoform. Furthermore, the results of the current

study do not explain the effect of RCAN1 phosphorylation on its ability to regulate the activity of calcineurin. Although in various other models the effect of RCAN1 phosphorylation on calcineurin activity has been looked at, the outcome has been contradictory. Some suggested a positive regulation and others the opposite. As this has not been looked at in β cells, future work could look at the effect of RCAN1 phosphorylation on its role in regulating calcineurin. It would also be interesting to understand the role of phosphorylated forms of RCAN1 in MIN6 β cells in regard to its half-life, interaction with GSK3β and other signaling pathways. In addition to these, the current results have identified the potential mechanisms in RCAN1 overexpression, however the generation of MIN6 cell lines with transgenic overexpression and knockdown of RCAN1 may help in further understanding the dynamic role of RCAN1 in glucose-induced changes in β-cell function.

In the current study the possible mechanisms of glucose-induced increase in RCAN1 expression was carried out in a β cell line. While transformed β cell lines such as MIN6 are phenotypically homogenous and proliferative in culture, they do have their limitations. Firstly, the cell line could exhibit impairment in some essential characteristics such as glucose transport or metabolism. Secondly, as these cells proliferate in culture as monolayers, the impaired response to glucose could be further aggravated by a reduction in cell-to-cell contact and gap junctional communication which is necessary in their response to nutrient stimuli (Vozzi et al., 1995). Hence, it would be necessary to repeat this in pancreatic islet cells to see if the mechanism suggested in modulating the glucose-induced RCAN1 expression is similar to that in the islets. In a physiological context, these mechanisms may be different as different cells making up the islets may contribute differently to the expression of RCAN1. Furthermore, work done using whole islets will provide a

more representative model of in vivo β-cell function when compared to MIN6 cell line. In addition to this as the islet is part of a larger signaling system in the body, there may be other factors contributing to the glucose-induced expression which may or may not be the same as that observed in a pure β cell line.

Previous work in our lab has provided a link between RCAN1 and the pathogenesis of β cell dysfunction during hyperglycemia. Complimentary to that work this current study has identified the mechanisms underlying the glucose-induced increase of RCAN1 expression. Taken together, understanding the mechanisms regulating RCAN1 could potentially allow for regulating β cell function in the presence of hyperglycemia via RCAN1 modulation to prolong normal β cell function in type 2 diabetes.

As for the work done in hypoxia, it would be interesting to see if hypoxic β cells have an increase in ROS production, as this is debatable. The quantification of ROS via markers such as Mitotracker for example would be useful in understanding this. The level of RCAN1 protein after hypoxic stress should also be looked at by Western blotting as hypoxia may have an effect on RCAN1 at the protein but not the gene level. A further point to look at would be to repeat the hypoxic treatment using whole islets instead of β cells as islets and β cells are affected at different oxygen tension and the use of islets will again be a more representative model of an *in vivo* effect of hypoxia on β cells.

REFERENCES

Abbasi, S., Lee, J. D., Su, B., Chen, X., Alcon, J. L., Yang, J., Kellems, R. E. & Xia, Y. 2006. Protein kinase-mediated regulation of calcineurin through the phosphorylation of modulatory calcineurin-interacting protein 1. *J Biol Chem,* 281**,** 7717-26.

Aihw 2011. Diabetes prevalence in Australia: detailed estimates for 2007-08. *In:* WELFARE, A. I. O. H. A. (ed.). Canberra.

Ainscow, E. K., Zhao, C. & Rutter, G. A. 2000. Acute overexpression of lactate dehydrogenase-A perturbs beta-cell mitochondrial metabolism and insulin secretion. *Diabetes,* 49**,** 1149-55.

Al-Daraji, W. I., Grant, K. R., Ryan, K., Saxton, A. & Reynolds, N. J. 2002. Localization of Calcineurin//NFAT in Human Skin and Psoriasis and Inhibition of Calcineurin//NFAT Activation in Human Keratinocytes by Cyclosporin A. 118**,** 779-788.

Aronoff, S. L., Berkowitz, K., Shreiner, B. & Want, L. 2004. Glucose Metabolism and Regulation: Beyond Insulin and Glucagon. *Diabetes Spectrum,* 17**,** 183-190.

Artavanis-Tsakonas, S., Rand, M. D. & Lake, R. J. 1999. Notch signaling: cell fate control and signal integration in development. *Science,* 284**,** 770-6.

Aruoma, O. I., Halliwell, B., Hoey, B. M. & Butler, J. 1989. The antioxidant action of N-acetylcysteine: its reaction with hydrogen peroxide, hydroxyl radical, superoxide, and hypochlorous acid. *Free Radic Biol Med,* 6**,** 593-7.

Arya, M. S. 2006. The Obese Patient with Diabetes Mellitus: From Research Targets to Treatment Options. *The American journal of medicine,* 119**,** S17-S23.

Asfari, M., Janjic, D., Meda, P., Li, G., Halban, P. A. & Wollheim, C. B. 1992. Establishment of 2-mercaptoethanol-dependent differentiated insulin-secreting cell lines. *Endocrinology,* 130**,** 167-78.

Beals, C. R., Sheridan, C. M., Turck, C. W., Gardner, P. & Crabtree, G. R. 1997. Nuclear export of NFATc enhanced by glycogen synthase kinase-3. *Science,* 275**,** 1930-1934.

Bendtzen, K., Mandrup-Poulsen, T., Nerup, J., Nielsen, J. H., Dinarello, C. A. & Svenson, M. 1986. Cytotoxicity of human pI 7 interleukin-1 for pancreatic islets of Langerhans. *Science (New York, N.Y.),* 232**,** 1545-7.

Berggren, P. O. & Larsson, O. 1994. Ca2+ and pancreatic B-cell function. *Biochem Soc Trans,* 22**,** 12-8.

Bernal-Mizrachi, E., Cras-Meneur, C., Ye, B. R., Johnson, J. D. & Permutt, M. A. 2010. Transgenic overexpression of active calcineurin in beta-cells results in decreased beta-cell mass and hyperglycemia. *Plos One,* 5**,** e11969.

Bigas, A., Martin, D. I. & Milner, L. A. 1998. Notch1 and Notch2 inhibit myeloid differentiation in response to different cytokines. *Mol Cell Biol,* 18**,** 2324-33.

Bluestone, J. A., Herold, K. & Eisenbarth, G. 2010. Genetics, pathogenesis and clinical interventions in type 1 diabetes. *Nature,* 464**,** 1293-300.

Brownlee, M. 2005. The pathobiology of diabetic complications: a unifying mechanism. *Diabetes,* 54**,** 1615-25.

Busciglio, J. & Yankner, B. A. 1995. Apoptosis and increased generation of reactive oxygen species in Down's syndrome neurons in vitro. *Nature,* 378**,** 776-779.

Camastra, S., Bonora, E., Del Prato, S., Rett, K., Weck, M. & Ferrannini, E. 1999. Effect of obesity and insulin resistance on resting and glucose-induced thermogenesis in man. EGIR (European Group for the Study of Insulin Resistance). *Int J Obes Relat Metab Disord,* 23**,** 1307-13.

Camello-Almaraz, C., Gomez-Pinilla, P. J., Pozo, M. J. & Camello, P. J. 2006. Mitochondrial reactive oxygen species and Ca2+ signaling. *Am J Physiol Cell Physiol,* 291**,** C1082-8.

Canellada, A., Ramirez, B. G., Minami, T., Redondo, J. M. & Cano, E. 2008. Calcium/calcineurin signaling in primary cortical astrocyte cultures: Rcan1-4 and cyclooxygenase-2 as NFAT target genes. *Glia,* 56**,** 709-22.

Cano, E., Canellada, A., Minami, T., Iglesias, T. & Redondo, J. M. 2005. Depolarization of neural cells induces transcription of the Down syndrome critical region 1 isoform 4 via a calcineurin/nuclear factor of activated T cells-dependent pathway. *J Biol Chem,* 280**,** 29435-43.

Cantley, J., Grey, S. T., Maxwell, P. H. & Withers, D. J. 2010. The hypoxia response pathway and beta cell function. *Diabetes, Obesity and Metabolism,* 12**,** 159-167.

Cantley, J., Selman, C., Shukla, D., Abramov, A. Y., Forstreuter, F., Esteban, M. A., Claret, M., Lingard, S. J., Clements, M., Harten, S. K., Asare-Anane, H., Batterham, R. L., Herrera, P. L., Persaud, S. J., Duchen, M. R., Maxwell, P. H. & Withers, D. J. 2009. Deletion of the von Hippel-Lindau gene in pancreatic beta cells impairs glucose homeostasis in mice. *J Clin Invest,* 119**,** 125-35.

Carlsson, P. O., Palm, F., Andersson, A. & Liss, P. 2001. Markedly decreased oxygen tension in transplanted rat pancreatic islets irrespective of the implantation site. *Diabetes,* 50**,** 489-95.

Casas, C., Martinez, S., Pritchard, M. A., Fuentes, J. J., Nadal, M., Guimera, J., Arbones, M., Florez, J., Soriano, E., Estivill, X. & Alcantara, S. 2001. Dscr1, a novel endogenous inhibitor of calcineurin signaling, is expressed in the primitive ventricle of the heart and during neurogenesis. *Mech Dev,* 101**,** 289-92.

Chan, B., Greenan, G., Mckeon, F. & Ellenberger, T. 2005. Identification of a peptide fragment of DSCR1 that competitively inhibits calcineurin activity in vitro and in vivo. *Proc Natl Acad Sci U S A,* 102**,** 13075-80.

Chandel, N. S., Maltepe, E., Goldwasser, E., Mathieu, C. E., Simon, M. C. & Schumacker, P. T. 1998. Mitochondrial reactive oxygen species trigger hypoxia-induced transcription. *Proc Natl Acad Sci U S A,* 95**,** 11715-20.

Chang-Chen, K. J., Mullur, R. & Bernal-Mizrachi, E. 2008. Beta-cell failure as a complication of diabetes. *Rev Endocr Metab Disord,* 9**,** 329-43.

Chang, K. & Min, K. T. 2005a. Drosophila melanogaster homolog of Down syndrome critical region 1 is critical. *Nat Neurosci,* 8**,** 1577-85.

Chang, K. T. & Min, K.-T. 2009. Upregulation of three Drosophila homologs of human chromosome 21 genes alters synaptic function: Implications for Down syndrome. *Proceedings of the National Academy of Sciences,* 106**,** 17117-17122.

Chang, K. T. & Min, K. T. 2005b. Drosophila melanogaster homolog of Down syndrome critical region 1 is critical for mitochondrial function. *Nat Neurosci,* 8**,** 1577-85.

Cheng, K., Ho, K., Stokes, R., Scott, C., Lau, S. M., Hawthorne, W. J., O'connell, P. J., Loudovaris, T., Kay, T. W., Kulkarni, R. N., Okada, T., Wang, X. L., Yim, S. H., Shah, Y., Grey, S. T., Biankin, A. V., Kench, J. G., Laybutt, D. R., Gonzalez, F. J., Kahn, C. R. & Gunton, J. E. 2010. Hypoxia-inducible factor-1alpha regulates beta cell function in mouse and human islets. *J Clin Invest,* 120**,** 2171-83.

Cho, K.-O., Kim, Y. S., Cho, Y.-J. & Kim, S. Y. 2008. Upregulation of DSCR1 (RCAN1 or Adapt78) in the peri-infarct cortex after experimental stroke. *Experimental Neurology,* 212**,** 85-92.

Clipstone, N. A. & Crabtree, G. R. 1992. Identification of calcineurin as a key signaling enzyme in T-lymphocyte activation. *Nature,* 357**,** 695-697.

Comellas, A. P., Dada, L. A., Lecuona, E., Pesce, L. M., Chandel, N. S., Quesada, N., Budinger, G. R., Strous, G. J., Ciechanover, A. & Sznajder, J. I. 2006. Hypoxia-mediated degradation of Na,K-ATPase via mitochondrial reactive oxygen species and the ubiquitin-conjugating system. *Circ Res,* 98**,** 1314-22.

Crawford, D. R., Leahy, K. P., Abramova, N., Lan, L., Wang, Y. & Davies, K. J. A. 1997. Hamster adapt78 mRNA is a down syndrome critical region homologue that is inducible by oxidative stress. *Arch Biochemistry Biophyscis,* 342**,** 6-12.

Dada, L. A., Chandel, N. S., Ridge, K. M., Pedemonte, C., Bertorello, A. M. & Sznajder, J. I. 2003. Hypoxia-induced endocytosis of Na,K-ATPase in alveolar epithelial cells is mediated by mitochondrial reactive oxygen species and PKC-zeta. *J Clin Invest,* 111**,** 1057-64.

Davies, K. J. 1999. The broad spectrum of responses to oxidants in proliferating cells: a new paradigm for oxidative stress. *IUBMB Life,* 48**,** 41-7.

Davies, K. J., Harris, C. D. & Ermak, G. 2001a. The essential role of calcium in induction of the DSCR1 (ADAPT78) gene. *Biofactors,* 15**,** 91-3.

Davies, K. J. A., Ermak, G., Rothermel, B. A., Pritchard, M., Heitman, J., Ahnn, J., Henrique-Silva, F. & Crawford, D. 2007. Renaming the DSCR1/Adapt78 gene family as RCAN;regulators of calcineurin. *The FASEB Journal,* 21**,** 3023-3028.

Davies, K. J. A., Harris, C. D. & Ermak, G. 2001b. The essential role of calcium in induction of the DSCR1 (ADAPT78) gene. *Biofactors,* 15.

Deedwania, P. C. & Fonseca, V. A. 2005. Diabetes, prediabetes, and cardiovascular risk: shifting the paradigm. *Am J Med,* 118**,** 939-47.

Demozay, D., Tsunekawa, S., Briaud, I., Shah, R. & Rhodes, C. J. 2011. Specific glucose-induced control of insulin receptor substrate-2 expression is mediated via Ca2+-dependent calcineurin/NFAT signaling in primary pancreatic islet beta-cells. *Diabetes,* 60**,** 2892-902.

Duan, L. & Cobb, M. H. 2010. Calcineurin increases glucose activation of ERK1/2 by reversing negative feedback. *Proc Natl Acad Sci U S A,* 107**,** 22314-9.

Efanova, I. B., Zaitsev, S. V., Zhivotovsky, B., Köhler, M., Efendić, S., Orrenius, S. & Berggren, P.-O. 1998. Glucose and Tolbutamide Induce Apoptosis in Pancreatic β-Cells. *Journal of Biological Chemistry,* 273**,** 33501-33507.

Ehleben, W., Bolling, B., Merten, E., Porwol, T., Strohmaier, A. R. & Acker, H. 1998. Cytochromes and oxygen radicals as putative members of the oxygen sensing pathway. *Respir Physiol,* 114**,** 25-36.

Epstein, F. H., Shepherd, P. R. & Kahn, B. B. 1999. Glucose Transporters and Insulin Action — Implications for Insulin Resistance and Diabetes Mellitus. *New England Journal of Medicine,* 341**,** 248-257.

Ermak, G. & Davies, K. J. A. 2001. Calcium and oxidative stress: from cell signaling to cell death. *Molecular Immunology,* 38**,** 713-721.

Ermak, G., Harris, C. D., Battocchio, D. & Davies, K. J. 2006. RCAN1 (DSCR1 or Adapt78) stimulates expression of GSK-3beta. *FEBS J,* 273**,** 2100-9.

Ermak, G., Harris, C. D. & Davies, K. J. A. 2002. The DSCR1(Adapt78) isoform 1 protein calcipressin1 inhibits calcineurin and proetcts against acute calcium-mediated stress damage, including transient oxidative stress. *FASEB,* 16**,** 814-824.

Ermak, G., Hench, K. J., Chang, K. T., Sachdev, S. & Davies, K. J. 2009. Regulator of calcineurin (RCAN1-1L) is deficient in Huntington disease and protective against mutant huntingtin toxicity in vitro. *J Biol Chem,* 284**,** 11845-53.

Ermak, G., Pritchard, M. A., Dronjak, S., Niu, B. & Davies, K. J. 2011. Do RCAN1 proteins link chronic stress with neurodegeneration? *FASEB J,* 25**,** 3306-11.

Evans, J. L., Goldfine, I. D., Maddux, B. A. & Grodsky, G. M. 2002. *Endocrine Reviews,* 23**,** 599-622.

Fandrey, J., Frede, S. & Jelkmann, W. 1994. Role of hydrogen peroxide in hypoxia-induced erythropoietin production. *Biochem J,* 303 (Pt 2)**,** 507-10.

Federici, M., Hribal, M. L. & Perego, L. 2001. High glucose causes apoptosis in cultured human pancreatic islets of Langerhans: a potential role for regulation of specific Bcl family genes toward an apoptotic cell death program. *Diabetes,* 50**,** 1290-1302.

Frye, R. A. 1999. Characterization of five human cDNAs with homology to the yeast SIR2 gene: Sir2-like proteins (sirtuins) metabolize NAD and may have protein ADP-ribosyltransferase activity. *Biochem Biophys Res Commun,* 260**,** 273-9.

Frye, R. A. 2000. Phylogenetic classification of prokaryotic and eukaryotic Sir2-like proteins. *Biochem Biophys Res Commun,* 273**,** 793-8.

Fuentes, J. J., Genesca, L., Kingsbury, T. J., Cunningham, K. W., Perez-Riba, M., Estivill, X. & De La Luna, S. 2000. DSCR1, overexpressed in Down Syndrome, is an inhibitor of calcineurin mediated signaling pathways. *Human Molecular Genetics,* 9**,** 1681-1690.

Fuentes, J. J., Pritchard, M. & Estivill, X. 1997. Genomic organiszation, alternative splicing and expression patterns of the DSCR1(Down syndrome candidate region 1) gene. *Genomics,* 44**,** 358-361.

Fuentes, J. J., Pritchard, M., Planas, A. M., Bosch, A., Ferrer, I. & Estivill, X. 1995. A new human gene from the Down syndrome critical region encodes a proline-rich protein highlky expressed in fetal brain and heart. *Human Molecular Genetics,* 4**,** 1935-1944.

Fujita, Y., Sasaki, T., Fukui, K., Kotani, H., Kimura, T., Hata, Y., Südhof, T. C., Scheller, R. H. & Takai, Y. 1996. Phosphorylation of Munc-18/n-Sec1/rbSec1 by Protein Kinase C. *Journal of Biological Chemistry,* 271**,** 7265-7268.

Gembal, M., Gilon, P. & Henquin, J. C. 1992. Evidence that glucose can control insulin release independently from its action on ATP-sensitive K+ channels in mouse B cells. *J Clin Invest,* 89**,** 1288-95.

Genesca, L., Aubareda, A., Fuentes, J. J., Estivill, X., De La Luna, S. & Perez-Riba, M. 2003. Phosphorylation of calcipressin 1 increases its ability to inhibit calcineurin and decreases calcipressin half-life. *Biochem J,* 374**,** 567-75.

Giacco, F. & Brownlee, M. 2010. Oxidative stress and diabetic complications. *Circ Res,* 107**,** 1058-70.

Graef, I. A., Chen, F. & Crabtree, G. R. 2001a. NFAT signaling in vertebrate development. *Current Opinion in Gentic and Development,* 11**,** 505-512.

Graef, I. A., Gastier, J. M., Francke, U. & Crabtree, G. R. 2001b. Evolutionary relationships among Rel domains indicate functional diversification by recombination. *Proc Natl Acad Sci U S A,* 98**,** 5740-5.

Greenwald, I. 1998. LIN-12/Notch signaling: lessons from worms and flies. *Genes Dev,* 12**,** 1751-62.

Griffith, J. P., Kim, J. L., Kim, E. E., Sintchak, M. D., Thomson, J. A., Fitzgibbon, M. J., Fleming, M. A., Caron, P. R., Hsiao, K. & Navia, M. A. 1995. X-ray structure of calcineurin inhibited by the immunophilin-immunosuppressant FKBP12-FK506 complex. *Cell,* 82**,** 507-22.

Groop, L. C., Bonadonna, R. C., Delprato, S., Ratheiser, K., Zyck, K., Ferrannini, E. & Defronzo, R. A. 1989. Glucose and free fatty acid metabolism in non-insulin-dependent diabetes mellitus. Evidence for multiple sites of insulin resistance. *The Journal of Clinical Investigation,* 84**,** 205-213.

Groop, L. C., Saloranta, C., Shank, M., Bonadonna, R. C., Ferrannini, E. & Defronzo, R. A. 1991. The Role of Free Fatty Acid Metabolism in the Pathogenesis of Insulin Resistance in Obesity and Noninsulin-Dependent Diabetes Mellitus. *J Clin Endocrinol Metab,* 72**,** 96-107.

Grunnet, L. G., Aikin, R., Tonnesen, M. F., Paraskevas, S., Blaabjerg, L., Storling, J., Rosenberg, L., Billestrup, N., Maysinger, D. & Mandrup-Poulsen, T. 2009. Proinflammatory cytokines activate the intrinsic apoptotic pathway in beta-cells. *Diabetes,* 58**,** 1807-15.

Gunton, J. E., Kulkarni, R. N., Yim, S., Okada, T., Hawthorne, W. J., Tseng, Y. H., Roberson, R. S., Ricordi, C., O'connell, P. J., Gonzalez, F. J. & Kahn, C. R. 2005. Loss of ARNT/HIF1beta mediates altered gene expression and pancreatic-islet dysfunction in human type 2 diabetes. *Cell,* 122**,** 337-49.

Gurda, G. T., Crozier, S. J., Ji, B., Ernst, S. A., Logsdon, C. D., Rothermel, B. A. & Williams, J. A. 2010. Regulator of Calcineurin 1 Controls Growth Plasticity of Adult Pancreas. *Gastroenterology,* 139**,** 609-619.e6.

Haber, C. A., Lam, T. K., Yu, Z., Gupta, N., Goh, T., Bogdanovic, E., Giacca, A. & Fantus, I. G. 2003. N-acetylcysteine and taurine prevent hyperglycemia-induced insulin resistance in vivo: possible role of oxidative stress. *Am J Physiol Endocrinol Metab,* 285**,** E744-53.

Haigis, M. C. & Guarente, L. P. 2006. Mammalian sirtuins--emerging roles in physiology, aging, and calorie restriction. *Genes Dev,* 20**,** 2913-21.

Halban, P. A., Praz, G. A. & Wollheim, C. B. 1983. Abnormal glucose metabolism accompanies failure of glucose to stimulate insulin release from a rat pancreatic cell line (RINm5F). *Biochem J,* 212**,** 439-43.

Hampton, T. 2005. Down syndrome protein deters cancer: scientists reveal molecular mechanism. *JAMA,* 293**,** 284-5.

Hannken, T., Schroeder, R., Zahner, G., Stahl, R. A. & Wolf, G. 2000. Reactive oxygen species stimulate p44/42 mitogen-activated protein kinase and induce p27(Kip1): role in angiotensin II-mediated hypertrophy of proximal tubular cells. *J Am Soc Nephrol,* 11**,** 1387-97.

Harmon, J. S., Gleason, C. E., Tanaka, Y., Oseid, E. A., Hunter-Berger, K. K. & Robertson, R. P. 1999. In vivo prevention of hyperglycemia also prevents glucotoxic effects on PDX-1 and insulin gene expression. *Diabetes,* 48**,** 1995-2000.

Harris, C. D., Ermak, G. & Davies, K. J. A. 2005. Multiple roles of the DSCR1 (Adapt 78 or RCAN1) gene and its protein product Calcipressin 1 (or RCAN1) in disease. *Cellular and Molecular Life Sciences,* 62**,** 2477-2486.

Hauge-Evans, A. C., Squires, P. E., Persaud, S. J. & Jones, P. M. 1999. Pancreatic beta-cell-to-beta-cell interactions are required for integrated responses to nutrient stimuli: enhanced Ca2+ and insulin secretory responses of MIN6 pseudoislets. *Diabetes,* 48**,** 1402-8.

Heit, J. J. 2007. Calcineurin/NFAT signaling in the Beta cell; from diabetes to new therapeutics. *BioEssays,* 29**,** 1011-1021.

Heit, J. J., Apelqvist, A. A., Gu, X., Winslow, M. M., Neilson, J. R., Crabtree, G. R. & Kim, S. K. 2006. Calcineurin/NFAT signalling regulates pancreatic beta cell growth amd function. *Nature,* 443**,** 345-349.

Henquin, J. C. 2000. Triggering and amplifying pathways of regulation of insulin secretion by glucose. *Diabetes,* 49**,** 1751-60.

Hilioti, Z., Gallagher, D. A., Low-Nam, S. T., Ramaswamy, P., Gajer, P., Kingsbury, T. J., Birchwood, C. J., Levchenko, A. & Cunningham, K. W. 2004. GSK-3 kinases enhance calcineurin signaling by phosphorylation of RCNs. *Genes Dev,* 18**,** 35-47.

Hirakawa, Y., Nary, L. J. & Medh, R. D. 2009. Glucocorticoid evoked upregulation of RCAN1-1 in human leukemic CEM cells susceptible to apoptosis. *J Mol Signal,* 4**,** 6.

Hisahara, S., Chiba, S., Matsumoto, H., Tanno, M., Yagi, H., Shimohama, S., Sato, M. & Horio, Y. 2008. Histone deacetylase SIRT1 modulates neuronal differentiation by its nuclear translocation. *Proc Natl Acad Sci U S A,* 105**,** 15599-604.

Hochachka, P. W., Buck, L. T., Doll, C. J. & Land, S. C. 1996. Unifying theory of hypoxia tolerance: molecular/metabolic defense and rescue mechanisms for surviving oxygen lack. *Proc Natl Acad Sci U S A,* 93**,** 9493-8.

Hoeffer, C. A., Dey, A., Sachan, N., Wong, H., Patterson, R. J., Shelton, J. M., Richardson, J. A., Klann, E. & Rothermel, B. A. 2007. The Down Syndrome Critical Region Protein RCAN1 Regulates Long-Term Potentiation and Memory via Inhibition of Phosphatase Signaling. *The Journal of Neuroscience,* 27**,** 13161-13172.

Hogan, P. G., Chen, L., Nardone, J. & Rao, A. 2003. Transcriptional regulation by calcium, calcineurin, and NFAT. *Genes Dev,* 17**,** 2205-32.

Holmes, K., Chapman, E., See, V. & Cross, M. J. 2010. VEGF stimulates RCAN1.4 expression in endothelial cells via a pathway requiring Ca2+/calcineurin and protein kinase C-delta. *Plos One,* 5**,** e11435.

Hoyal, C. R., Thomas, A. P. & Forman, H. J. 1996. Hydroperoxide-induced increases in intracellular calcium due to annexin VI translocation and inactivation of plasma membrane Ca2+-ATPase. *J Biol Chem,* 271**,** 29205-10.

Huang, C., Li, J., Costa, M., Zhang, Z., Leonard, S. S., Castranova, V., Vallyathan, V., Ju, G. & Shi, X. 2001. Hydrogen peroxide mediates activation of nuclear factor of activated T cells (NFAT) by nickel subsulfide. *Cancer Res,* 61**,** 8051-7.

Idf 2011. IDF Diabetes Atlas Fifth Edition. *IDF Diabetes Atlas* Fifth edition ed.: International Diabetes Federation.

Ihara, Y., Toyokuni, S., Uchida, K., Odaka, H., Tanaka, T., Ikeda, H., Hiai, H., Seino, Y. & Yamada, Y. 1999. Hyperglycemia causes oxidative stress in pancreatic beta-cells of GK rats, a model of type 2 diabetes. *Diabetes,* 48**,** 927-32.

Im, S. H. & Rao, A. 2004. Activation and deactivation of gene expression by Ca2+/calcineurin-NFAT-mediated signaling. *Mol Cells,* 18**,** 1-9.

Imai, S., Armstrong, C. M., Kaeberlein, M. & Guarente, L. 2000. Transcriptional silencing and longevity protein Sir2 is an NAD-dependent histone deacetylase. *Nature,* 403**,** 795-800.

Ishihara, H., Asano, T., Tsukuda, K., Katagiri, H., Inukai, K., Anai, M., Kikuchi, M., Yazaki, Y., Miyazaki, J. I. & Oka, Y. 1993. Pancreatic beta cell line MIN6 exhibits characteristics of glucose metabolism and glucose-stimulated insulin secretion similar to those of normal islets. *Diabetologia,* 36**,** 1139-45.

Iso, T., Kedes, L. & Hamamori, Y. 2003. HES and HERP families: multiple effectors of the Notch signaling pathway. *J Cell Physiol,* 194**,** 237-55.

Jegasothy, B. V., Ackerman, C. D., Todo, S., Fung, J. J., Abu-Elmagd, K. & Starzl, T. E. 1992. Tacrolimus (FK 506)--a new therapeutic agent for severe recalcitrant psoriasis. *Arch Dermatol,* 128**,** 781-5.

Jensen, M. V., Joseph, J. W., Ronnebaum, S. M., Burgess, S. C., Sherry, A. D. & Newgard, C. B. 2008. Metabolic cycling in control of glucose-stimulated insulin secretion. *Am J Physiol Endocrinol Metab,* 295**,** E1287-1297.

Jin, L. & Harrison, S. C. 2002. Crystal structure of human calcineurin complexed with cyclosporin A and human cyclophilin. *Proc Natl Acad Sci U S A,* 99**,** 13522-6.

Jonas, J. C., Bensellaam, M., Duprez, J., Elouil, H., Guiot, Y. & Pascal, S. M. A. 2009. Glucose regulation of islet responses and beta-cell failure in type 2 diabetes. *Diabetes, Obesity and Metabolism,* 11(Supplement 4)**,** 65-81.

Kahn, S. E. 2003. The relative contribution of insulin resistance and beta cell dysfunction to the pathophysiology of type 2 diabetes. *Diabetologica,* 46**,** 3-19.

Kahn, S. E., Hull, R. L. & Utzschneider, K. M. 2006. Mechanisms linking obesity to insulin resistance and type 2 diabetes. *Nature,* 444**,** 840-6.

Kajimoto, Y. & Kaneto, H. 2004. Role of oxidative stress in pancreatic beta-cell dysfunction. *Ann N Y Acad Sci,* 1011**,** 168-76.

Kaneto, H., Kajimoto, Y., Miyagawa, J., Matsuoka, T., Fujitani, Y., Umayahara, Y., Hanafusa, T., Matsuzawa, Y., Yamasaki, Y. & Hori, M. 1999. Beneficial effects of

antioxidants in diabetes: Possible protection of Pancreatic beta cells against glucose toxicity. *Diabetes,* 48**,** 2398-2406.

Kaneto, H., Sharma, A., Suzuma, K., Laybutt, D. R., Xu, G., Bonner-Weir, S. & Weir, G. C. 2002. Induction of c-Myc expression suppresses insulin gene transcription by inhibiting NeuroD/BETA2-mediated transcriptional activation. *J Biol Chem,* 277**,** 12998-3006.

Keating, D. J., Dubach, D., Zanin, M. P., Yu, Y., Martin, K., Zhao, Y.-F., Chen, C., Porta, S., Arbonés, M. L., Mittaz, L. & Pritchard, M. A. 2008a. DSCR1/RCAN1 regulates vesicle exocytosis and fusion pore kinetics: implications for Down syndrome and Alzheimer's disease. *Human Molecular Genetics,* 17**,** 1020-1030.

Keating, D. J., Dubach, D., Zanin, M. P., Yu, Y., Martin, K., Zhao, Y. F., Chen, C., Porta, S., Arbones, M. L., Mittaz, L. & Pritchard, M. A. 2008b. DSCR1/RCAN1 regulates vesicle exocytosis and fusion pore kinetics: implications for Down syndrome and Alzheimer's disease. *Human Molecular Genetics,* 17**,** 1020-30.

Kim, A., Miller, K., Jo, J., Kilimnik, G., Wojcik, P. & Hara, M. 2009. Islet architecture: A comparative study. *Islets,* 1**,** 129-36.

Kim, S. S., Oh, Y., Chung, K. C. & Seo, S. R. 2012. Protein kinase A phosphorylates Down syndrome critical region 1 (RCAN1). *Biochem Biophys Res Commun,* 418**,** 657-61.

Kingsbury, T. J. & Cunningham, K. W. 2000. A conserved family of calcineurin regulators. *Genes Dev,* 14**,** 1595-604.

Kissinger, C. R., Parge, H. E., Knighton, D. R., Lewis, C. T., Pelletier, L. A., Tempczyk, A., Kalish, V. J., Tucker, K. D., Showalter, R. E., Moomaw, E. W. & Et Al. 1995. Crystal structures of human calcineurin and the human FKBP12-FK506-calcineurin complex. *Nature,* 378**,** 641-4.

Kitsou-Mylona, I., Burns, C. J., Squires, P. E., Persaud, S. J. & Jones, P. M. 2008. A role for the extracellular calcium-sensing receptor in cell-cell communication in pancreatic islets of langerhans. *Cellular Physiology and Biochemistry,* 22**,** 557-566.

Klee, C. B., Draetta, G. F. & Hubbard, M. J. 1988. Calcineurin. *Adv Enzymol Relat Areas Mol Biol,* 61**,** 149-200.

Knip, M., Veijola, W., Virtanen, S. M., Hyoty, H., Vaarala, O. & Akerblom, H. K. 2005. Environmental triggers and determinants of type 1 diabetes. *Diabetes,* 54**,** S125-S136.

Kobayashi, N., Okitsu, T., Lakey, J. R. & Tanaka, N. 2004. The current situation in human pancreatic islet transplantation: problems and prospects. *J Artif Organs,* 7**,** 1-8.

Kulkarni, R. N., Jhala, U. S., Winnay, J. N., Krajewski, S., Montminy, M. & Kahn, C. R. 2004. PDX-1 haploinsufficiency limits the compensatory islet hyperplasia that occurs in response to insulin resistance. *J Clin Invest,* 114**,** 828-36.

Ladner, C. J., Czech, J., Maurice, J., Lorens, S. A. & Lee, J. M. 1996. Reduction of calcineurin enzymatic activity in Alzheimer's disease: correlation with neuropathologic changes. *J Neuropathol Exp Neurol,* 55**,** 924-31.

Lange, A. W., Molkentin, J. D. & Yutzey, K. E. 2004. DSCR1 gene expression is dependent on NFATc1 during cardiac valve formation and colocalizes with anomalous organ development in trisomy 16 mice. *Developmental Biology,* 266**,** 346-360.

Lawrence, M. C., Bhatt, H. S. & Easom, R. A. 2002. NFAT regulates insulin gene promoter activity in response to synergistic pathways induced by glucose and glucagon-like peptide-1. *Diabetes,* 51**,** 691-698.

Lawrence, M. C., Bhatt, H. S., Watterson, J. M. & Easom, R. A. 2001. Regulation of insulin gene transcription by a Ca(2+)-responsive pathway involving calcineurin and nuclear factor of activated T cells. *Mol Endocrinol,* 15**,** 1758-67.

Laybutt, D. R., Kaneto, H., Hasenkamp, W., Grey, S., Jonas, J. C., Sgroi, D. C., Groff, A., Ferran, C., Bonner-Weir, S., Sharma, A. & Weir, G. C. 2002. Increased expression of antioxidant and antiapoptotic genes in islets that may contribute to beta-cell survival during chronic hyperglycemia. *Diabetes,* 51**,** 413-23.

Leahy, J. L. 2005. Pathogenesis of type 2 diabetes mellitus. *Arch Med Res,* 36**,** 197-209.

Leahy, K. P. & Crawford, D. R. 2000. adpat78 protects cells against stress damage and suppresses cell growth. *Arch Biochemistry Biophyscis,* 379**,** 221-228.

Leahy, K. P., Davies, K. J. A., Dull, M., Kort, J. J., Lawrence, K. W. & Crawford, D. R. 1999. adapt78, a stress-inducible mRNA, is related to the glucose-regulated protein family of genes. *Arch Biochemistry Biophysics,* 368**,** 67-74.

Lee, J. E., Jang, H., Cho, E. J. & Youn, H. D. 2009. Down syndrome critical region 1 enhances proteolytic cleavage of calcineurin. *Experimental and Molecular Medicine,* 41**,** 471-477.

Leibowitz, G., Bachar, E., Shaked, M., Sinai, A., Ketzinel-Gilad, M., Cerasi, E. & Kaiser, N. 2010. Glucose regualtion of beta-cell stress in type 2 diabetes. *Diabetes, Obesity and Metabolism,* 12**,** 66-75.

Li, F. & Mahato, R. I. 2011. RNA interference for improving the outcome of islet transplantation. *Advanced Drug Delivery Reviews,* 63**,** 47-68.

Li, J. J., Oberley, L. W., Fan, M. & Colburn, N. H. 1998. Inhibition of AP-1 and NF-kappaB by manganese-containing superoxide dismutase in human breast cancer cells. *FASEB J,* 12**,** 1713-23.

Li, N., Brun, T., Cnop, M., Cunha, D. A., Eizirik, D. L. & Maechler, P. 2009. Transient oxidative stress damages mitochondrial machinery inducing persistent beta-cell dysfunction. *The Journal of Biological Chemistry,* 284**,** 23602-23612.

Li, X., Zhang, L., Meshinchi, S., Dias-Leme, C., Raffin, D., Johnson, J. D., Treutelaar, M. K. & Burant, C. F. 2006. Islet microvasculature in islet hyperplasia and failure in a model of type 2 diabetes. *Diabetes,* 55**,** 2965-73.

Limbert, C., Path, G., Jakob, F. & Seufert, J. 2008. Beta-cell replacement and regeneration: Strategies of cell-based therapy for type 1 diabetes mellitus. *Diabetes Res Clin Pract,* 79**,** 389-99.

Lin, H. Y., Michtalik, H. J., Zhang, S., Andersen, T. T., Van Riper, D. A., Davies, K. K., Ermak, G., Petti, L. M., Nachod, S., Narayan, A. V., Bhatt, N. & Crawford, D. R. 2003. Oxidative and calcium stress regulate DSCR1 (Adapt78/MCIP1) protein. *Free Radic Biol Med,* 35**,** 528-39.

Lin, Y., Berg, A. H., Iyengar, P., Lam, T. K., Giacca, A., Combs, T. P., Rajala, M. W., Du, X., Rollman, B., Li, W., Hawkins, M., Barzilai, N., Rhodes, C. J., Fantus, I. G., Brownlee, M. & Scherer, P. E. 2005. The hyperglycemia-induced inflammatory response in adipocytes: the role of reactive oxygen species. *J Biol Chem,* 280**,** 4617-26.

Liu, C., J.O. 2009a. Calmodulin-dependent phosphatase, kinases and transcriptional corepressors involved in T-cell activation. *Immunological Review,* 228**,** 184-198.

Liu, J., Farmer, J. D., Jr., Lane, W. S., Friedman, J., Weissman, I. & Schreiber, S. L. 1991. Calcineurin is a common target of cyclophilin-cyclosporin A and FKBP-FK506 complexes. *Cell,* 66**,** 807-15.

Liu, J. O. 2009b. Calmodulin-dependent phosphatase, kinases, and transcriptional corepressors involved in T-cell activation. *Immunol Rev,* 228**,** 184-98.

Liu, Q., Busby, J. C. & Molkentin, J. D. 2009. Interaction between TAK1-TAB1-TAB2 and RCAN1-calcineurin defines a signalling nodal control point. *Nat Cell Biol,* 11**,** 154-61.

Liu, X., Zhao, D., Qin, L., Li, J. & Zeng, H. 2008. Transcription enhancer factor 3 (TEF3) mediates the expression of Down syndrome candidate region 1 isoform 1 (DSCR1-1L) in endothelial cells. *J Biol Chem,* 283**,** 34159-67.

Longo, V. D. & Kennedy, B. K. 2006. Sirtuins in aging and age-related disease. *Cell,* 126**,** 257-68.

Ma, H., Xiong, H., Liu, T., Zhang, L., Godzik, A. & Zhang, Z. 2004. Aggregate formation and synaptic abnormality induced by DSCR1. *J Neurochem,* 88**,** 1485-96.

Macdonald, P. E. & Rorsman, P. 2006. Oscillations, Intercellular Coupling, and Insulin Secretion in Pancreatic β Cells. *PLoS Biol,* 4**,** e49.

Maechler, P. 2002. Mitochondria as the conductor of metabolic signals for insulin exocytosis in pancreatic beta cells. *Cellular and Molecular Life Sciences,* 59**,** 1803-1818.

Maedler, K., Fontana, A., Ris, F., Sergeev, P., Toso, C., Oberholzer, J., Lehmann, R., Bachmann, F., Tasinato, A., Spinas, G. A., Halban, P. A. & Donath, M. Y.

2002a. FLIP switches Fas-mediated glucose signaling in human pancreatic β cells from apoptosis to cell replication. *Proceedings of the National Academy of Sciences of the United States of America,* 99**,** 8236-8241.

Maedler, K., Sergeev, P., Ris, F., Oberholzer, J., Joller-Jemelka, H. I., Spinas, G. A., Kaiser, N., Halban, P. A. & Donath, M. Y. 2002b. Glucose-induced β cell production of IL-1β contributes to glucotoxicity in human pancreatic islets. *The Journal of Clinical Investigation,* 110**,** 851-860.

Maedler, K., Spinas, G. A., Dyntar, D., Moritz, W., Kaiser, N. & Donath, M. Y. 2001. Distinct Effects of Saturated and Monounsaturated Fatty Acids on β-Cell Turnover and Function. *Diabetes,* 50**,** 69-76.

Mammucari, C., Tommasi Di Vignano, A., Sharov, A. A., Neilson, J., Havrda, M. C., Roop, D. R., Botchkarev, V. A., Crabtree, G. R. & Dotto, G. P. 2005. Integration of Notch 1 and calcineurin/NFAT signaling pathways in keratinocyte growth and differentiation control. *Dev Cell,* 8**,** 665-76.

Mandrup-Poulsen, T., Bendtzen, K., Nielsen, J. H., Bendixen, G. & Nerup, J. 1985. Cytokines Cause Functional and Structural Damage to Isolated Islets of Langerhans. *Allergy,* 40**,** 424-429.

Marchetti, P., Del Prato, S., Lupi, R. & Del Guerra, S. 2006. The pancreatic beta-cell in human Type 2 diabetes. *Nutr Metab Cardiovasc Dis,* 16 Suppl 1**,** S3-6.

Marchetti, P., Dotta, F., Lauro, D. & Purrello, F. 2008. An overview of pancreatic beta-cell defects in human type 2 diabetes: Implications for treatment. *Regulatory Peptides,* 146**,** 4-11.

Masa Skelin, M. R. a. a. C. 2010. Pancreatic beta cell line and their applications in diabetes mellitus research. *ALTEX,* 27**,** 105-113.

Mcclenaghan, N. H. & Flatt, P. R. 1999. Engineering cultured insulin-secreting pancreatic B-cell lines. *J Mol Med (Berl),* 77**,** 235-43.

Meng, T. C., Fukada, T. & Tonks, N. K. 2002. Reversible oxidation and inactivation of protein tyrosine phosphatases in vivo. *Mol Cell,* 9**,** 387-99.

Michtalik, H. J., Narayan, A. V., Bhatt, N., Lin, H. Y., Mulligan, M. T., Zhang, S. L. & Crawford, D. R. 2004. Multiple oxidative stress-response members of the Adapt78 family. *Free Radic Biol Med,* 37**,** 454-62.

Mitchell, A. N., Jayakumar, L., Koleilat, I., Qian, J., Sheehan, C., Bhoiwala, D., Hushmendy, S. F., Heuring, J. M. & Crawford, D. R. 2007a. Brain expression of the calcineurin inhibitor RCAN1 (Adapt78). *Arch Biochem Biophys,* 467**,** 185-92.

Mitchell, A. N., Jayakumar, L., Koleilat, I., Qian, J., Sheehan, C., Bhoiwala, D., Hushmendy, S. F., Heuring, J. M. & Crawford, D. R. 2007b. Brain expression of the calcineurin inhibitor RCAN1 (Adapt78). *Archives of Biochemistry and Biophysics,* 467**,** 185-192.

Miyazaki, J., Araki, K., Yamato, E., Ikegami, H., Asano, T., Shibasaki, Y., Oka, Y. & Yamamura, K. 1990. Establishment of a pancreatic beta cell line that retains glucose-inducible insulin secretion: special reference to expression of glucose transporter isoforms. *Endocrinology,* 127**,** 126-32.

Mohanty, P., Hamouda, W., Garg, R., Aljada, A., Ghanim, H. & Dandona, P. 2000. Glucose challenge stimulates reactive oxygen species (ROS) generation by leucocytes. *J Clin Endocrinol Metab,* 85**,** 2970-3.

Moritz, W., Meier, F., Stroka, D. M., Giuliani, M., Kugelmeier, P., Nett, P. C., Lehmann, R., Candinas, D., Gassmann, M. & Weber, M. 2002. Apoptosis in hypoxic human pancreatic islets correlates with HIF-1alpha expression. *The FASEB Journal*.

Neal, J. W. & Clipstone, N. A. 2001. Glycogen synthase kinase-3 inhibits the DNA binding activity of NFATc *Jounal of Biological Chemistry,* 276**,** 3666-3673.

Newsholme, P., Gaudel, C. & Mcclenaghan, N. H. (eds.) 2010. *The islets of Langerhans*

Newsholme, P., Haber, E. P., Hirabara, S. M., Rebelato, E. L. O., Procopio, J., Morgan, D., Oliveira-Emilio, C. H., Carpinelli, A. R. & Curi, R. 2007. Diabetes associated cell stress and dysfunction: role of mitochondrial and non-mitochondrial ROS production and activity. *Journal of Physiology,* 583**,** 9-24.

O'driscoll, L., Gammell, P. & Clynes, M. 2004. Mechanisms associated with loss of glucose responsiveness in beta cells. *Transplant Proc,* 36**,** 1159-62.

O'driscoll, L., Gammell, P., Mckiernan, E., Ryan, E., Jeppesen, P. B., Rani, S. & Clynes, M. 2006. Phenotypic and global gene expression profile changes between low passage and high passage MIN-6 cells. *J Endocrinol,* 191**,** 665-76.

O'keefe, S. J., Tamura, J. I., Kincaid, R. L., Tocci, M. J. & O'neill, E. A. 1992. FK-506- and CsA-sensitive activation of the interleukin-2 promoter by calcineurin. *Nature,* 357**,** 692-694.

Olson, L. K., Redmon, J. B., Towle, H. C. & Robertson, R. P. 1993. Chronic exposure of HIT cells to high glucose concentrations paradoxically decreases insulin gene transcription and alters binding of insulin gene regulatory protein. *The Journal of Clinical Investigation,* 92**,** 514-519.

Osborne, B. & Miele, L. 1999. Notch and the immune system. *Immunity,* 11**,** 653-63.

Pan, D. A., Lillioja, S., Kriketos, A. D., Milner, M. R., Baur, L. A., Bogardus, C., Jenkins, A. B. & Storlien, L. H. 1997. Skeletal muscle triglyceride levels are inversely related to insulin action. *Diabetes,* 46**,** 983-988.

Park, J., Oh, Y. & Chung, K. C. 2009. Two key genes closely implicated with the neuropathological characteristics in Down syndrome: DYRK1A and RCAN1. *BMB Rep,* 42**,** 6-15.

Park, S., Uesugi, M. & Verdine, G. L. 2000. A second calcineurin binding site on the NFAT regulatory domain. *Proc Natl Acad Sci U S A,* 97**,** 7130-5.

Peiris, H. 2011. ***The Role of Regulator of Calcineurin 1 (RCAN1) In The Regulation of Glucose Homoeostasis And β-Cell Function***

Doctor of Philosophy, Flinders University.

Planas, R., Pujol-Borrell, R. & Vives-Pi, M. 2010. Global gene expression changes in type 1 diabetes: insights into autoimmune response in the target organ and in the periphery. *Immunol Lett,* 133**,** 55-61.

Poitout, V., Olson, L. K. & Robertson, R. P. 1996. Chronic exposure of betaTC-6 cells to supraphysiologic concentrations of glucose decreases binding of the RIPE3b1 insulin gene transcription activator. *The Journal of Clinical Investigation,* 97**,** 1041-1046.

Porta, S., Marti, E., De La Luna, S. & Arbones, M. L. 2007a. Differential expression of members of the RCAN family of calcineurin regulators suggests selective functions for these proteins in the brain. *Eur J Neurosci,* 26**,** 1213-26.

Porta, S., Serra, S. A., Huch, M., Valverde, M. A., Llorens, F., Estivill, X., Arbones, M. L. & Marti, E. 2007b. RCAN1 (DSCR1) increases neuronal susceptibility to oxidative stress: a potential pathogenic process in neurodegeneration. *Human Molecular Genetics,* 16**,** 1039-50.

Prentki, M. & Nolan, C. J. 2006. Islet beta cell failure in type 2 diabetes. *J Clin Invest,* 116**,** 1802-12.

Prozorovski, T., Schulze-Topphoff, U., Glumm, R., Baumgart, J., Schroter, F., Ninnemann, O., Siegert, E., Bendix, I., Brustle, O., Nitsch, R., Zipp, F. & Aktas, O. 2008. Sirt1 contributes critically to the redox-dependent fate of neural progenitors. *Nat Cell Biol,* 10**,** 385-94.

Rabinovitch, A. 1998. *Diabetes Metabolic Review,* 14**,** 129-151.

Rajala, M. W. & Scherer, P. E. 2003. Minireview: The adipocyte--at the crossroads of energy homeostasis, inflammation, and atherosclerosis. *Endocrinology,* 144**,** 3765-73.

Ramadan, J. W., Steiner, S. R., O'neill, C. M. & Nunemaker, C. S. 2011. The central role of calcium in the effects of cytokines on beta-cell function: implications for type 1 and type 2 diabetes. *Cell Calcium,* 50**,** 481-90.

Rao, A., Luo, C. & Hogan, P. G. 1997. Transcription factors of the NFAT family; regulation and function. *Annual Review of Immunology,* 15**,** 707-747.

Ravussin, E. & Smith, S. R. 2002. Increased fat intake, impaired fat oxidation, and failure of fat cell proliferation result in ectopic fat storage, insulin resistance, and type 2 diabetes mellitus. *Ann N Y Acad Sci,* 967**,** 363-78.

Recchioni, R., Marcheselli, F., Moroni, F. & Pieri, C. 2002. Apoptosis in human aortic endothelial cells induced by hyperglycemic condition involves mitochondrial

depolarization and is prevented by N-acetyl-L-cysteine. *Metabolism-Clinical and Experimental,* 51**,** 1384-8.

Rizzuto, R., Brini, M., Murgia, M. & Pozzan, T. 1993. Microdomains with high Ca2+ close to IP3-sensitive channels that are sensed by neighboring mitochondria. *Science,* 262**,** 744-7.

Robertson, R. P. 2004. Chronic oxidative stress as a central mechanism for glucose toxicity in pancreatic islet beta cells in diabetes. *The Journal of Biological Chemistry,* 279**,** 42351-42354.

Robertson, R. P. & Harmon, J. S. 2006. Diabetes, glucose toxicity, and oxidative stress: A case of double jeopardy for the pancreatic islet beta cell. *Free Radic Biol Med,* 41**,** 177-84.

Robertson, R. P., Zhang, H. J., Pyzdrowski, K. L. & Walseth, T. F. 1992. Preservation of insulin mRNA levels and insulin secretion in HIT cells by avoidance of chronic exposure to high glucose concentrations. *The Journal of Clinical Investigation,* 90**,** 320-325.

Rolo, A. P. & Palmeira, C. M. 2006. Diabetes and mitochondrial function: role of hyperglycemia and oxidative stress. *Toxicol Appl Pharmacol,* 212**,** 167-78.

Rorsman, P. 2005. Insulin secretion: function and theraphy of pancreatic beta-cells in diabetes. *The British Journal of Diabetes and Vascular Disease,* 5**,** 187-191.

Rorsman, P., Braun, M. & Zhang, Q. 2011. Regulation of calcium in pancreatic alpha- and beta-cells in health and disease. *Cell Calcium*.

Rothermel, B., Vega, R. B., Yang, J., Wu, H., Bassel-Duby, R. & Williams, R. S. 2000. A protein encoded within the Down syndrome critical region is enriched in striated muscles and inhibits calcineurin signaling. *J Biol Chem,* 275**,** 8719-25.

Rothermel, B. A., Vega, R. B. & Williams, R. S. 2003a. The Role of Modulatory Calcineurin-Interacting Proteins in Calcineurin Signaling. *Trends in Cardiovascular Medicine,* 13**,** 15-21.

Rothermel, B. A., Vega, R. B. & Williams, R. S. 2003b. The role of modulatory calcineurin-interacting proteins in calcineurin signaling. *Trends Cardiovasc Med,* 13**,** 15-21.

Rusnak, F. & Mertz, P. 2000. Calcineurin: Form and Function. *Physiological Review,* 80.

Rutter, G., T., T. & Ravier, M. A. 2006a. Ca2+ microdomains and the control of insulin secretion. *Cell Calcium,* 40**,** 539-551.

Rutter, G. A., Theler, J. M., Murgia, M., Wollheim, C. B., Pozzan, T. & Rizzuto, R. 1993. Stimulated Ca2+ influx raises mitochondrial free Ca2+ to supramicromolar levels in a pancreatic beta-cell line. Possible role in glucose and agonist-induced insulin secretion. *J Biol Chem,* 268**,** 22385-90.

Rutter, G. A., Tsuboi, T. & Ravier, M. A. 2006b. Ca^{2+} microdomains and the control of insulin secretion. *Cell Calcium,* 40**,** 539-51.

Saltiel, A. R. & Kahn, C. R. 2001. Insulin signalling and the regulation of glucose and lipid metabolism. *Nature,* 414**,** 799-806.

Schulla, V., Renstrom, E., Feil, R., Feil, S., Franklin, I., Gjinovci, A., Jing, X. J., Laux, D., Lundquist, I., Magnuson, M. A., Obermuller, S., Olofsson, C. S., Salehi, A., Wendt, A., Klugbauer, N., Wollheim, C. B., Rorsman, P. & Hofmann, F. 2003. Impaired insulin secretion and glucose tolerance in beta cell-selective Ca(v)1.2 Ca2+ channel null mice. *EMBO J,* 22**,** 3844-54.

Semenza, G. L. 1999. Regulation of mammalian O2 homeostasis by hypoxia-inducible factor 1. *Annu Rev Cell Dev Biol,* 15**,** 551-78.

Semenza, G. L., Agani, F., Feldser, D., Iyer, N., Kotch, L., Laughner, E. & Yu, A. 2000. Hypoxia, HIF-1, and the pathophysiology of common human diseases. *Adv Exp Med Biol,* 475**,** 123-30.

Semenza, G. L. & Wang, G. L. 1992. A nuclear factor induced by hypoxia via de novo protein synthesis binds to the human erythropoietin gene enhancer at a site required for transcriptional activation. *Mol Cell Biol,* 12**,** 5447-54.

Shen, J. B., Jiang, B. & Pappano, A. J. 2000. Comparison of L-type calcium channel blockade by nifedipine and/or cadmium in guinea pig ventricular myocytes. *J Pharmacol Exp Ther,* 294**,** 562-70.

Sher, E., Giovannini, F., Codignola, A., Passafaro, M., Giorgi-Rossi, P., Volsen, S., Craig, P., Davalli, A. & Carrera, P. 2003. Voltage-operated calcium channel heterogeneity in pancreatic beta cells: physiopathological implications. *J Bioenerg Biomembr,* 35**,** 687-96.

Shin, S. Y., Yang, H. W., Kim, J. R., Do Heo, W. & Cho, K. H. 2011. A hidden incoherent switch regulates RCAN1 in the calcineurin-NFAT signaling network. *J Cell Sci,* 124**,** 82-90.

Sieber, M. & Baumgrass, R. 2009. Novel inhibitors of the calcineurin/NFATc hub-allternatives to CsA and FK506. *Cell Communication and SIgnaling,* 7.

Stie, J. & Fox, D. 2008. Calcineurin regulation in fungi and beyond. *Eukaryot Cell,* 7**,** 177-86.

Su, A. I., Wiltshire, T., Batalov, S., Lapp, H., Ching, K. A., Block, D., Zhang, J., Soden, R., Hayakawa, M., Kreiman, G., Cooke, M. P., Walker, J. R. & Hogenesch, J. B. 2004. A gene atlas of the mouse and human protein-encoding transcriptomes. *Proceedings of the National Academy of Sciences of the United States of America,* 101**,** 6062-6067.

Sun, 孙., Xiulian, 秀莲, Wu, 吴., Yili, 伊丽, Chen, B., Zhang, Z., Zhou, W., Tong, 童., Yigang, 贻刚, Yuan, J., Xia, K., Gronemeyer, H., Flavell, R. A. & Song, 宋., Weihong, 伟宏 2011. Regulator of Calcineurin 1 (RCAN1) Facilitates Neuronal

Apoptosis through Caspase-3 Activation. *Journal of Biological Chemistry,* 286**,** 9049-9062.

Takahashi, N., Hayano, T. & Suzuki, M. 1989. Peptidyl-prolyl cis-trans isomerase is the cyclosporin A-binding protein cyclophilin. *Nature,* 337**,** 473-475.

Tanaka, Y., Gleason, C. E., Tran, P. O., Harmon, J. S. & Robertson, R. P. 1999. Prevention of glucose toxicity in HIT-T15 cells and Zucker diabetic fatty rats by antioxidants. *Proc Natl Acad Sci U S A,* 96**,** 10857-62.

Tarasov, A., Dusonchet, J. & Ashcroft, F. 2004. Metabolic regulation of the pancreatic beta-cell ATP-sensitive K+ channel: a pas de deux. *Diabetes,* 53 Suppl 3**,** S113-22.

Thiebaud, D., Jacot, E., Defronzo, R. A., Maeder, E., Jequier, E. & Felber, J. P. 1982. The effect of graded doses of insulin on total glucose uptake, glucose oxidation, and glucose storage in man. *Diabetes,* 31**,** 957-963.

Timmerman, L. A., Clipstone, N. A., Ho, S. N., Northrop, J. P. & Crabtree, G. R. 1996. Rapid shuttling of NF-AT in discrimination of Ca2+ signals and immunosuppression. *Nature,* 383**,** 837-40.

Ulrich, A. B., Schmied, B. M., Standop, J., Schneider, M. B. & Pour, P. M. 2002. Pancreatic cell lines: a review. *Pancreas,* 24**,** 111-20.

Vega, R. B., Rothermel, B. A., Weinheimer, C. J., Kovacsw, A., Naseem, R. H., Bassel-Duby, R., Williams, R. S. & Olson, E. N. 2003. Dual roles of modulatory calcineurin-interacting protein1 in cardiac hypertrophy. *Proc Natl Acad Sci U S A,* 100**,** 669-674.

Vega, R. B., Yang, J., Rothermel, B. A., Bassel-Duby, R. & Williams, R. S. 2002. Multiple domains of MCIP1 contribute to inhibition of calcineurin activity. *Journal of Biological Chemistry,* 277**,** 30401-30407.

Vettor, R., Fabris, R., Serra, R., Lombardi, A. M., Tonello, C., Granzotto, M., Marzolo, M. O., Carruba, M. O., Ricquier, D., Federspil, G. & Nisoli, E. 2002. Changes in FAT/CD36, UCP2, UCP3 and GLUT4 gene expression during lipid infusion in rat skeletal and heart muscle. *International journal of obesity and related metabolic disorders : journal of the International Association for the Study of Obesity,* 26**,** 838-47.

Vozzi, C., Ullrich, S., Charollais, A., Philippe, J., Orci, L. & Meda, P. 1995. Adequate connexin-mediated coupling is required for proper insulin production. *J Cell Biol,* 131**,** 1561-72.

Weir, G. C. & Bonner-Weir, S. 2007. A dominant role for glucose in beta cell compensation of insulin resistance. *J Clin Invest,* 117**,** 81-3.

Wollheim, C. B. & Sharp, G. W. 1981. Regulation of insulin release by calcium. *Physiological Review,* 61**,** 914-973.

Wu, H., Kao, S.-C., Barrientos, T., Baldwin, S. H., Olson, E. N., Crabtree, G. R., Zhou, B. & Chang, C.-P. 2007. Down Syndrome Critical Region-1 Is a Transcriptional Target of Nuclear Factor of Activated T Cells-c1 within the Endocardium during Heart Development. *Journal of Biological Chemistry,* 282**,** 30673-30679.

Wykoff, C. C., Beasley, N. J., Watson, P. H., Turner, K. J., Pastorek, J., Sibtain, A., Wilson, G. D., Turley, H., Talks, K. L., Maxwell, P. H., Pugh, C. W., Ratcliffe, P. J. & Harris, A. L. 2000. Hypoxia-inducible expression of tumor-associated carbonic anhydrases. *Cancer Res,* 60**,** 7075-83.

Xu, G. G. & Rothenberg, P. L. 1998. Insulin receptor signaling in the beta-cell influences insulin gene expression and insulin content: evidence for autocrine beta-cell regulation. *Diabetes,* 47**,** 1243-52.

Xu, H., Barnes, G. T., Yang, Q., Tan, G., Yang, D., Chou, C. J., Sole, J., Nichols, A., Ross, J. S., Tartaglia, L. A. & Chen, H. 2003. Chronic inflammation in fat plays a crucial role in the development of obesity-related insulin resistance. *J Clin Invest,* 112**,** 1821-30.

Yanagawa, S., Lee, J. S., Kakimi, K., Matsuda, Y., Honjo, T. & Ishimoto, A. 2000. Identification of Notch1 as a frequent target for provirus insertional mutagenesis in T-cell lymphomas induced by leukemogenic mutants of mouse mammary tumor virus. *J Virol,* 74**,** 9786-91.

Yang, J., Rothermel, B., Vega, R. B., Frey, N., Mckinsey, T. A., Olson, E. N., Bassel-Duby, R. & Williams, R. S. 2000a. Independent signals control expression of the calcineurin inhibitory proteins MCIP1 and MCIP2 in striated muscles. *Circ Res,* 87**,** E61-8.

Yang, J., Rothermel, B. A., Vega, R. B., Frey, N., Mckinsey, T., Olson, E. N., Bassel-Duby, R. & Williams, R. S. 2000b. Independent signals control expression of the calcineurin inhibitory proteins MCIP1 and MCIP2 in striated muscle *Circulation Research,* 87**,** E61-E68.

Yang, S. N. & Berggren, P. O. 2006. The role of voltage-gated calcium channels in pancreatic beta-cell physiology and pathophysiology. *Endocrine Reviews,* 27**,** 621-76.

Yang, T. T., Suk, H. Y., Yang, X., Olabisi, O., Yu, R. Y., Durand, J., Jelicks, L. A., Kim, J. Y., Scherer, P. E., Wang, Y., Feng, Y., Rossetti, L., Graef, I. A., Crabtree, G. R. & Chow, C. W. 2006. Role of transcription factor NFAT in glucose and insulin homeostasis. *Mol Cell Biol,* 26**,** 7372-87.

Yoon, J. W. & Jun, H. S. 2001. Cellular and Molecular Pathogenic Mechanisms of Insulin-Dependent Diabetes Mellitus. *Annals of the New York Academy of Sciences,* 928**,** 200-211.

Zhang, L. & Jope, R. S. 1999. Oxidative stress differentially modulates phosphorylation of ERK, p38 and CREB induced by NGF or EGF in PC12 cells. *Neurobiol Aging,* 20**,** 271-8.

Zhang, W., Efanov, A., Yang, S.-N., Fried, G., Kölare, S., Brown, H., Zaitsev, S., Berggren, P.-O. & Meister, B. 2000. Munc-18 Associates with Syntaxin and Serves as a Negative Regulator of Exocytosis in the Pancreatic β-Cell. *Journal of Biological Chemistry,* 275**,** 41521-41527.

Zhao, P., Xiao, X., Kim, A. S., Leite, M. F., Xu, J., Zhu, X., Ren, J. & Li, J. 2008. c-Jun inhibits thapsigargin-induced ER stress through up-regulation of DSCR1/Adapt78. *Exp Biol Med (Maywood),* 233**,** 1289-300.

Zierler, K. 1999. Whole body glucose metabolism. *American Journal of Physiology-Endocrinology and Metabolism,* 276**,** E409-E426.

APPENDIX 1: Primer Sequences

Gene	Primer	Sequence (5' ➔ 3')
18S rRNA	18S rRNA (F)	CCGCAGCTAGGAATAATGGA
	18S rRNA (R)	AGTCGGCATCGTTTATGGTC
RCAN1-1	RCAN1-1 (F)	ATGGAGGAGGTGGATCTGC
	RCAN1-1(R)	TTTATCCGGACACGTTTGAAG
RCAN1-4	RCAN1-4 (F)	CTGATTGCTTGTGTGGCAAA
	RCAN1-4 (R)	GCAGATAAGGGGTTGCTGAA
RCAN1-NS	RCAN1-NS (F)	CAAGGACACCACCTTCCAGT
	RCAN1-NS (R)	GGAACTGTTTGTCGGGATTG
CA9	CA9 (F)	AGGCTCAGAACACACAGTCA
	CA9 (R)	TGGGACAGCAACTGTTCGTA